THE JOURNAL
OF
CHEMICAL PHYSICS

VOLUME 4 MARCH, 1936 NUMBER 3

The Far Ultraviolet Absorption Spectra and Ionization Potentials of H_2O and H_2S

W. C. PRICE,* *Laboratory of Physical Chemistry, Cambridge, England*

(Received December 30, 1935)

The absorption spectra of H_2O and H_2S in the region below 1600A have been found to consist of various electronic series accompanied by comparatively little vibrational structure. The electronic series conform fairly well to Rydberg formulas the limits of which give 12.56 ± 0.02 and 10.42 ± 0.01 volts, respectively, for the ionization potentials of these molecules. The analysis fits in very well with Mulliken's prediction that the bands should be due to the excitation and removal of a nonbonding electron localized near the oxygen or the sulphur atom. A tentative rotational analysis given for some of the bands in H_2S indicates that the moments of inertia suffer little change by the excitation. Suggestions with regard to plausible atomic term series related with the molecular series are put forward.

A CONSIDERABLE amount of correlation between the far ultraviolet absorption spectra and the ionization potentials of polyatomic molecules has now been accomplished. It has been found[1] that the far ultraviolet absorption spectra of a number of polyatomic molecules consist of bands which can be arranged in various Rydberg series. This is especially so when the excitation is of a nonbonding electron. The limit of the series gives a very accurate value for the ionization potential of the molecule and in addition the absorption spectrum usually yields a great deal of information about the nature of the electron removed. Thus the subject is of considerable importance in the theory of the electronic structure of polyatomic molecules.

A description of the apparatus and the technique employed by the author in obtaining these spectra has appeared elsewhere.[2] A vacuum spectrograph of the grazing incidence type having a dispersion of ~ 2.3 A/mm is used. The grating is of glass to avoid the danger of impairing its surface with corrosive gases. The Lyman continuum serves as the continuous background against which the absorption is observed and the gas under investigation is allowed to flow through the body of the spectrograph. Absorption bands in the region below 2000A are extremely strong. They usually appear at pressures of a few hundredths of a mm in a path length of the order of a meter and thus correspond to electronic transitions of the highest probability.

The two molecules H_2O and H_2S have been selected for treatment in this article because of the similarity of their electronic structures and the fact that, on account of their low moments of inertia, the bands of both molecules exhibit wide rotational structure. The electronic configurations of the normal states of H_2O and H_2S have been given by R. S. Mulliken.[3] The minimum ionization potential is predicted as being due to the removal of a nonbonding electron localized near the oxygen or the sulphur atom, respectively. The nature of the absorption bands

* Senior 1851 Exhibitioner, Trinity College.

[1] W. C. Price, Phys. Rev. **47**, 444 (1935); J. Chem. Phys. **3**, 256, 439 (1935).

[2] Collins and Price, Rev. Sci. Inst. **5**, 423 (1934).

[3] R. S. Mulliken, J. Chem. Phys. **3**, 506 (1935).

reported here is in agreement with Mulliken's prediction.

We will consider the spectrum of H_2S first as many of the bands in it have strong sharp Q branches by which they can be conveniently located. Most of the bands of H_2O on the other hand do not possess such Q branches and their positions cannot be specified so easily on this account. A reproduction of the spectrum of H_2S in the region below 1700A is shown in Fig. 1. The first discrete bands start around 1600A. They are strong and well separated. As we go to shorter wave-lengths the bands become weaker and get closer together eventually merging into a continuous absorption around 1190A. These are the characteristics of absorption bands which go to an ionization potential and it is worthy of note that the wave-length at which the continuum starts corresponds very closely to 10.4 electron volts which is the value obtained by Mackay[4] from electron impact experiments for the ionization potential of H_2S.

A striking feature of the spectrum is the large number of bands with very strong and sharp Q branches accompanied on either side by weaker R and P branches. Fig. 2 is an enlargement of the band at 1391A. It resembles strongly a near infrared vibration rotation band. The R and P branches are degraded only very slightly. In fact no departure from even spacing could be observed in the P branch to within the error of measurement. Further, the extreme sharpness of the Q branch is a sign that the change in the moment of inertia in going from the ground to the excited state has been very slight. As the band corresponds to an electronic jump of nearly 9 electron volts we must conclude that the electron is of a nonbonding type. This is in conformity also with the fact that very little vibrational structure accompanies the excitation. A few vibration bands were found to accompany the first electronic state but these faded out for all higher electronic jumps. This phenomenon is characteristic of the spectra of the alkyl halides, formaldehyde and benzene where the excitation is also that of a nonbonding electron.

The rotational structure of the band at 1391A seems at first sight rather simple to be associated with a molecule like H_2S. However we will discuss it in a later paragraph. What we wish to say now is that a whole set of bands of exactly similar structure appeared in the spectrum and that the heads of the Q branches of these bands were found to fit into the following Rydberg series.

$$\nu_0^n = 84{,}420 - R/(n-2.04)^2, \quad n=5, 6, 7, \text{etc.} \quad (1)$$

The above formula represents very well all the bands of this type and the diminution in intensity of the bands with increasing 'n' is just what is expected for such a Rydberg series. They correspond to series E in Fig. 1.

Another set of discrete bands possessing strong and sharp Q branches is also present in the spectrum. They are marked as the A series in Fig. 1. They can be distinguished from the bands of the previous type on account of the fact that their P branches are extremely weak compared with their R branches. This gives them an unsymmetrical appearance. It is indeed hard to ascertain whether some of them have any P branch at all. However their Q branches can be fitted fairly well into a Rydberg series which runs as follows.

$$\nu_0^n = 84{,}520 \pm R/(n-1.57)^2, \quad n=4, 5, 6, \text{etc.} \quad (2)$$

A large number of terms were found for both the series (1) and (2) and an idea of the accuracy with which they conform to the respective Rydberg formulas can be obtained from an inspection of Table I. The limits are so slightly different as probably to come within the error of extrapolation in Rydberg series. Their mean corresponds to an ionization potential of 10.420 ± 0.005 volts as compared with Mackay's value of 10.4 volts for H_2S. There is therefore no doubt that the bands are those which lead to ionization at this voltage. (The quantum defects in the Rydberg formulas are chosen so as to bring out the relation with certain associated atomic term series.)

In addition to the A and E series a number of other series were found in the band system (Table II). To the long wave-length side of all the E bands there appear strong diffuse bands called the D bands. These rapidly approach the E bands with increase in "n." Again to the long wave-length side of the D bands another set of

[4] C. A. Mackay, Phys. Rev. **24**, 319 (1924).

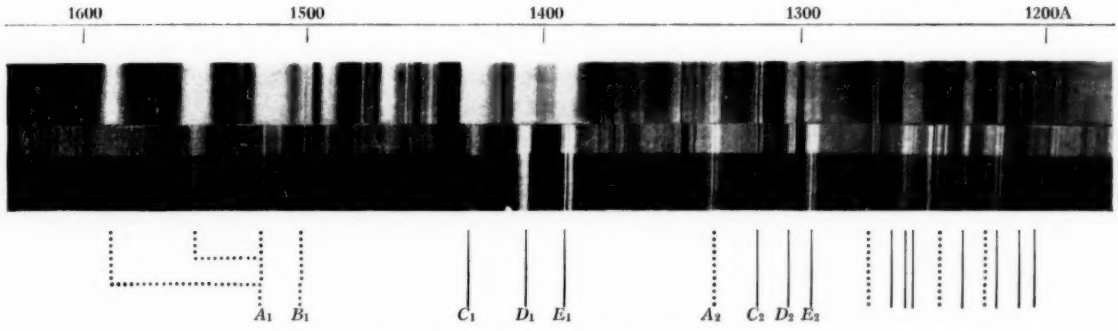

FIG. 1. The far ultraviolet absorption spectrum of H_2S.

bands called C is found. These are not so diffuse as the D bands. They are similar to the A system in that they possess strong sharp Q branches their R branches being fairly strong and their P branches being extremely weak or possibly nonexistent. In general they are somewhat weaker and more diffuse than the A set. Both the C and the D bands approach the E bands fairly rapidly with increase in 'n' and eventually fuse into them around 1028A.

The above classification is considered satisfactory for all the bands below 1460A. The weaker bands in the region from 1600–1460A must be explained as a set of vibration bands accompanying one or two main electronic transitions. We will now proceed to the analysis of the bands in this region. Our first clue comes from the longest wave-length bands at 1579.1 and 1545.3A. These are bands which only come out at relatively high pressures and as they lie to the long wave-length side of the main electronic transition, they are therefore of the nature of transitions from an initial vibrational state. It is found that they are separated from the strong low pressure band A_1 at 1516A by distances of 1250 cm^{-1} and 2630 cm^{-1}, respectively. These frequency differences correspond to the ν_δ and ν_π (or ν_σ) vibrations of the ground state of H_2S. The conclusion is therefore that they belong to the same electronic jump as the A_1 band but that they are transitions from initial vibrational states. A number of other weak bands accompanying the main electronic transitions appear in the region between A_1B_1 and $C_1D_1E_1$. They can be explained partly as transitions to upper vibrational levels of the A_1B_1 states and

TABLE I. *Table showing the observed and calculated frequencies of the bands of series (1) and (2) of H_2S.*

	Series 1 (E)				Series 2 (A)		
n	I	ν obs.	ν calc.	n	I	ν obs.	ν calc.
5	10	71895	71893	4	10	65963	65930
6	9	77437	77422	5	9	75121	75192
7	7	79998	79958	6	7	78945	78926
8	6	81350	81330	7	5	80789	80797
9	4	82141	82154	8	3	81866	81866
10	3	82692	82688	9	2	82534	82532
11	2	83068	83053	10	1	82964	82975
12	2	83325	83314				
13	1	83500	83507				
14	0	83654	83654				

TABLE II. *Table giving the observed frequencies of the bands assigned to the C and D series of H_2S.*

	Series C			Series D	
n	I	ν obs.	n	I	ν obs.
5	8	69850	5	10D	71060
6	6	76220	6	8D	76900
7	4	79353	7	6D	79760
8	2	81251	8	4D	81310

For bands with sharp Q branches the frequency given corresponds to the head of this branch and the values are probably correct to 5 or 10 cm^{-1}. For the more diffuse bands the errors in the estimated centers may be considerably larger than this.

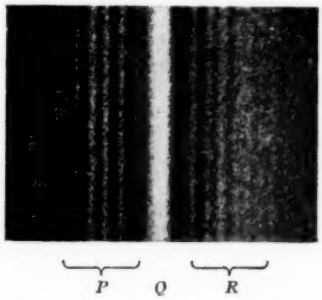

FIG. 2. Band in H_2S at 1391A.

partly as transitions from initial vibrational states to the $C_1D_1E_1$ states. Frequency differences of 1110–1160 cm^{-1} were found to accompany the A_1 and B_1 bands on their short wave-length side and differences very closely equalling $(\nu_\delta)_0$ and $(\nu_{\pi \text{ or } \sigma})_0$ were found to accompany the C_1, D_1 and E_1 bands on their long wave-length side. The former are explained as transitions to final vibrational levels of the A_1 and B_1 states. The latter, which are transitions from initial vibrational states, are of course important in associating the $C_1D_1E_1$ states with H_2S. These bands are a little too diffuse to make this identification absolutely certain by measurement. It is therefore desirable to leave the exact vibrational analysis in this region until the spectrum of D_2S has been obtained. This will then give an unambiguous assignment of the vibrational bands. The ones which correspond to upper vibrational states will be shifted toward the red while those which are transitions from initial vibrational states will be shifted toward the violet. The author plans to obtain this spectrum in the near future.

Rotational Structure

The main objection to the rotational structure of the E system as exemplified by the band at 1391A (Fig. 2) is that it is unusually simple to be associated with a molecule like H_2S. An easy way out of the difficulty would be to try and ascribe it to the diatomic SH molecule which is the only other conceivable possibility. However, it is felt that the evidence is sufficient to rule this out entirely. In the first place the bands are obtained in absorption at extremely low pressures (~0.01 mm). Any SH that might be formed by photodissociation must immediately pass out of the path of the light and be lost in the huge volume of the spectrograph. (The ratio of the volume of the absorbing column to the volume of the spectrograph is at least as low as 1/100.) It is hardly conceivable that a secondary effect of this nature should give rise to bands as strong as the primary bands. From the analysis, the A_1, D_1 and E_1 bands can probably be definitely ascribed to H_2S as they are accompanied on the long wave-length side by bands whose frequency differences from them correspond to the known vibration frequencies associated with the ground state of H_2S. It must also be remembered that these bands are linked up with those at shorter wave-lengths through the various Rydberg series going to the same ionization potential. On these grounds it is believed that all the bands reported here are due to the H_2S molecule.

The weakness or apparent absence of the P branch in the A and C sets of bands is rather a curious phenomenon. The sharpness of the Q branches shows that the moment of inertia is not changed a great deal by the transition (even at considerably high pressures the Q branches retain most of their sharpness). This weakness of the P branch is hard to explain if the bands are due to the SH molecule though it must be admitted that its explanation in terms of H_2S is not obvious either.

We perhaps get our best clues for explaining the rotational structure of the E system by considering the nature of the electronic transitions which give rise to the bands. The electron configuration of the normal state of H_2S has been given by R. S. Mulliken.[3] The bands going

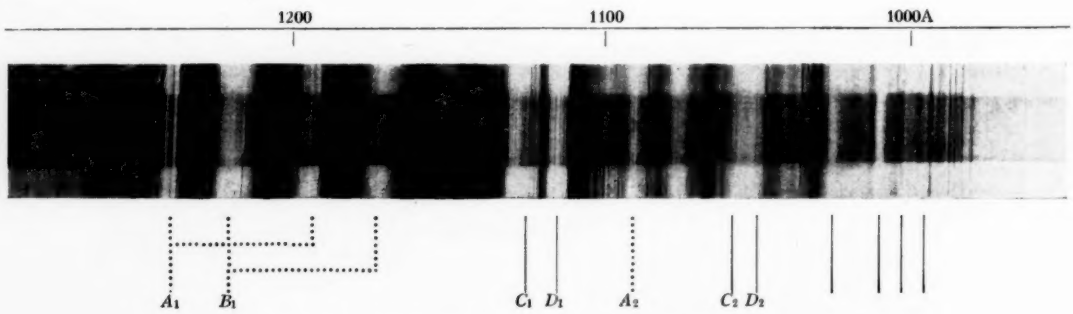

Fig. 3. The far ultraviolet absorption spectrum of H_2O.

to the lowest ionization potential, presumably the ones we have here, are due to the removal of a nonbonding $3xb$ electron, i.e., $3p_x$, 'x' axis perpendicular to the HSH plane. It thus seems possible that the electric moment corresponding to the E transitions vibrates in the 'x' direction. This of course depends also on the nature of the upper states. However, these might easily be suitable in the case of the E series. Now H_2S approximates to a symmetrical top rotator, the axis of symmetry from this point of view being through the center of gravity and parallel to the 'x' axis. An electric moment changing along this axis gives rise to a parallel band and the rotational transitions are governed by the selection rules $\Delta j=0, \pm 1$ and $\Delta k=0$. The spacing observed in the E bands thus corresponds to a mean of the two lower moments of inertia if neither is changed greatly by the excitation. The $\Delta\nu$ of the bands which remains constant for the qP branch to within the error of measurement is 20 cm^{-1}. This corresponds to a moment of inertia of 2.77×10^{-40} g cm^2 as compared with the values $A=2.667\times10^{-40}$ and $B=3.076\times10^{-40}$ g cm^2 given by Cross[5] for the values in the ground state. The absence of any alternation of intensity indicates that the rotation is mainly about the 'y' axis. The diffuseness of the qR branch is probably not due to predissociation but to a splitting of the rotational levels due to deviations from the symmetrical top. This would be expected to occur for the rotational states of higher quantum numbers.

The absorption spectrum of H_2O

The ultraviolet absorption spectra of H_2O and H_2S are similar in many respects. Both possess regions of continuous absorption at longer wave-lengths. The continuum in H_2S lies between 2070–1880A and in H_2O between 1785–1550A. To the short wave-length side of these we find relatively discrete bands which form series going to the first ionization potentials of the molecules. The absorption spectrum of water vapor in the region below 1250A was first investigated by Rathenau.[6] The bands he obtained were so broad and diffuse that a complete analysis was impossible with the dispersion at his disposal. The spectrograph used in the present work has about seven times the dispersion of the one used by Rathenau. While this enabled a great deal of the rotational structure to be resolved, it was found to be too complicated to analyze completely. Further many of the bands were spoiled by being crossed by emission lines which from the nature of the continuum it is impossible to remove. However a clearer picture of the system was obtained and this has led to the analysis given here.

Fig. 3 shows the absorption spectrum of H_2O in the region below 1300A. The first bands which are of sufficient intensity to correspond to the first strong resonance bands of the molecule occur at 1240A. They are apparently of the nature of two Q branches, A_1 and A_1', i.e., an electronic doublet $\Delta\nu=170$ cm^{-1}. On the short wave-length side of them appear two very similar bands of much reduced intensity. The separation of these from the former bands is 3170 cm^{-1}. They thus probably correspond to a $\nu_{\pi \text{ or } \sigma}$ type vibration in the upper state. A strong but rather diffuse band B_1 at about 1220A is also accompanied by a much weaker band about 3240 cm^{-1} to the short wave-length side of it. These frequencies do not differ much from $\nu_\pi=3600$ cm^{-1} or $\nu_\sigma=3756$ cm^{-1} of the ground state of H_2O and thus probably correspond to vibrations of the same type. Bands which may be second members of A_1 and B_1 occur at 1091 and 1078A. However, the Rydberg series corresponding to the A and B types are weak and few members could be observed, so we will pass on to the consideration of the stronger systems C and D. (It is a significant fact that a similar phenomenon occurs in H_2S, i.e., the Rydberg series starting at longer wave-lengths are considerably weaker and less well developed than those which start further down in the ultraviolet. A possible explanation of this will be given later.) The bands C_1 and D_1 show rotational structure spreading out over a range of more than 10A. Two other bands C_2 and D_2 which are, however, closer together fall around 1058 and 1052A.*

[5] P. C. Cross, Phys. Rev. **47**, 7 (1935).
[6] G. Rathenau, Zeits. f. Physik **87**, 32 (1934).

* Emission lines in the continuum also tend to affect the appearance of the bands, e.g., the dark centers appearing in C_2 and D_2 are actually emission lines coming through the absorption bands.

TABLE III. *Table showing the mean observed and calculated frequencies of the CD series of H_2O along with the molecular term values and the mean values of the $(^4S)ns$, $^5, ^3S$ term series of $O(I)$.*

n	I	ν obs.	ν calc.	T_M	T_A	Δ
4	10	89170	89170	12610	13895	−1375
5	9	94780	94750	7000	7535	− 573
6	8	97320	97300	4460	4745	− 285
7	7	98690	98680	3090	3251	− 161
8	5	99500	99508	2280	2370*	− 90
9	3	100040	100044	1740	1800*	− 60

T_A* means that the atomic term value has been estimated.

C_3D_3 is the next doublet in the series. Here the C and D bands have fused into one another and for all subsequent states they overlap. The mean of the corresponding C and D bands were taken to form the following Rydberg series.

$$\nu_0^n = 101{,}780 - R/(n-1.05)^2 \quad n=4, 5, 6, \text{etc.} \quad (3)$$

Seven members of this series were observed. An idea of the accuracy with which the centers conform to the Rydberg formula can be obtained from Table III. The limit corresponds to an ionization potential of 12.56 volts, the error being probably not more than two-hundredths of a volt. It is to be compared with the value 12.7 volts obtained by Smyth and Mueller[7] from electron impact experiments.

Tables of the frequencies and assignments of the strong bands are appended (Table IV). The frequency given corresponds to the estimated center of all the rotational lines in the band. All the bands given by Rathenau which lie on the long wave-length side of A_1 must correspond to transitions from various initial vibrational states. The fact that they only come out at high pressures and become rapidly weaker as we go to long wave-lengths supports this. The bands are however too broad to make the identification certain. Many plausible classifications were found but none could be established definitely enough to be recorded.

Now that we have a fairly large amount of data on the Rydberg series of molecules it is both interesting and profitable to try and find the related atomic series. To do this we use the equation given below at the same time combining with it as many data on the structure of the bands as are available.

[7] H. D. Smyth and D. W. Mueller, Phys. Rev. **43**, 116 (1933).

TABLE IV. *Table giving the frequencies and assignments of bands in H_2O.*

n	I	νA	I	$\nu A'$	I	νB	I	νC	I	νD
4	8	80600	9	80770	9D	82070	10	88660	10	89680
5	6	91690	7	91730	4	92050	9	94530	9	95090
6	3	95880		—	1	96080	components overlap			

$$T_M{}^n - T_A{}^n = (D_n - D_\infty) = \Delta, \quad (4)$$

where $T_M{}^n$ stands for the term value of an excited molecular state "n" and $T_A{}^n$ stands for the term value of an excited atomic state "n." D_n stands for the energy required to increase all internuclear distances indefinitely and thus localize the excitation in one particular atom. As the bonding (or antibonding) power of an electron rapidly falls to zero with increase in electronic quantum number, Δ should become very small for the higher series members and thus the molecular term values should approach those of the related atomic term series. If Δ is positive the excited orbitals are bonding, if negative they are antibonding. The equation has not been applied extensively for diatomic molecules on account of the fact that the ionization potentials of few of these are known well enough to enable the term values of their excited states to be given accurately. However, the ionization potentials of a number of polyatomic molecules are now known fairly accurately from molecular Rydberg series and thus the equation is the natural one to use in these cases. It must, however, be used with caution and due regard to any evident structure of the bands. We proceed to apply it here to the spectra of H_2O and H_2S. Its application to a number of other molecules will appear in a subsequent article.

Let us consider first the spectrum of H_2O. An investigation of the term values of the C and D series indicates that they are related to the $2p^3$ $(^4S)ns$, ^5S and ^3S terms of O(I). The mean term values* of the molecular and atomic Rydberg series† are given in Table III. It is seen

* Mean term values are given because the higher states of the molecular Rydberg series fuse into one another and it is impossible to give the individual term values on account of overlapping.

† It is considered that the choice of any other atomic term series would make the Δ's too large for the bands to be associated with the excitation of a nonbonding electron, and it must be remembered that all the other features of the spectrum are in agreement with this hypothesis.

that the values of the Δ's are negative and therefore the orbitals of the excited states are of a slightly antibonding type. These values, which decrease rapidly with "n" are of the same order of magnitude as those found in known diatomic cases. An inspection of the Rydberg formula for the *CD* series shows that another term is predicted to lie around 1600A. This is in the region of continuous absorption. Mulliken has already attributed this absorption to a transition to an upper state $(2xa_1)(3sa_1)$, $^{3,1}A_1$, stating that the continuum is probably due to predissociation. This conclusion is supported by the fact that Rathenau finds some structure in the continuum. A frequency difference of about 1300 cm^{-1} was found to be associated with the structure, which might easily be related to a vibration of the type ν_3 in the upper state. The diminution in this frequency which has a value of 1600 cm^{-1} in the ground state, may well be due to the increased antibonding power of the orbitals of these low excited states as can be predicted from the antibonding powers of the higher series members. Extending Mulliken's assignment of the transitions in this region to cover the rest of the *CD* series, the upper states are thus in his notation $\cdots(2xa_1)(nsa_1)$, $^{3,1}A_1$.

Sufficient term values of the *A* and *B* series could not be found to make the correlations certain but an examination of those available indicates strongly that the related atomic term series are $2p^3$ $(^4S)np$, ^5P and ^3P. The comparative weakness of the transitions is possibly connected with the fact that combinations with the ground state $2s^22p^4$, ^3P are forbidden in the atomic case.

Attention has already been called to the great similarity between the spectra of H_2O and H_2S. As in H_2O, two sets of Rydberg series have been obtained in H_2S. These two sets have quite different term values, and in the case of H_2O they were correlated to atomic term series of the types $(^4S)np$ and $(^4S)ns$. A similar correlation exists for H_2S. A comparison of the term values of the *A* series in H_2S with those given for $S(I)$ by Frerichs[8] indicates that the upper states for this set probably dissociate into $(^4S)np$, $^{5,3}P$ states of $S(I)$. For the *CDE* series the only plausible atomic term series are $(^4S)ns$, $^{5,3}P$ states of $S(I)$. Actually as shown in Table V there is a rather striking agreement between the *A* term series and the ^3P atomic term series. A similar agreement is found to exist between the *E* term series and the ^3S term series. However, the existence of several series makes the interpretation a little uncertain. As in H_2O the first member of the *CDE* series is predicted to lie in the continuum (i.e., around 2000A). This continuum has been interpreted by Mulliken in an exactly analogous way to that in H_2O and it is satisfying to find that it is also linked up with the bands at shorter wave-lengths in the same way for both molecules.

TABLE V. *Table showing how the term values of the A and E series in H_2S approach the $(^4S)np$, ^3P and $(^4S)ns$, ^3S atomic term series.*

n	$T_M(A)$	^3P	n	$T_M(E)$	^3S
4	18557	18668	5	12525	12207
5	9399	9290	6	6983	6839
6	5575	5574*	7	4422	4374
7	3731	3722*	8	3064	3039

Besides their intrinsic value the spectra of H_2O and H_2S are important because, as Mulliken has pointed out, they are the type molecules for the spectra of the alcohols and ethers, and the mercaptans and sulphides, respectively. In all these cases the absorption spectra can be attributed to the excitation of a nonbonding electron from the oxygen or sulphur atom. In conclusion the author wishes to thank Dr. W. G. Penney and Dr. G. B. B. M. Sutherland for their valuable criticism of the manuscript. He also wishes to express his appreciation of the hospitality of the staff of The Johns Hopkins University, where the experimental work connected with this article was carried out.

[8] R. Frerichs, Zeits. f. Physik **80**, 150 (1933).

The Infrared Absorption Spectra of Mixtures of Acetone and Water

DUDLEY WILLIAMS AND E. K. PLYLER, *Department of Physics, University of North Carolina*

(Received November 20, 1935)

A study of the infrared absorption spectra of acetone containing water revealed an associational band in the region 2.7μ. This band was studied for concentrations of water varying from 0.5 percent to 70 percent by weight. The intensity of the associational band increased with the water content of the mixture. When the water content was large, the 3μ water band overlapped the associational band. Absorption spectra were obtained for ten mixtures. It was found that concentrations of water as low as 0.1 percent could be detected by the presence of this band.

IN previous infrared absorption studies[1] of aqueous solutions of several acids and bases, certain bands were observed which were not characteristic of either the pure solvent or solute. These bands were interpreted as arising from hydration effects in the solutions. The absorption spectra of alcoholic solutions of hydroxides were found to contain similar bands.[2] The presence of these solvation bands in the spectra of these two types of solutions suggested the possible existence of associational bands in still other types of solutions and mixtures.

Fajans[3] has applied the first law of thermodynamics to the problem of thermal effects in the formation of solutions. His work shows that in aqueous solutions the heat of hydration of the ions makes up the greater part of the total heat of solution. In the case of nonionizing solvents, the heat of solution is probably due to solvation effects. These results indicate that substances generating heat on mixing should have absorption bands arising from their associational energies. If these energies are of sufficient magnitude, the resulting absorption would be expected to occur in the near infrared.

In tests on several mixtures it was found that the addition of a small amount of water to acetone resulted in a rise of temperature of several degrees. The absorption spectra of various mixtures of acetone and water were investigated and the results are discussed below. The methods of measurement have been previously described.[4]

The absorption of a sample of Baker's absolute acetone was studied in the region from 1.0μ to 6.5μ. Intense bands were observed at 3.3μ and 5.8μ, and weaker bands at 1.4μ, 2.1μ, 2.7μ, and 4.7μ. This absorption curve is shown in Fig. 1. The second curve of Fig. 1 shows the absorption of a mixture of nine parts of acetone to four parts of water. The small band at 2.7μ in the first curve appears with greatly increased intensity in the second curve. The water bands at 4.7μ and 6.2μ were also observed in the mixture. It should be noted that the intense absorption in the region of 2.9μ in the second curve is due in part to the 3μ water band.

These radical changes in the spectra indicated that the absorption at 2.7μ was possibly due to an associational effect in mixtures of acetone and water. In order to examine the absorption in this region in a more detailed manner, it was decided to measure this absorption with various known concentrations of water in acetone. In order to obtain water-free acetone for use in this investigation a sample of Baker's chemically pure acetone was dried for three days over $CaCl_2$ and then distilled in a system with drying tubes. Several concentrations varying from 0.5 percent to 70 percent by weight of water were prepared and sealed in dry bottles until needed. The fluorite windows used for the cells were kept in a desiccator with P_2O_5 for several hours before being used.

In Fig. 2 are shown the results obtained in the region from 2.3μ to 3.5μ. The concentrations of water in the mixtures used for these curves vary from zero percent to 70 percent. The first curve, which represents the transmission of the supposedly absolute acetone, shows a slight absorption at 2.7μ, indicating the presence of a small amount of water, which was probably

[1] E. K. Plyler and E. S. Barr, J. Chem. Phys. **2**, 306 (1934). E. K. Plyler and W. Gordy, J. Chem. Phys. **2**, 470 (1934).
[2] E. K. Plyler and F. D. Williams, J. Chem. Phys. **2**, 565 (1934).
[3] H. S. Taylor, *Treatise on Physical Chemistry* (D. Van Nostrand Co., 1930), p. 334.
[4] W. Gordy and D. Williams, J. Chem. Phys. **3**, 664 (1935).

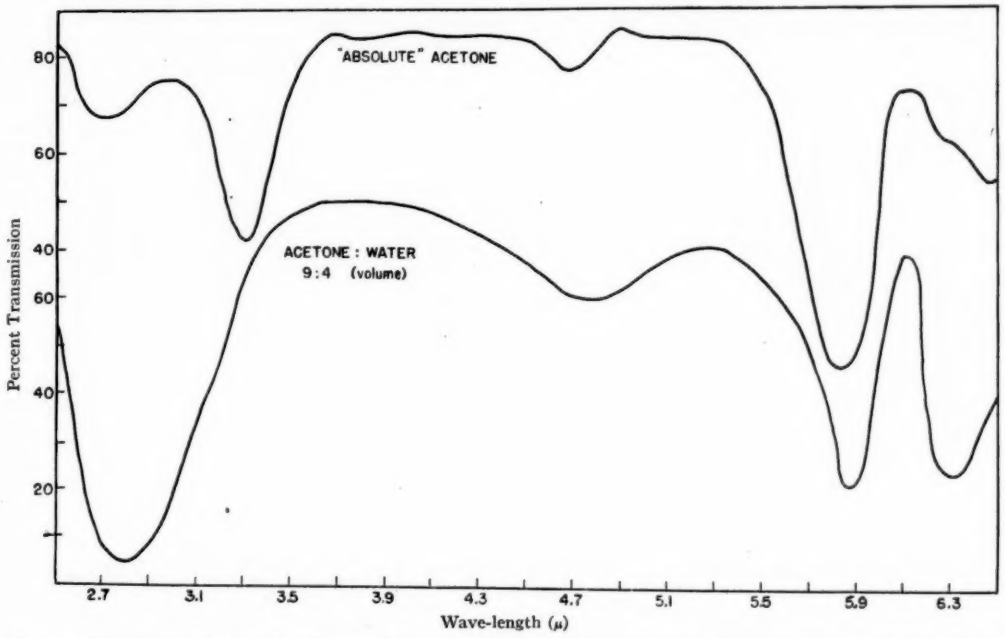

FIG. 1. The transmission of "absolute" acetone and a water-acetone mixture from 2.5μ to 6.5μ. Cell thickness: 0.03 mm.

absorbed from the air while the cell was being prepared. The curves for 5 percent and 10 percent water show clearly the associational band at 2.7μ and also the acetone band at 3.3μ. The absorption curves for the higher concentrations of water do not show two distinct bands on account of the absorption of water at 3μ. This water band is predominant for the 50 and 70 percent solutions of water. At these concentrations the band actually observed is broad and intense, extending from 2.5μ to 3.4μ, and arises from the combined absorption of the water, the acetone, and the associated molecules.

In Fig. 2 the absorption curve for the 5 percent concentration of water shows that the intensity of the 2.7μ associational band is greater than that of the 3.3μ acetone band. This suggested the possibility of using this associational band for detecting the presence of small amounts of water in acetone. In Fig. 3 are shown the transmission curves for low concentrations of water in acetone. A freshly prepared sample of absolute acetone was used for comparison, and no appreciable absorption was observed in the region of 2.7μ. At a concentration of 0.5 percent water, a strong associational band appeared, and the intensity of this band increased with increasing

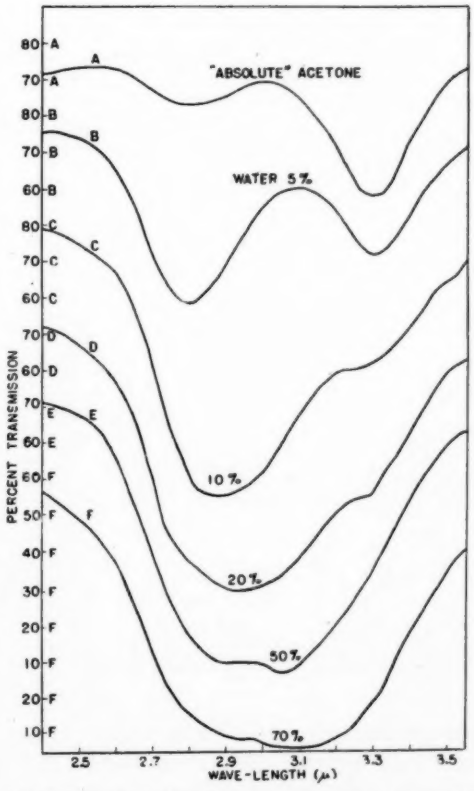

FIG. 2. The transmission of several water-acetone mixtures from 2.3μ to 3.5μ. Cell thickness: 0.03 mm.

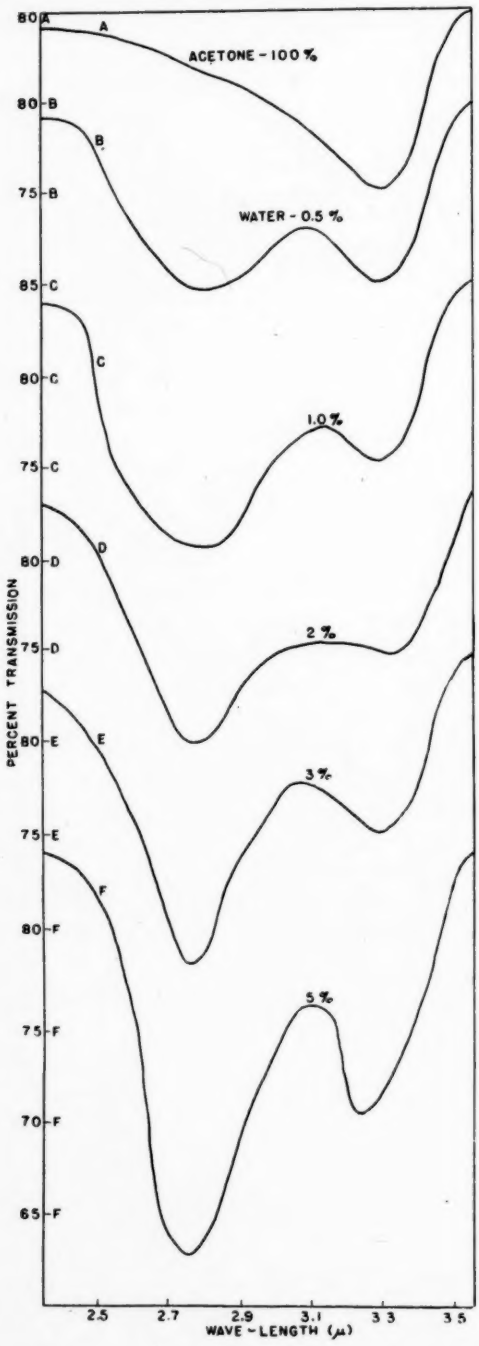

FIG. 3. The transmission of low concentrations of water in acetone from 2.3μ to 3.5μ. Cell thickness: 0.01 mm.

concentrations of water. The bands appearing in Fig. 3 are sharper than those shown in Fig. 2 as a result of the use of thinner absorbing layers.

As it has been stated above, the absorption at

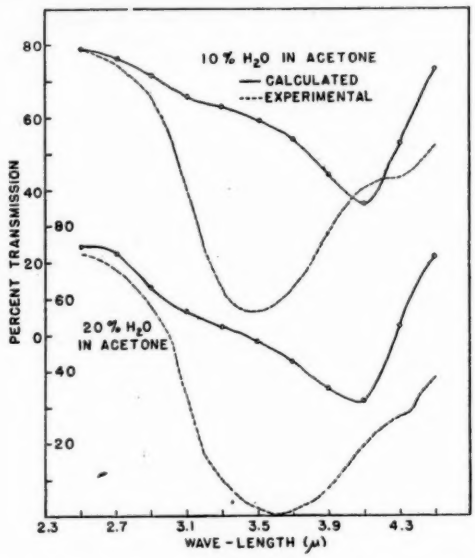

FIG. 4. The theoretical and experimental transmission of the water-acetone mixtures. Cell thickness: 0.03 mm.

2.7μ is attributed to an associational effect. In order to show that this band is not merely an apparent effect arising from the superposition of water and acetone absorptions, theoretical transmission curves have been plotted showing the absorption to be expected in a purely mechanical mixture of the two liquids, in which there is no association. These curves are shown in Fig. 4 and are developed on the assumption that the coefficient of absorption at any wave-length is equal to a suitably weighted mean of the absorption coefficients at the same wave-length; i.e.,

$$\alpha_{12}x=\alpha_1 n_1 x+\alpha_2 n_2 x. \qquad (1)$$

where α_{12}, α_1, and α_2 are the coefficients of absorption of the mixture, the water, and the acetone, respectively, and x is the cell thickness. Here n_1 is the ratio of the number of water molecules in the cell to the total number of water molecules in a cell of equal thickness when only water is present; n_2 is the same ratio for acetone. As is evident from the figure the sharp absorption band actually observed at 2.7μ is not present in the theoretical curves.

There are two different types of association which would give rise to the 2.7μ band. First, the band may arise from a modified vibration of the water molecule. Second, the band may be

produced by the molecules of an association compound. Although it is impossible from the observation of only one absorption band to determine definitely the nature of the mechanism producing it, the authors are inclined toward a belief in the existence of an association compound, since the absorption coefficient at 2.7μ for an acetone-water mixture is several times greater than the absorption of water at the 3μ water band.

By comparison with the set of absorption curves in Fig. 3, small amounts of water in acetone can be determined in a quantitative manner. For example, the absorption curve for the sample of supposedly absolute acetone used for Fig. 2 shows a band which by comparison with the curves of Fig. 3 indicates the presence of approximately 0.3 percent water. Concentrations of water as low as 0.1 percent give rise to appreciable absorption bands in the 2.7μ region. As a test for the presence of water in acetone this method is more rapid and more accurate than the usual tests involving anhydrous copper sulphate.

MARCH, 1936 JOURNAL OF CHEMICAL PHYSICS VOLUME 4

The Infrared Absorption Spectra of Deuteroxide Solutions in Deuterium Oxide

E. K. PLYLER AND DUDLEY WILLIAMS, *Department of Physics, University of North Carolina*

(Received January 15, 1936)

The infrared aborption spectra of deuterium oxide and deuteroxide solutions in D_2O have been measured in the region from 2.5μ to 9μ. Also solutions of Na_2CO_3 and K_2CO_3 in D_2O have been studied in the same region. The spectra of deuterium oxide possess strong bands at 4.0μ and 8.2μ and the results agree with those of other workers. The absorption at 4.0μ is probably composed of several overlapping bands. Intense bands were observed in the NaOD solutions at 3.1μ, 4.95μ and 7.1μ. The hydrolyzing salts in D_2O gave rise to bands in these regions, but with some shifts in wave-length. The changes in the spectra were probably caused by the absorption of the CO_3 ion and D_2CO_3 which was formed in the solution. The relation of the absorption of NaOD in D_2O to the absorption of NaOH in H_2O is discussed. It is concluded that the OD ion has an absorption band at 3.1μ and that the bands at 4.95μ and 7.1μ are produced by hydration.

THE infrared absorption spectra of several hydroxides in aqueous solutions have already been measured.[1] Absorption bands were found at 3.65μ and 5.2μ. Grantham[2] had previously found a band at 2.3μ which was characteristic of all hydroxide solutions. He concluded that this band was due to the absorption of the OH ion. By studying the intensity of the 2.3μ band in solutions of hydrolyzing salts it has been shown[1] that this band is due to the OH ion. The bands produced by alcoholic solutions of hydroxides have also been measured.[3] There is little difference in the absorption spectra of the hydroxides in solutions of water or alcohol except for the shift of the band at 3.65μ in aqueous solutions to 3.8μ for the alcoholic solutions.

The present work was undertaken to find the change in these bands due to the substitution of deuterium for hydrogen in the aqueous solutions. On account of the increase in mass there should be an appreciable shift to the longer wavelengths of the vibrational frequencies which were observed for the ordinary aqueous solutions. Deuterium oxide, marked 99.5 percent, was obtained from the California Isotope Company, Berkeley, California, and also a solution of NaOD in deuterium oxide. A large type Hilger infrared spectrometer with a fluorite prism was used in the region from 2.5μ to 6.9μ and a rocksalt prism from 6μ to 9μ. In order to observe the band in the 7μ region with a single prism the observations with the rocksalt prism were started at 6μ. The effective slit width at 4μ was

[1] E. K. Plyler and Walter Gordy, J. Chem. Phys. **2**, 470 (1934).
[2] G. E. Grantham, Phys. Rev. **18**, 339 (1921).
[3] E. K. Plyler and Dudley Williams, J. Chem. Phys. **2**, 566 (1934).

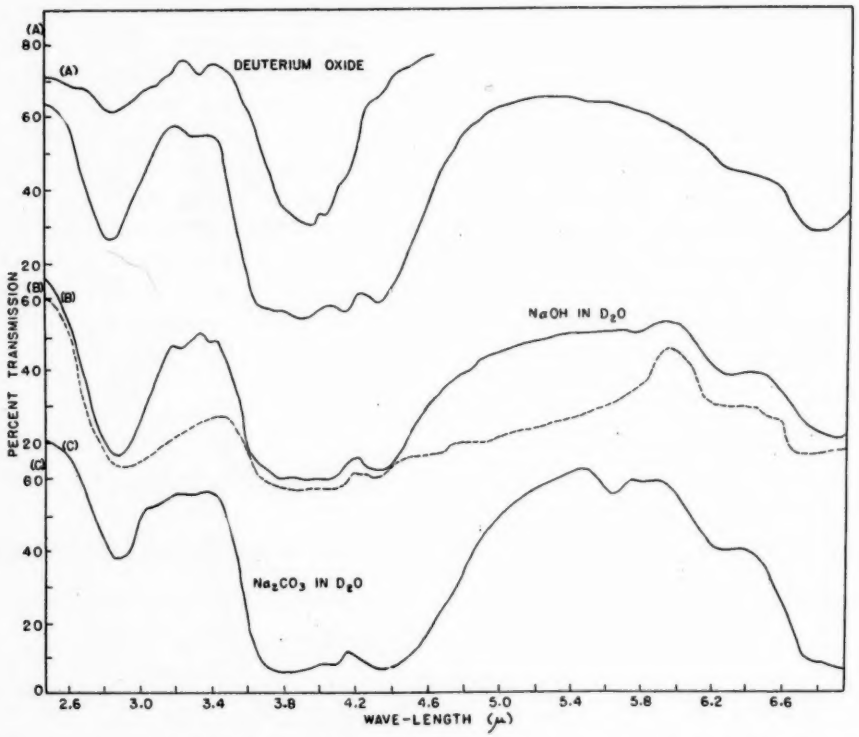

FIG. 1. The percent transmission of deuterium oxide and of certain concentrated solutions from 2.5μ to 6.9μ.

0.03μ and at 8μ was 0.04μ. Narrow slits were possible on account of the use of a thermorelay for increasing the deflections. Fluorite windows were used on the cells and they did not absorb very much below 9μ because they were about 2 mm thick. The absorption cell was made by placing mica washers 0.03 mm in thickness between the fluorite plates.

The infrared absorption spectra of deuterium oxide were first measured in order to have a comparison spectra to be used with the hydroxide solutions. The results obtained are represented in Fig. 1 and Fig. 2. Deuterium oxide has already been studied by Ellis and Sorge[4] and also by Casselman.[5] The absorption spectra found in the present work agree well with those previously found. In fact the intensity and position of the stronger bands are markedly similar to those found by Ellis and Sorge. Intense bands were observed at 2.85μ, 4.00μ, 6.80μ and 8.20μ. The broad band in the region of 4.0μ appeared to have four maxima. A thin cell was made by placing a drop of deuterium oxide between fluorite windows and pressing them together. The first curve in Fig. 1 shows the transmission through the thin cell. From the intensity of the bands it is estimated that

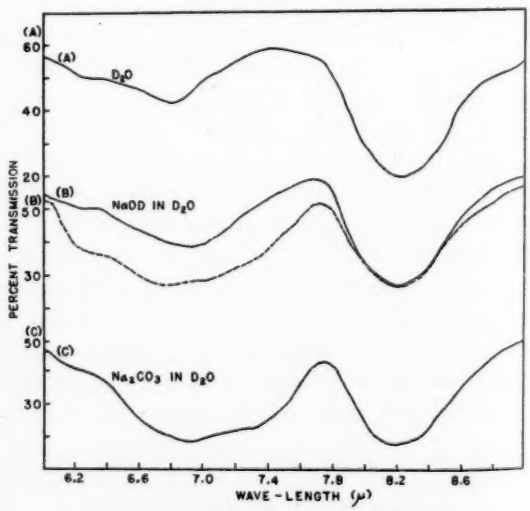

FIG. 2. The percent transmission of heavy water and solutions from 6.0μ to 9.0μ. Cell thickness: 0.03 mm.

[4] J. W. Ellis and B. W. Sorge, J. Chem. Phys. **2**, 559 (1934).
[5] A. L. Casselman, Phys. Rev. **45**, 221 (1934).

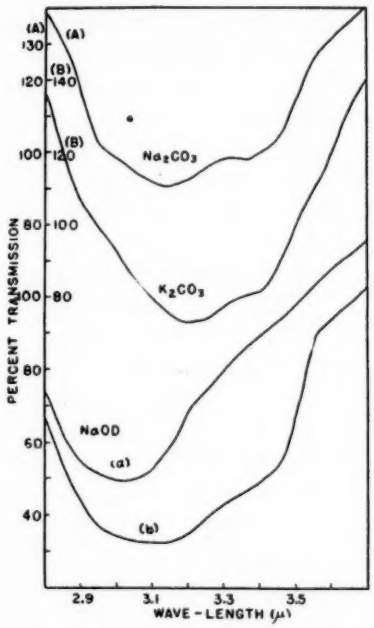

FIG. 3. Ratio of the transmission of certain solutions to that of the solvent. Region: 2.8μ to 3.8μ. (a) 0.18 g of NaOD dissolved in 0.66 g D_2O; (b) 0.18 g of NaOD dissolved in 1.00 g D_2O. The K_2CO_3 and Na_2CO_3 solutions were saturated at 26°C.

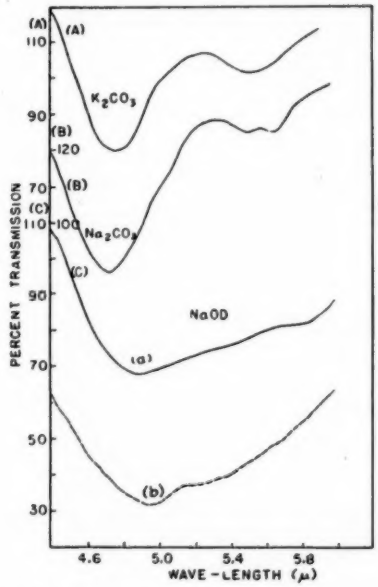

FIG. 4. Ratio of the transmission of solutions in D_2O to that of D_2O. Region: 4.4μ to 6.2μ. Concentrations of (a) and (b) are the same as in Fig. 3.

the cell thickness is 0.01 mm. Weak bands appear at 2.65μ and 3.35μ, but it was impossible to separate the bands in the region of 4.0μ. In ordinary water two fundamental bands occur at 2.78μ and 2.92μ. If the absorption at 4.0μ in D_2O represents the two similar fundamental bands, they may overlap so that it is impossible to resolve them. Also the first harmonic of the 8.20μ band falls in the 4.0μ region. This may in part account for the difficulty in separating the band into its components. Because of the presence of small amounts of H_2O and HOD many small bands will be present. For example, the absorption band at 2.85μ may in part be due to H_2O and the combination of the 4.0μ and 8.20μ bands. Also, the region of 6.8μ appears to have several bands overlapping.

The solutions of NaOD in D_2O were studied with the same cell thickness as used for D_2O. The two concentrations were plotted to the same scale and show the regions of increase in absorption due to the presence of NaOD in solution. This absorption is readily observed without the necessity of plotting the ratio of the transmission of the solution to that of water. The greater absorption is in the regions of 3.1μ, 4.9μ and 7.1μ. Solutions (saturated at 26°C) of Na_2CO_3 and K_2CO_3 in D_2O were also studied. Sodium and potassium carbonates were chosen for study because on hydrolysis these salts produce OD ions and because they are easily freed from H_2O. However, these compounds produce bands arising from the CO_3 group and these bands add to the complexity of the spectra of the solution. For example the strong absorption observed in the region of 7μ is due in part to the CO_3 group. All compounds containing CO_3 have an intense band in this region, which has only been observed by reflection.

In Fig. 3 the absorption in the region of 3.1μ is shown. The percent transmission of these curves was obtained by taking the ratio of the transmission of the solutions to that of D_2O. The transmission of the more concentrated NaOD is about 30 percent at 3.1μ. Since the cells were of the same thickness (0.03 mm) for solutions and D_2O, the water content of the solution cells is less than in D_2O cell. This causes the percent transmission of the solutions, when the ratio to D_2O is taken, to be greater than the actual value for cells containing equal numbers of D_2O molecules. The effect due to

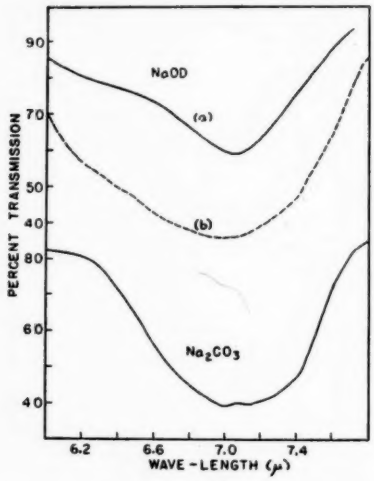

FIG. 5. Transmission of certain solutions compared with D_2O. Region: 6.0μ to 7.8μ. Concentrations of (a) and (b) are the same as in Fig. 3.

effective cell thickness is greatest in the regions of most intense D_2O absorption and in some of the curves the transmission ratio is greater than 100 percent. On account of the narrow band in D_2O at 2.85μ, the absorption band in the solutions of NaOD at 3.1μ vary in position. In the more concentrated solution of NaOD another band is present at 3.45μ. This band may be the first harmonic of the absorption in the region of 7μ. The curve *a* has a weak absorption band in this region. Curves *a* and *b* are plotted to the same scale and show the increase in absorption in this region as the amount of NaOD in the solution is increased.

The absorption bands of Na_2CO_3 and K_2CO_3 are more complex in this region. The maximum absorption occurs at about 3.2μ. The absorption band at 3.4μ is in part due to the CO_3 group, which has an intense band in this region. The D_2CO_3 formed by hydrolyzing salts may produce bands in this part of the spectrum. However, the absorption in this region is probably in part due to deuteroxide.

In Fig. 4 the absorption for the 4.9μ region is plotted. No appreciable absorption bands were observed between 3.1μ and 4.9μ. The intensity of the bands in the 4.9μ region is about the same as observed at 3.1μ. The bands observed in K_2CO_3 and Na_2CO_3 solutions are much sharper than in the NaOD solutions and appear at a shorter wave-length. The positions are 4.75μ and 4.95μ, respectively. Further differences are shown in the appearance of bands at 5.5μ for the salt solutions. These bands may have their origin in D_2CO_3 or the CO_3 ion.

In Fig. 5 is represented the absorption in the region of 7μ. The Na_2CO_3 and K_2CO_3 absorption is here equal to that of the stronger solution of NaOD. This increase in intensity of absorption of the salt solutions is due to the intense absorption of the CO_3 ion in this region. The K_2CO_3 and Na_2CO_3 salt solutions have similar absorption at these wave-lengths and only Na_2CO_3 has been plotted in Fig. 5.

There is a similarity in the absorption spectra of the solutions of hydroxides in ordinary water and that of solutions of deuteroxide in D_2O. Three intense bands were found at 3.1μ, 4.95μ and 7.1μ for compounds containing deuterium. The distribution of these bands in the spectra is similar to that of ordinary hydroxides, which have bands at 2.3μ, 3.65μ and 5.2μ. Also the ratio of the frequencies of the bands in the hydroxide solutions to those appearing in the spectra of deuteroxide solutions is approximately equal to the change calculated by replacing H with D in the OH ion oscillator. The absorption band which is found at 4.95μ for the NaOD solutions occurs at 4.75μ in the hydrolyzing salts. This change in position may be produced by decrease in absorption of D_2O in this region. However, the same effect is found in the hydroxide solutions, the corresponding band being shifted from 3.65μ in hydroxides to 3.45μ in the hydrolyzing salt solutions. From the present study it is impossible to determine the origin of the bands. However, on account of the similarity to the absorption of hydroxide solutions it is concluded that the absorption band at 3.1μ for NaOD is produced by the OD ion. This corresponds to OH band at 2.3μ. The two bands at 4.95μ and 7.1μ are probably due to hydration and correspond to the bands at 3.65μ and 5.2μ in hydroxide solutions.

The Raman Spectrum of Tetraethyl Silane. Vibrational Resonance of Tetraalkyls*

THOMAS F. ANDERSON, *Gates Chemical Laboratory, California Institute of Technology, Pasadena*

(Received December 21, 1935)

The Raman spectrum of tetraethyl silane is reported. Assignments of frequencies for this compound and for other tetraalkyls are made. An analysis of resonance between vibrations $\nu_1+\nu_2$ and ν_3 explains the presence of extra lines which appear in the Raman spectra of each of these compounds. Resonance between frequencies $2\nu_2$ and ν_4 explains the presence of two additional lines observed in $Si(C_2H_5)_4$. Resonance between ethyl vibrations in $Si(C_2H_5)_4$ and in $Pb(C_2H_5)_4$ accounts for a split in the frequencies characteristic of the ethyl group. First-order perturbation calculations of the observed resonance effects are given in some detail.

INTRODUCTION

THE Raman spectra of a number of tetraalkyl compounds of fourth group elements have been observed; namely, tetramethylmethane,[1,2] tetramethyl silane,[2] tetramethyl tin,[3] tetramethyl lead[4] and tetraethyl lead.[3,4] All exhibit an extra line in the vibration spectrum which has been ascribed to vibrational resonance within the molecule.[2] Previous authors have discussed such resonance in the case of carbon dioxide[5] and the methyl group.[6]

In this paper are presented the results of an investigation of the Raman spectrum of tetraethyl silane together with a somewhat detailed discussion of resonance between vibrational levels in the tetraalkyl molecules whose Raman spectra have been reported.

EXPERIMENTAL

The silicon tetraethyl used was prepared by Professor W. C. Johnson of the University of Chicago. After careful fractional distillation, a 10-ml portion had the following properties: b_{746} 153.3–153.8°C; d_4^{25} 0.7635; n_D^{25} 1.4249. The Raman spectrum of this portion was obtained by using light from a water-cooled mercury arc filtered through a solution containing quinine sulfate and rhodamine *B* which absorbed all but the 4300A lines of mercury.

RESULTS AND GENERAL DISCUSSION

All the lines observed for $Si(C_2H_5)_4$ were broad. The results of the measurements together with the data available for other tetraalkyls are given in Table I. The data are also presented graphically in Fig. 1 where the assignments are indicated.

TABLE I. *Raman spectra of tetraalkyls.*

$C(CH_3)_4$ (cm^{-1})	$Si(CH_3)_4$ (cm^{-1})	$Si(C_2H_5)_4$ (cm^{-1})	$Sn(CH_3)_4$ (cm^{-1})	$Pb(CH_3)_4$ (cm^{-1})	$Pb(C_2H_5)_4$ (cm^{-1})
	202(20)	160(4)	152(7)	130(8)	96(4)
	239(15)	249(3)	262(4)		165(2)
332(10)	598(20)	303(6)			239(1)
415(3)	696(15)	393(2)			444(4)
731(20)	863(10)	553(10)	506(8)	460(10)	
790(2)		625(3)	526(5)	473(5)	463(3)
921(2)		736(3)		577(0)	535(1)
		865(1)		767(1)	
		978(5)	952(0)	930(0)	941(1)
		1021(5)	1046(0)	1155(5)	1013(2)
1250(20)	1264(10)	1200(7)	1200(5)	1170(4)	1165(3)
1453(15)	1427(15)	1423(7)	1262(0)		1460(1)
2711(5)		1467(8)			
2745(2)		2734(1)		2292(1)	1781(1)
2790(3)		2813(3)		2918(7)	2869(1)
2864(7)		2885(10)		2999(6)	2927(5)
2892(3)		2912(6)	2915(3)	3679(1)	
2911(10)		2950(5)	2979(2)	3755(1)	
2937(3)					
2954(7)					

Numbers in parentheses indicate relative intensities.

With Bennet and Meyer's notation,[6,7] lines characteristic of the methyl group, *C*, *D*, *E*, and *F* are easily recognized from the values of the frequencies. In the case of tetramethylmethane other lines in the neighborhood of *E* and *F* are doubtless due to interactions of hydrogens on methyl groups. A double line $\nu \approx 950$, 1020 cm^{-1} is observed only in tetraethyl silane and tetraethyl lead. It is therefore ascribed to the vibrations characteristic of the ethyl group. These lines will be discussed in more detail later.

If the alkyl groups are considered to be units

* Contribution No. 524.

[1] Kohlrausch and Barnes, Annales Fisica y Quimica **30**, 733 (1932); Kohlrausch and Köppl, Zeits. f. physik. Chemie **B26**, 209 (1934).

[2] D. H. Rank and E. R. Bordner, J. Chem. Phys. **3**, 248 (1935).

[3] N. G. Pai, Proc. Roy. Soc. **A149**, 29 (1935).

[4] A. B. F. Duncan and J. W. Murray, J. Chem. Phys. **2**, 636 (1934).

[5] E. Fermi, Zeits. f. Physik **71**, 250 (1931); Adel and Dennison, Phys. Rev. **43**, 716 (1933); **44**, 99 (1933).

[6] Adel and Barker, J. Chem. Phys. **2**, 627 (1934).

[7] Bennet and Meyer, Phys. Rev. **32**, 888 (1928).

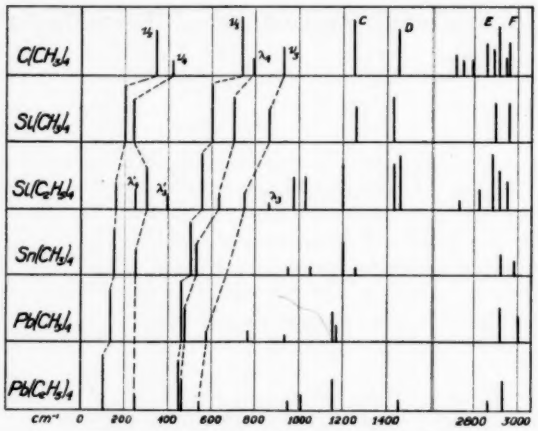

FIG. 1. Raman spectra of tetraalkyls.

at tetrahedral corners about the central atom, all lower frequencies can be ascribed to tetrahedral vibrations. In a number of cases[4] depolarization measurements have indicated that the most intense frequency in the spectra is due to ν_1, the symmetrical stretching vibration. The lowest frequency in each case is assigned to ν_2, the doubly degenerate bending vibration. The assignments of ν_3 and ν_4, the triply degenerate vibrations are indicated in Fig. 1. The presence of the remaining lines in the spectra can then be ascribed to resonance between vibrational levels having approximately equal energies.

On the basis of these assignments the infrared absorption bands observed[8] for $Sn(CH_3)_4$ and $Pb(CH_3)_4$ can be assigned to the combinations of frequencies indicated in Table II. ν_4 is not observed in the Raman spectrum of $Pb(CH_3)_4$; its value was obtained from the frequency at 777 cm^{-1}, $\nu_3+\nu_4$. As might be expected both ν_3 and ν_4 occur frequently in the combinations. It is interesting to note that $3D$ predicted by Adel and Barker to be a split frequency appears as a single frequency.

TABLE II. *Infrared spectra of $Sn(CH_3)_4$ and $Pb(CH_3)_4$.*

$Sn(CH_3)_4$			$Pb(CH_3)_4$		
νobs (cm^{-1})	νcalc (cm^{-1})	COMBINATION	νobs (cm^{-1})	νcalc (cm^{-1})	COMBINATION
777(10)	768	$\nu_1+\nu_4$	777(9)	(777)	$(\nu_3+\nu_4)$
943(2)	922	$\nu_3+\nu_4$	935(3)	977	$\nu_3+2\nu_4$
1036(2)	1034	$2\nu_4+\nu_1$	1064(1)	1037	$\nu_1+\nu_3$
1262(R)	1276	$2\nu_1+\nu_4$	1170(6)	1163	C
1205(9)	1200	C	1300(3)	1284	$2\nu_3+\nu_2$
1369(4)	1352	$C+\nu_2(?)$	1470(6)	(1470)	D
1470(7)	1468	$2\nu_3+\nu_2$, D	1610(5)	1614	$2\nu_3+\nu_1$
1724(3)	1706	$C+\nu_1(?)$	1890(0)	1860	$3\nu_3+\nu_2$
2330(1)	2328	$2\nu_3+2\nu_1$	2174(0)	2190	$3\nu_3+\nu_1$
2464(1)	2480	$3\nu_3+\nu_1$	3030(9)	3024	G
3030(9)	3024	$G^{(4)}$	3704(0)	3490	$3C$
3700(1)	3600	$3C$	4348(0)	(4300)	$3D^{(4)}$
4350(1)	(4300)	$3D^{(4)}$			

[8] Kettering and Sleator, Physics **4**, 39 (1933).

VIBRATIONAL RESONANCE IN TETRAALKYLS

To treat the problem of resonance between vibrational levels in a molecule we may first set down the wave equation in normal coordinates and obtain the solutions as products of the normalized orthogonal Hermite functions of the normal coordinates. To obtain interactions between the normal vibrations third-order and higher terms in the normal coordinates consistent with the symmetry of the molecule must be included in the potential energy expression. These additional terms are then considered as a perturbation H^1 on the zeroth order solutions just obtained.

The perturbation energy will be appreciable, and additional lines in the Raman spectrum may be observed if a degeneracy of the type

$$V_1\nu_1+V_2\nu_2+\cdots=\nu_4\cdots \qquad (1)$$

can be considered to exist, and if the symmetry of the molecule permit such an interaction. If only third-order terms are included in the potential energy expression and none of the fundamental frequencies ν_1, ν_2, $\cdots$ ν_4 is degenerate, the first-order perturbation energies are zero and second-order perturbations must be considered. If, however, one or more of the vibrations ν_1, ν_2, $\cdots$, ν_4 is degenerate, first-order perturbation energies will not vanish. The perturbation method[9] consists in finding the correct zeroth order wave function for the perturbation H' as a linear combination of all the wave functions which correspond to the energy ν_4. In order that the equations determining the coefficients in this combination of eigenfunctions have a solution the new energies resulting from the interaction must satisfy a secular equation. One can then solve this equation for the energy levels of the perturbed system.

The presence of the lines indicated as λ_3 and λ_4 in Fig. 1 can be ascribed to resonance between the doubly degenerate level $\nu_1\{1\}+\nu_2\{2\}$ and

[9] Pauling and Wilson, *Introduction to Quantum Mechanics* (McGraw-Hill Book Co., 1935), p. 165.

TABLE III. *Resonance in tetraalkyls.*

COMPOUND	$\nu_1+\nu_2$ (cm^{-1})	ν_3 (cm^{-1})	$\nu_1+\nu_2-\nu_3$ (cm^{-1})	λ_4 (cm^{-1})	$\frac{1}{2}(\nu_1+\nu_2+\nu_3)-\lambda_4$($cm^{-1}$)	($\lambda_3$calc) (cm^{-1})	($\lambda_3$obs) (cm^{-1})	P (cm^{-1})	B ($cm^{-5/2}\times10^{-4}$)	C ($cm^{1/2}\times10^{4}$)
$C(CH_3)_4$	1063	921	142	790	202	1194	—	77	117	51
$Si(CH_3)_4$	800	863	−63	696	136	968	—	54	55	53
$Si(C_2H_5)_4$	713	736	−23	625	100	825	865	41	33	51
$Sn(CH_3)_4$	658	(658)	(0)	526	(132)	(790)	748	(54)	(39)	(75)
$Pb(CH_3)_4$	590	577	13	473	111	694	656	45	26.5	(77)
$Pb(C_2H_5)_4$	540	535	5	463	75	613	—	31	14.5	(64)

the triply degenerate frequency $\nu_3\{3\}$. Numbers in braces denote degeneracies of the respective fundamental frequencies. We may assume initially that $\nu_1+\nu_2=\nu_3$. The term in the potential energy which will give rise to interactions between these levels is[10]

$$H_1'=\beta_1 Q_1(Q_2+Q_2')(Q_3+Q_3'+Q_3'')$$

where Q_i is the normal coordinate having the frequency ν_i. Primes affixed to the Q_i's distinguish the normal coordinates having the same frequency from each other. Omitting zero-point energies, the secular equation turns out to be

$$\begin{vmatrix} \nu_1+\nu_2-\lambda & 0 & P_1 & P_1 & P_1 \\ 0 & \nu_1+\nu_2-\lambda & P_1 & P_1 & P_1 \\ P_1 & P_1 & \nu_3-\lambda & 0 & 0 \\ P_1 & P_1 & 0 & \nu_3-\lambda & 0 \\ P_1 & P_1 & 0 & 0 & \nu_3-\lambda \end{vmatrix}=0.$$

P_1 is the perturbation integral,

$$P_1=\beta_1 h^{\frac{1}{2}}/16\sqrt{2}\pi^3(\nu_1\nu_2\nu_3)^{\frac{1}{2}}=B_1/(\nu_1\nu_2\nu_3)^{\frac{1}{2}}.$$

The secular equation has the following solutions for the λ's the energy levels resulting from resonance:

$$\lambda_1\{1\}=\nu_1+\nu_2,$$
$$\lambda_2\{2\}=\nu_3,$$
$$\lambda_3\{1\}=\tfrac{1}{2}[\nu_1+\nu_2+\nu_3+\{(\nu_1+\nu_2-\nu_3)^2+24P_1^2\}^{\frac{1}{2}}],$$
$$\lambda_4\{1\}=\tfrac{1}{2}[\nu_1+\nu_2+\nu_3-\{(\nu_1+\nu_2-\nu_3)^2+24P_1^2\}^{\frac{1}{2}}].$$

$\lambda_1\{1\}$, a combination frequency, may be expected to be weak in the Raman effect, while $\lambda_2\{2\}$, $\lambda_3\{1\}$ and $\lambda_4\{1\}$ are permitted but not necessarily with equal intensities.

Assignments of frequencies and results of calculations are presented in Table III. Both λ_4 and ν_3 have been observed for all but $Sn(CH_3)_4$, in which case it appears that λ_4 is observed while ν_3 is not. ν_3 was obtained in this case by assuming that $\nu_1+\nu_2=\nu_3$. In each case λ_3, P_1 and B_1 were calculated from values of λ_4 and ν_3. λ_3 is observed in the Raman spectrum of $Si(C_2H_5)_4$ and in the infrared spectra of $Sn(CH_3)_4$ and $Pb(CH_3)_4$,[8] where it appears as a satellite of strong absorption lines. The agreement of observed and calculated values of λ_3 is satisfactory considering the approximations made in assuming Eq. (1).

The values of P_1 obtained are of the same order of magnitude as those for vibrational interactions in the carbon dioxide molecule and for the interactions of hydrogen vibrations in methyl groups. The magnitude of the effect is greater because of the degeneracy of the resonating levels. Inasmuch as the normal coordinates for tetrahedral molecules are not known it seems impossible at this time to relate the B's to actual displacements of the groups in the molecules.

In the last column of Table III are given values of

$$C_1=B_1/\nu_1\nu_2\nu_3=P_1/(\nu_1\nu_2\nu_3)^{\frac{1}{2}},$$

which, interestingly enough, turn out to be nearly constant, i.e., independent of the nature of the central atom and of the character of the alkyl group.

If the above analysis is correct, one must conclude that Raman lines resulting from resonance may be more intense than those from fundamental modes, as is the case in $Si(CH_3)_4$ and $Pb(C_2H_5)_4$. In an extreme case, such as apparently exists in $Sn(CH_3)_4$, the resonance line may appear strongly and the fundamental not at all. Without a somewhat detailed analysis of the possibility of resonance between normal

[10] Tetrahedral symmetry does not permit H_1'. However the tetraalkyl molecules have tetrahedral symmetry only for very special orientations of the alkyl groups. For general orientations, the term H_1' is then allowed. If the assignments of frequencies, ν_2 and ν_4, were interchanged, tetrahedral symmetry would permit such a term as H_1'. However if this were done certain of the infrared combinations would not be allowed and there would be absolutely no agreement with valence force criteria (Rosenthal, Phys. Rev. **45**, 538 (1934); **46**, 730 (1934).

modes, extreme caution must be taken in applying the results of normal coordinate treatments to observed frequencies.

Apparently another case of resonance exists in $Si(C_2H_5)_4$, namely, that brought about by the fact that $2\nu_2(2) \approx \nu_4(3)$. The term in the potential energy expression which gives rise to resonance between these levels is:

$$H_2' = \beta_2(Q_2^2 + Q_2Q_2' + Q_2'^2)(Q_3 + Q_3' + Q_3'').$$

The secular equation in this case has the same form as in the previous case, with $2\nu_2$, ν_4, and P_2 replacing $(\nu_1+\nu_2)$, ν_3, and P_1, respectively. In this case

$$P_2 = \frac{\beta_2 h^{\frac{1}{2}}}{16\sqrt{2}\pi^3\nu_2(\nu_4)^{\frac{1}{2}}} = \frac{B_2}{\nu_2(\nu_4)^{\frac{1}{2}}}$$

and the levels permitted by the secular equation are

$$\lambda_1'\{3\} = 2\nu_2,$$
$$\lambda_2'\{2\} = \nu_4,$$
$$\lambda_3'\{1\} = \tfrac{1}{2}[2\nu_2+\nu_4+\{(2\nu_2-\nu_4)^2+24P^2\}^{\frac{1}{2}}],$$
$$\lambda_4'\{1\} = \tfrac{1}{2}[2\nu_2+\nu_4-\{(2\nu_2-\nu_4)^2+24P^2\}^{\frac{1}{2}}].$$

Taking $2\nu_2 = 320$, $\nu_4 = 303$, and $\lambda_4' = 249$ cm^{-1}, one obtains 63 cm^{-1} for $\frac{1}{2}(2\nu_2+\nu_4)-\lambda_4$, 12.4 cm^{-1} for P_2, 3.4×10^4 cm$^{-5/2}$ for B_2 and 44×10^{-4} cm$^{\frac{1}{2}}$ for C_2. The value for C_2 is very nearly equal to that for C_1. The calculated value, 375 cm^{-1} for λ_3' is in good agreement with the observed value, 393 cm^{-1}.

The double lines observed at 980 cm^{-1} in $Si(C_2H_5)_4$ and $Pb(C_2H_5)_4$ may be ascribed to C–C vibrations in the ethyl groups. Its frequency is equal to the C–C frequencies in ethane (990 cm^{-1}), ethyl chloride (966), bromide (960), iodide (950), which have been discussed in some detail by Cross and Van Vleck.[11] If there were no interactions between ethyl groups there would be a single fourfold degenerate level ω_0 with this frequency. The splitting of the level may be due to interactions between the ethyl groups represented by a term in the potential energy expression

$$H'_{C_2H_5} = \beta_{C_2H_5}(q_1q_2+q_1q_3+q_1q_4+q_2q_3+q_2q_4+q_3q_4),$$

where q_i is the normal coordinate for the C–C vibration for the ith ethyl group. The secular equation for this interaction is

$$\begin{vmatrix} \omega_0-\lambda & P & P & P \\ P & \omega_0-\lambda & P & P \\ P & P & \omega_0-\lambda & P \\ P & P & P & \omega_0-\lambda \end{vmatrix} = 0,$$

where $P = \beta_{C_2H_5}h/8\pi^2\omega_0 = B_{C_2H_5}/\omega_0$. The solutions of the secular equation are

$$\lambda_1''\{3\} = \omega_0 - P,$$
$$\lambda_2''\{1\} = \omega_0 + 3P.$$

In Table IV are given values of λ_1'', λ_2'', ω_0 and P for the two compounds for which data are available. Here again it is difficult to relate the P's directly to physical quantities since the q's are not known; moreover, $H'_{C_2H_5}$ is difficult to interpret since the ethyl groups may rotate and consequently may be oriented in many ways with respect to one another. One might have predicted, however, that the interaction, P, would be greater in $Pb(C_2H_5)_4$ than in $Si(C_2H_5)_4$. Because both have a smaller electronegativity than carbon, the central atom will in each case have a slight positive charge; Pb would have a greater positive charge than Si since it has a smaller electronegativity than Si. As a result, the methylene groups in $Pb(C_2H_5)_4$ have greater negative charges than those in $Si(C_2H_5)_4$. Consequently the interaction between methylene groups might well be greater in $Pb(C_2H_5)_4$. Apparently this effect overcomes the opposing effect of the distance between methylene groups, which distance is greater in $Pb(C_2H_5)_4$. A study of tetraethyl methane, in which electronegativities play no part, would greatly clarify the situation.

TABLE IV. *Vibrational resonance between ethyl groups.*

COMPOUND	λ_1'' (cm^{-1})	λ_2'' (cm^{-1})	ω_0 (cm^{-1})	P (cm^{-1})	$B_{C_2H_5}\times10^{-4}$ (cm^{-2})
$Si(C_2H_5)_4$	978	1021	989	11	11
$Pb(C_2H_5)_4$	941	1013	959	18	17.3

In conclusion I should like to express my appreciation to Professor Don M. Yost for helpful advice and criticism, and to Dr. G. W. Wheland for his kindness in working out the combination selection rules for tetrahedral molecules from group theory considerations.

[11] Cross and Van Vleck, J. Chem. Phys. **1**, 350 (1933).

The Rate of Reaction of Deuterium with Hydrogen Chloride

PH. GROSS AND H. STEINER, *First Chemistry Laboratory, University of Vienna*

(Received December 4, 1935)

The reaction $D_2+HCl=HD+DCl$ has been investigated at temperatures from 765°K to 843°K. The reaction is almost entirely homogeneous, and, up to temperatures of the order of 830°K, bimolecular. The fraction which proceeds heterogeneously is determined in a vessel packed with tubes. The constant of the homogeneous bimolecular reaction can be represented by the following equation:

$$K_c=6.27\times10^{13}\times T^{\frac{1}{2}}\times e^{-26.200/T} \text{ mole}^{-1} \text{ cm}^3 \text{ sec.}^{-1}.$$

At the maximum measured temperature of 843°K deviations were noticed which may have been due to atomic reaction.

I. INTRODUCTION

THIS investigation into the reaction of heavy hydrogen with light hydrogen halides was undertaken to gain acquaintance with the mechanism of exchange reactions of this nature. After it had been found that the process proceeds substantially homogeneously and bimolecularly, the investigation gained in interest, since the reaction turned out to be a typical example of the few reactions of the type $A_2+BC=AB+AC$ which proceed without complications.

II. EXPERIMENTAL

(1) Materials used

(a) Deuterium was obtained for the greater part by electrolysis of a 0.3 N solution of heavy sodium hydroxide. The electrolysis vessel consisted of a U-tube into which platinum electrodes were sealed. The escaping deuterium diffused through a heated palladium tube closed towards the U-tube, and was collected in a flask. To equalize the pressure on both sides of the U-tube the oxygen evolved was drawn off by means of a water-jet pump controlled by a valve with precision regulation. By prolonged electrolysis it proved possible to produce gas containing 100 percent D_2. This gas however was only used for calibration purposes, while for the experiments there was used a gas with an HD content varying from five to ten percent. A small quantity of D_2 was prepared from heavy water containing D_2O to the extent of 99.2 percent by decomposition with the aid of metallic sodium.

(b) Light hydrogen, which was used for calibration purposes, was taken from a cylinder. It diffused from a hydrogen flame through a palladium tube into the apparatus.

(c) Hydrogen chloride was produced from sodium chloride and sulphuric acid (both Merck p.a.) in an apparatus consisting throughout of glass. After passing through a wash-bottle and a vessel cooled to −70°C, the hydrogen chloride was frozen out with the aid of liquid air. After sealing and evacuation, the hydrogen chloride was distilled twice and finally after repeated evacuation conducted into a receiving flask. It was found that dry hydrogen chloride does not appreciably attack mercury and stopcock grease, so that it was possible to work without any particular precautionary measures.

(2) The determination of the deuterium content

The deuterium content of the gas was deduced from its heat conductivity which was determined by Schleiermacher's method[1] of the electrically heated wire. With the aid of the cell, which has been described previously,[2] it was possible with 0.2 cm³ gas at atmospheric pressure to ascertain the total deuterium concentration to within 0.5 percent and consequently that of HD to within one percent. The resistance of the cell amounted to approximately 85 ohms, and the excess temperature of the wire over that of the wall amounted to approximately 20°C. The voltage applied was measured while the resistance was kept constant, and likewise the temperature of the wall. The wall temperature was kept constant

[1] Schleiermacher, Wied. Ann. **34**, 623 (1888).
[2] Ph. Gross and H. Steiner, Zeits. f. Mikrochemie **17**, 43 (1935).

TABLE I.

p(mm Hg)	$E_{D_2}^2$(99.2)%	$E_{H_2}^2$	$E_{H_2}^2/(E_{D_2}^2 \times 0.975)$	Corrected for 100% D_2
200	2353	3188	1.390	1.391
300	2417	3311	1.405	1.407
400	2464	3386	1.411	1.412
500	2484	3423	1.414	1.414
600	2499	3452	1.417	1.417

by immersing the cell in ice water agitated by a current of air. Since only relative values of the heat conductivity were needed, we used the square of the scale divisions (E^2) read off at the potentiometer for our computations, since this square is proportional to the heat conductivity. Fluctuations in the voltage of the accumulator used for compensation were of course allowed for.

Since the heat conductivity thus measured showed some dependence on pressure it was determined at different pressures. Table I shows that from 400 mm Hg upwards the relation given by the kinetic theory of gases,

$$E_{H_2}^2/(E_{D_2}^2 \times 0.975) = \sqrt{2},$$

is fulfilled to a great extent at 400 mm Hg and higher pressures, the factor 0.975 being given by the ratio of the specific heats of H_2 and D_2 at 0°C.[3] In order to save hydrogen the measurements were made at a pressure of 200 mm Hg, slight deviations from this pressure being allowed for empirically. The values for (E^2) were corrected for each gas separately from a pressure of 500 mm Hg to a pressure of 200 mm Hg. The value for HD was computed at a pressure of 500 mm Hg from the relation

$$E_{HD}^2/E_{D_2}^2 = 2/\sqrt{3}$$

and was corrected to a pressure of 200 mm Hg by multiplication by the geometric mean of the factors of correction for D_2 and H_2. Since the experiments were confined to the start of the reaction, it was assumed that the gas consisted solely of D_2 and HD, and the HD concentration was accordingly determined by linear interpolation between the values for D_2 and HD.

Before each run the value of ($E_{H_2}^2$) for light hydrogen, which served as a reference value was determined. Table II shows that in general the fluctuations in the reference value are not very great, greater displacements being however observable at times.

TABLE II.

DATE OF RUN	E^2H_2
Oct. 1	3196
	3198
Oct. 2	3192
Oct. 3	3184
Oct. 4	3185
Oct. 5	3179
Oct. 7	3179

(3) Apparatus

As reaction vessels (Fig. 1, *A*) cylindrical tubes of quartz of approximately 200 cm³ capacity in which there were sealed on the one side a quartz capillary tube for charging, and on the other side a quartz tube *B* for the introduction of the thermocouple were used. Two empty vessels and one packed with quartz tubes were used to determine the fraction of the reaction which proceeded heterogeneously. The ratio between the superficial area of the empty vessels to that of the packed vessel was as 1 : 10.

The reaction furnace consisted of a shell *C* made from "Eternit," into which a firebrick pipe *D* was cemented. In this latter there was disposed an iron tube *E* on which the heating wire was wound with the interposition of an insulating layer of asbestos. The reaction vessel held in position by means of perforated brass disks *F* was suspended inside the iron tube. With the exception of the inner space, the furnace was packed with silicate wool. As a result of this precaution the temperature in the inner space did not vary more than 0.1°C from any one part to another. During the run the temperature could be kept constant within 0.5°C by hand control of the current supply.

A silver-platinum thermocouple the voltage of which was measured in a potentiometer using a galvanometer as a null-point-instrument was used for measuring the temperature. The arrangement used allowed of reading accurately to within 0.1°. The thermocouple was calibrated at the boiling point of benzophenone and melting points of zinc and antimony, and was checked against a platinum-platinum rhodium thermo-

[3] See A. Farkas, *Ortho-, Para- and Heavy Hydrogen*, (Cambridge, University Press, 1935).

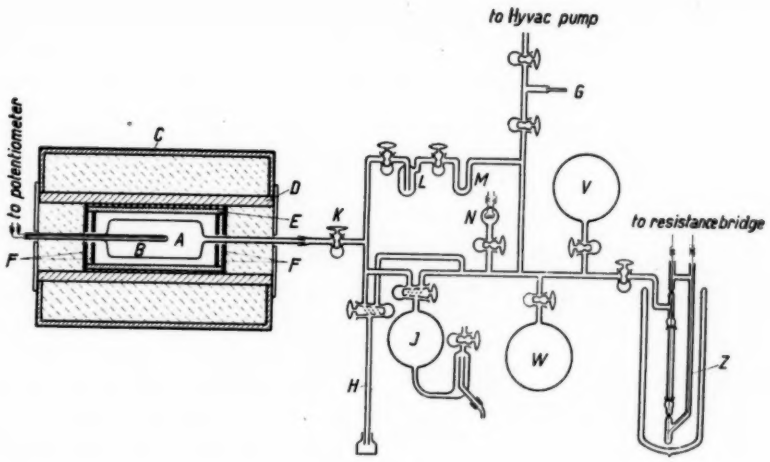

FIG. 1.

couple calibrated by the Physikalisch-Technische Reichsanstalt at Berlin. The maximum deviation was found to be 1°C.

(4) Procedure

The runs were conducted as follows: After evacuation of the apparatus to 10^{-4} mm Hg, the heat conductivity determining cell Z was filled with light hydrogen from the palladium tube G, for the purpose of determining the reference value of $E_{H_2}{}^2$.

A manometer H which could be selectively connected to the reaction vessel or to the measuring apparatus was used for the adjustment of the temperature. After repeated evacuation, deuterium of known concentration was forced into the reaction vessel from the storage flask V with the aid of the Töpler pump I and the pressure read off at the manometer. After repeated evacuation, hydrogen chloride was likewise forced into the reaction vessel from the storage flask W, the time at which the reaction started being simultaneously noted. After reading off the additional pressure, the stopcock K was closed, and the remainder of the apparatus once more evacuated. After conclusion of the run, in order to freeze out the hydrogen chloride, the gas was drawn through the trap L and U-tube M, (both of which were cooled with liquid air) into the Töpler pump and thence forced into the cell. At high concentrations of hydrogen chloride, even with repeated pumping through the freezing traps, traces of hydrogen chloride were left behind, the percentage of which was very small but which prevented the measurement of heat conductivity. In this case the gas was introduced into the adjoining sealed-on incandescent lamp N the filament of which was heated to white heat. After this treatment the last traces of hydrogen chloride appeared to have been eliminated. It should, however, be noted that at the incandescent filament the equilibrium of the reaction $H_2+D_2=2HD$ becomes established, thus causing an alteration of the heat conductivity of the original gas consisting exclusively of HD and D_2. However these alterations are insignificant at a total-D-content of 85–90 percent and come within the limits of error of the heat conductivity determination.

III. Evaluation of Results

In Table III complete minutes of two of the runs are given. The constant given in column 13 is calculated from the following equation of differences:

$$\Delta p_{D_2}/\Delta t = K_p \times p_{D_2 m} \times p_{HCl m}.$$

Since merely the start of the reaction was measured the accuracy of the equation using differences is adequate, as can be demonstrated by series expansion. In Table IV an account of all the runs is given. In this table the first column specifies the vessel used (e=empty, t=tubes), the second, the mean temperature in degrees

TABLE III.

No. of Run	T(°K)	t	$E^2_{D_2}(100\%)$	E^2	% D_2	$p(D_2+HD)$	pD_2	ΔpD_2	pD_2m	pHCl	pHClm	$K_p\times10^{-6}$
11	826	0	2364	2404	88.0	162	142.5	18.8	133	142	133	3.47
		30.6		2444	76.3		123.7					
27	826	0	2351	2375	92.5	149	138.0	21.7	127	153	142	3.54
		34.0		2425	78.0		116.3					

Explanation of Table III. In the first column there is given the number of the run, in the second the temperature in degrees K, in the third the duration of the run or the time at which reading was made, in the fourth the value of E^2 for 100% D_2, in the fifth the value of E^2 at the commencement and at the end of the run, in the sixth the resulting percentage of D_2 in the gas, in the seventh the total pressure of D_2+HD, in the eighth the partial pressure of D_2 at the commencement and at the end of the run, in the ninth the decrease in pressure of D_2, in the tenth the mean partial pressure of D_2 (pD_2m), in the eleventh the total pressure of HCl+DCl, in the twelfth the mean partial pressure of HCl (pHClm) and in the thirteenth the constant K_p.

Kelvin, the third the mean partial pressure of D_2, the fourth the mean partial pressure of HCl, and the fifth the constant K_p.

IV. Results

It was found that the reaction is bimolecular and for the greater part homogeneous over a range of D_2 and HCl partial pressures from 80 mm Hg to 300 mm Hg. As is shown by the increase of the constants, the conditions appear to change at pressures below 50 mm Hg, but this fact was not followed up for the time being. Measurements made in the packed vessel showed that the reaction proceeded to a slight extent on the wall and that at the most to the extent of 15 percent at the lowest temperature.

In the further evaluation of the results the heterogeneous reaction was included in the calculation, which could all the more easily be done since its order was the same as that of the homogeneous reaction. The constant of the reaction in the empty vessel was subtracted from that in the packed vessel. Seeing that the ratio between the superficial areas was 1 : 10; dividing this difference by ten gave the constant of the heterogeneous reaction in the empty vessel. From the measurements in the packed vessel for two temperatures the values for the remaining temperatures were calculated from the resulting activation energy of the heterogeneous reaction amounting to 44 kcal. In Table V there are given, in the first column the temperatures of the runs in degrees Kelvin, in the second the mean values of K_p with the omission of the values below a pressure of 50 mm Hg, in the third the values of K_p after allowance is made for the heterogeneous reaction, and in the fourth the values for K_c in mole^{-1} cm^3 sec.$^{-1}$.

When the values of log K_c are plotted against $1/T$ (Fig. 2), it is found, that they lie in a straight line, the lowest value deviating somewhat, corresponding to the higher limit of error caused by the long duration of the run and the small amount reacted. On the other hand the value for the highest temperature lies considerably too high, beyond the limit of error. This deviation is believed to be due to atomic reactions occuring when measuring at the highest temperature. The deviations at low pressures may be due to

TABLE IV.

Reaction Vessel	T(°K)	pD_2	pHCl	$K_p\times10^{-6}$
e	843	62.4	72.1	11.4
e	843	39.3	62.0	13.2
e	843	137	146	11.1
e	826	269	312	3.75
e	826	134	133	3.47
e	826	129	142	3.55
e	826	126	138	3.77
e	826	58.2	142	3.74
e	826	39.7	134	4.88
e	826	37.2	148	5.19
e	806	266	319	1.78
e	806	134	176	1.69
e	784	285	291	0.725
e	784	144	156	0.802
e	784	139	157	0.689
e	765	283	306	0.236
e	765	267	311	0.332
t	826	112	215	6.27
t	826	119	140	5.51
t	826	120	123	6.78
t	826	46	124	6.44
t	784	124	248	1.38
t	784	36	243	1.29

TABLE V.

T(°K)	$K_p\times10^{-6}$	$K_{p\text{corr.}}\times10^{-6}$	K_c	K_c theor. I.	K_c theor. II.
765	2.84	2.49	1.99	2.18	2.25
784	7.17	6.48	5.28	5.02	5.08
806	17.4	16.0	13.4	13.2	12.9
826	36.5	33.8	29.0	28.6	27.4
843	112	107	93.8	54.8	51.4

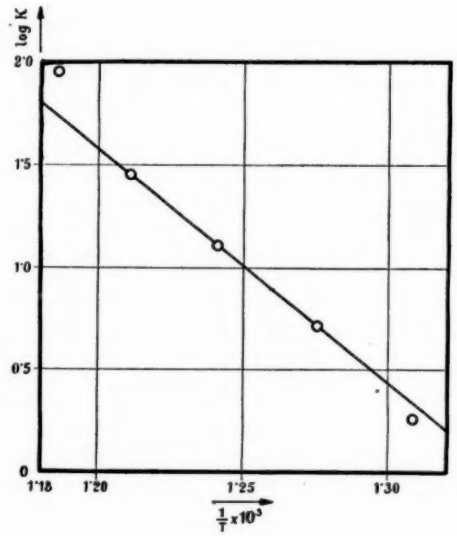

FIG. 2.

the same fact. The authors intend to study this reaction at higher temperatures with modified apparatus. Apart from the change in the energy of activation, there should then be observed a change in the order of the reaction.

The activation energy found from the values determined at the four lower temperatures, taking account of the dependence of the collision number on temperature, amounts to 52.1 kcal./mole. If the collision diameter be calculated according to the simple theory of bimolecular reactions using the formula $K_c=\alpha A e^{-Q/RT}$ (A being the collision number, Q the energy of activation, α the steric factor) there is obtained, assuming $\alpha=1$, a mean value of 6.5×10^{-8} cm for the collision diameter. By inserting these values in the general equation for the constant of the reaction rate, one obtains

$$K_c=6.27\times10^{13}T^{\frac{1}{2}}e^{-26{,}200/T}\ \text{mole}^{-1}\ \text{cm}^3\ \text{sec.}^{-1}.$$

The values calculated from this equation are given in the fifth column of Table V.

V. Discussion

A collision diameter of 6A appears to be too great. At the highest temperatures at which the reaction rate of the hydrogen iodide decomposition has been measured, which approximately correspond to those in the present investigation, collision diameters of the same order of magnitude can be computed with the aid of this simple formula. If the simple theory be modified by the introduction of a part of the non-translational degrees of freedom, which leads to the equation

$$K_c=\alpha A\frac{1}{(S/2-1)!}(Q/RT)^{(S/2-1)}e^{-Q/RT},$$

in which s is the number of the square terms participating, a steric factor of 0.2 will be found, assuming $s=6$, the collision-diameter = 3A and the energy of activation = 53.8 kcal. The values for K_c calculated from the latter equation are to be found in the sixth column of Table V. These values appear to be somewhat less in agreement with the experimental results than the values resulting from the former equation. Assuming that a larger number of square terms participate, there are obtained low steric factors and a dependence of the reaction rate on temperature which is out of agreement with the experimental results. In order to arrive at an exact determination of the dependence of the reaction rate on temperature experiments are to be made at lower temperatures in apparatus modified to suit the necessarily long duration of the runs. After conclusion of these experiments, and possibly of similar experiments with other simple hydrogen compounds, the authors intend to furnish a more detailed theoretical discussion.

Reactions Involving Hydrogen Molecules and Atoms

J. HIRSCHFELDER, H. EYRING AND B. TOPLEY, *Frick Chemistry Laboratory, Princeton University*

(Received December 23, 1935)

The criticisms of Coolidge and James of activation energy calculations are discussed. It is pointed out that their criticisms of the original London proposal do not apply to the semi-empirical method which in its present form has little more than a formal resemblance to the original scheme. Until a satisfactory quantum-mechanical derivation of the semi-empirical method is provided, it must depend for acceptance on its usefulness and the fact that it is a reasonable interpolation formula for calculating the energies of polyatomic molecules from diatomic ones. The best surface for three hydrogen atoms is constructed and from it the rates of all the possible hydrogen-deuterium reactions are calculated by means of the general theory of absolute rates, these rates are found to be in excellent agreement with the experimental values. The transmission coefficient for reactions on this surface is investigated. Diagrams showing the angular dependence of the potential energy for an H and for a Cl atom approaching a hydrogen molecule are given.

I. INTRODUCTION

IN this paper the absolute rates of all the reactions involving hydrogen and deuterium are calculated theoretically using the best available potential energy surface. The results are compared with the experimental values.[1]

It is advantageous to consider the methods for calculating suitable potential energy surfaces for use in the interpretation of reaction rates. Since the early work of Arrhenius,[2] chemists have realized that the intermediate in a reaction was a state of high energy. In many reactions, this was interpreted as a state of high potential energy which could be reached only by the collision of two molecules having unusually great relative kinetic energy.[3] Thus it was clear that energy surfaces were required. However, there was no theoretical way of supplying this need before the advent of quantum mechanics. In 1928, London[4] proposed that a large body of reactions might be considered as proceeding adiabatically in the Ehrenfest sense and that a single eigenfunction be used to represent the electronic state throughout the course of the chemical reaction, i.e., no electron jumps are involved and just one potential energy surface is required. Villars[5] also proposed a rather specialized procedure of calculating the potential energy for the reaction $H_2+I_2\rightarrow 2HI$. London's suggestion included a first-order perturbation theory formula for constructing the necessary potential surface for three and four-atom reactions. These formulae were derived from first-order perturbation theory when the following assumptions were made:

1. Certain complicated types of electronic interactions known as multiple exchange integrals were neglected.
2. The nonorthogonality of the electronic charge distributions, i.e., overlap integrals, was considered to be negligibly small.
3. The remaining integrals were idealized to the point where they could be calculated from knowledge of corresponding diatomic integrals, and they were expressed in terms of the simplest atomic eigenfunctions.

This last assumption made the energy of the polyatomic configuration a function of diatomic energies only. Eyring and Polanyi[6] first applied this method unmodified to the triatomic hydrogen system using the exchange and coulombic integrals calculated by Heitler and London[7] and by Sugiura.[8] They obtained the activation energy of 29 kcal./mole for the reaction H_2+H

[1a] A. Farkas and L. Farkas, Proc. Roy. Soc. **A152**, 124 (1935).

[1b] L. Farkas and E. Wigner, Proc. Faraday Soc. in press. We wish to thank the authors for the opportunity of seeing their manuscript in advance of publication. They consider some of the questions treated in this paper but from the point of view of going from the experimental rates to a potential surface. Here all of our results are calculated from the surface considered best *a priori*.

[2] Arrhenius, Zeits. f. physik. Chemie **4**, 226 (1889).

[3] M. Polanyi, Zeits. f. Physik **1**, 90 (1920); Zeits. f. Elektrochemie **62**, 228 (1920); and Tolman, *Statistical Mechanics* (Chemical Catalog Co., 1927).

[4] London, *Probleme der Moderne Physik* (Sommerfeld-Festschrift); (S. Hirzel, Leipzig, 1928), page 104; Zeits. f. Elektrochemie **35**, 552 (1929).

[5] Villars, Phys. Rev. **34**, 1063 (1929).

[6] Eyring and Polanyi, Zeits. f. physik. Chemie **B12**, 279 (1931).

[7] Heitler and London, Zeits. f. Physik **44**, 455 (1927).

[8] Sugiura, Zeits. f. Physik **45**, 484 (1927).

$\rightarrow H+H_2$ and this is to be compared with the experimental value of 7 kcal./mole. This discrepancy is not surprising since the energy of the normal H_2 molecule calculated from these integrals is only -72.2 kcal./mole instead of the experimental value of -108.6. This activation energy agrees as regards order of magnitude but is far from the accuracy which is necessary for the quantitative calculation of reaction rates. In more complicated reactions, the required integrals were not available. Clearly some improvements were required if the method was to be more than suggestive in the treatment of reactions. The suggestion for the improvement and extension made by Eyring and Polanyi was that the small coulombic energy could be calculated and the exchange energy could then be obtained by subtracting this coulombic energy from the spectroscopically known total binding of the diatomic molecules. In later treatments, the coulombic energy was assumed to be a certain constant percentage of the total binding. This assumption is born out by the Heitler-London-Sugiura integrals for hydrogen and what is more important it is justified empirically by the fact that the same constant percentage gives very nearly the experimental activation energy for a wide variety of cases. It will be shown elsewhere that the constant percentage assumption for three like atoms really leads to the conclusion that the activation energy is directly proportional to the energy of binding of the diatomic molecule. When the spectroscopic and other experimental data are used in the London formulae in place of the integrals which are supposed to be calculated with approximate charge distributions, the assumptions involved lose their original significance but the formulae themselves remain at least an interpolation mechanism for going from diatomic to polyatomic knowledge. When the atoms are widely separated, the London assumptions and the semi-empirical method are equally valid. When only pairs of univalent atoms are together, although the London scheme is inaccurate, the semi-empirical method is still correct. Since the percentage of additive energy is chosen to give the right activation energy and the potential energy goes smoothly into the correct values as the atoms separate into individuals or into pairs, the semi-empirical method must be nearly accurate in its important features. The details of the surface which are necessary to calculate the rate of chemical reactions are:

1. The activation energy.
2. The vibration frequencies.
3. The position of the activated state.
4. The probability that the system having once passed through the activated state will not return.

For each of these, the semi-empirical surface cannot be far wrong. When sufficient accurate data become available so that a precise empirical analysis of these features may be obtained, an improved interpolation formula may be indicated. In the meantime, these semi-empirical surfaces represent our best information as to the nature of interatomic forces and provide a very practical tool for investigating the nature of chemical problems.

Coolidge and James[9] have analyzed the London assumptions and find no way of justifying them in their original form. Since no adequate theoretical derivation of the semi-empirical scheme has ever been proposed it is impossible at the present time to say how rigorously it can be derived from quantum mechanics for the interesting intermediate configurations. The London treatment and the semi-empirical one are sufficiently different to make it impossible to base a criticism of the latter on the basis of the former. An accurate quantum-mechanical surface would be very desirable and we are making some progress in this direction. In a recent paper Rosen and two of the present authors[10] derive the energy of the triatomic hydrogen molecule to the Wang plus polar states approximation by the variation method but the calculated activation energy is 25 kcal. On the basis of these calculations which include and go considerably beyond the calculations of Coolidge and James we find that, for the present at least, the only surfaces adequate for the treatment of chemical reactions are the semi-empirical ones.

The Potential Energy Surface for H_3

The semi-empirical potential energy surface of constant percentage additive energy is given

[9] Coolidge and James, J. Chem. Phys. **2**, 811 (1934).
[10] Hirschfelder, Eyring and Rosen, J. Chem. Phys. **4**, 121ff (1936).

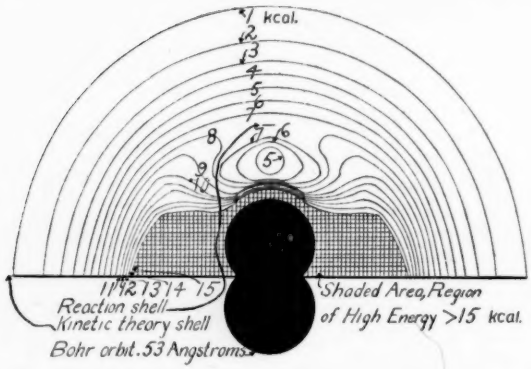

FIG. 1. Potential for an H atom approaching an H_2 molecule.

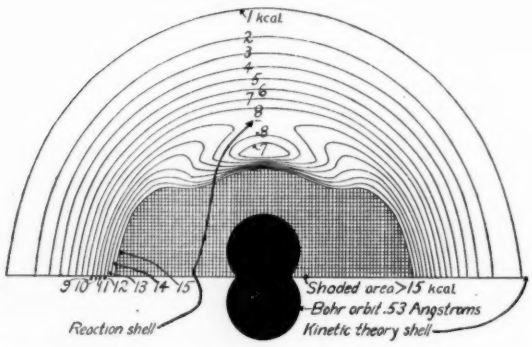

FIG. 2. Potential for a Cl atom approaching an H_2 molecule.

by the lowest root:

$$E = D' + n(w_{ab} + w_{bc} + w_{ac}) \mp (1-n)(w_{ab}^2 + w_{bc}^2 + w_{ac}^2 - w_{ab}w_{bc} - w_{ab}w_{ac} - w_{bc}w_{ac})^{\frac{1}{2}} \quad (1)$$

where D' is the heat of dissociation of H_2 minus the half-quanta of zero-point energy,

w_{ab} is the energy of H_2 for the internuclear separation r_{ab} and similarly for w_{bc} and w_{ac},

n is the fraction of the total binding energy of H_2 which is taken to be additive.

w_{ab}, w_{bc}, w_{ac} are taken from the spectroscopically determined Morse[11] curve for H_2.

Certain features of the surface are exhibited in Fig. 1. In this case two atoms of a hydrogen molecule are held at the normal internuclear distance. The contour lines are the lines of constant potential energy for the various positions of the third atom. The third atom approaching in any direction is first attracted by weak van der Waals forces. Coming closer, the attraction changes to repulsion. An atom of only average thermal velocity (at room temperatures) will be repelled before it reaches the first contour line. At large distances the equipotential surfaces are very nearly spherical. A colliding atom with very high energy penetrates into the interior where it becomes easier to advance parallel to the line of nuclei than perpendicular to this line. If the atom approaches along the line of nuclei and has sufficient energy, it will cross over the energy pass marked, "reaction shell." From this point, it is now attracted for a short distance as previously stated. In Fig. 1 we have kept the two atoms of the original hydrogen molecule at a fixed distance apart. If left to itself the molecule expands slightly as the atom approaches, and after the atom has reached the reaction shell all three atoms vibrate violently. One of the outer atoms departs. If the departing atom belonged to the original molecule a chemical reaction has taken place. The similarity between surfaces of this type is seen by a comparison of Figs. 1 and 2. In the latter the equipotentials for a hydrogen molecule and a chlorine atom are given. As before, the energy pass lies along the molecular axis but at a somewhat greater interatomic separation.

The more nearly the atom approaches along the molecular axis the less the energy required for reaction. For this reason, it is desirable to examine the motion of the three atoms in a line in greater detail; the angular motion is treated by the method of small vibrations and so to this approximation the two motions are separable. The equipotential energy surface for three atoms colliding along a straight line is given in Fig. 3. Only the portion of the surface in the neighborhood of the activated state is shown here. This is the important region for this reaction. The initial state for the system is far to the right and the final state is correspondingly far above the figure as drawn. This surface is drawn so that a mass point having the potential energy indicated by the contour lines and moving in the plane faithfully describes the behavior of a three H atom system. The significance of the

[11] P. Morse, Phys. Rev. **34**, 57 (1929).

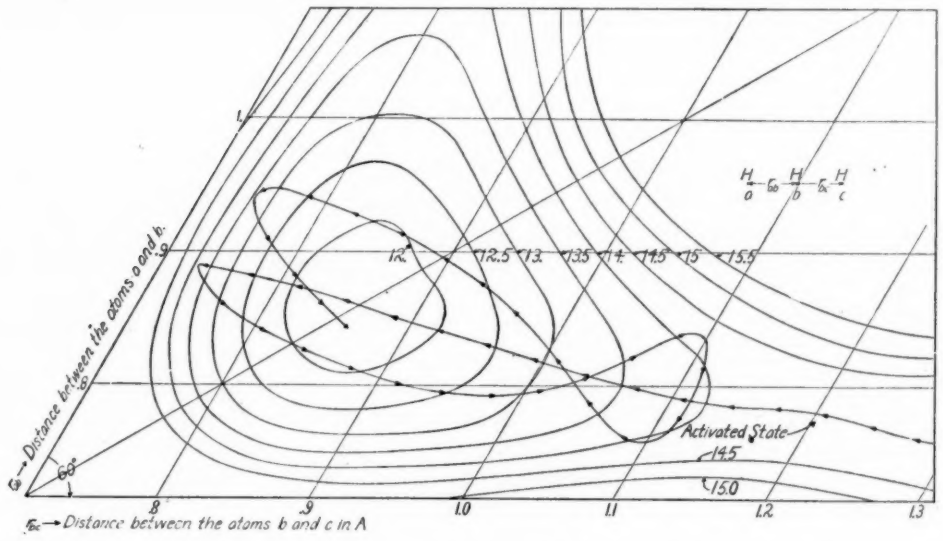

FIG. 3. A detailed vibrational trajectory for linear H_3 is indicated by the line with arrows.

coordinates are made clear in Fig. 3. The line with the arrows represents a trajectory calculated point by point from the classical equations of motion. It is interesting to note that although the system has 300 cal. more energy than is required for reaction (i.e., to pass up beyond the top of the diagram) it wanders about in the potential basin a considerable time. Eventually the system will either react or pass back into the valley from which it came. Which it will do is a mechanically determined problem if we use classical theory. Using classical theory approximately half of a group of such particles entering at various angles will react and half will return to the initial state. Although this problem has not been treated quantum mechanically (and it is not easy to do so) it seems safe to anticipate this same result. If the true surface instead of having the basin shown in Fig. 3 should have the activated state on the symmetrical line this probability of reaction will be considerably increased over one-half but the factor cannot exceed one. However, we will find that when the two outer atoms are identical the symmetry now possessed by the activated complex introduces a statistical factor acting to slow down the rate by a factor of two so that there will be very little net change. We shall therefore restrict our considerations to the surface of Fig. 3. At present it is impossible to say whether the existence of this basin is a virtue or defect of the semi-empirical method of calculating surfaces.

One of the most interesting applications of a potential energy surface is in the determination of the rates of a chemical reaction. The specific reaction rate, k', i.e., the rate at which a reaction takes place when the concentrations of the reacting substances are each equal to unity, has usually been expressed in the form:

$$k' = cZe^{-E/kT}, \tag{2}$$

where Z is the number of collisions which the molecules make in unit time. E is the activation energy of the reaction. The c is the collision efficiency or the ratio of the number of chemical reactions to the number of collisions between the desired molecules which have a kinetic energy relative to its center of mass of more than the energy E. The objections to the form (5) are that c is not defined in terms of molecular properties, it varies from unity to 10^{-8} in magnitude,[12] and it is often found experimentally to be a function of the temperature. Pelzer and

[12] Moelwyn-Hughes, *Kinetics of Reactions in Solutions* (Oxford Press, 1933); L. Kassel, *Kinetics of Reactions* (Chemical Catalog Co., 1932), p. 16; Gershinowitz and Eyring, J. Am. Chem. Soc. **57**, 985 (1935).

Wigner[13] considered explicitly the reaction $H+H_2$ (*ortho*) $\rightarrow H_2$ (*para*)$+H$. They used classical statistical mechanics to determine the density of systems in phase space within prescribed velocity ranges and in the vicinity of the activated state. With this information, they were able to determine the specific reaction rate as the number of systems crossing the activated state from right to left in unit time multiplied by the fraction of these reactions which lead to H_2 (para). They treated the vibrations of the activated complex as classical simple harmonic motion and have given a justification of treating the motion of the atoms as adiabatic. In a subsequent paper Wigner[14] has given a correction to the classical calculation of the rate of crossing the barrier which we discuss below. Eyring[15] generalized the statistical treatment of reaction rates by considering:

$$k'=\kappa\frac{F_a^*}{F_n}\frac{kT}{h}\exp(-E_0/kT), \qquad (3)$$

where F_a and F_n are the partition functions for the activated and the initial configurations of the system. The zero of energy for F_a^* is the lowest state at the top of the barrier while the energy for F_n is the lowest initial state. These states differ by E_0. κ is the transmission coefficient or the fraction of the systems which having reached the activated state leads to a chemical reaction. F_a^* is the product of translational, rotational, and vibrational functions for all except the degree of freedom in the direction in which the complex is decomposing. The partition function for this degree of freedom multiplied by the velocity of crossing the barrier is included in the frequency factor kT/h if we treat crossing the barrier as a pure translation. To take into account the curvature of the barrier we must introduce the additional factor $1-(1/24)(h\nu_i/kT)^2$ which is a quantum-mechanical correction. ν_i^2 is negative and is the square of the imaginary frequency which the theory of small vibrations give for the degree of freedom normal to the barrier. This correction is due to Wigner.[14] It becomes negligible at high temperatures or for small curvatures. When barriers of sufficiently high curvature are encountered the correction should be carried to higher powers of h to give the tunnel effect. Such calculations have been made exactly by Eckart[16] for a special potential surface of one degree of freedom and have been considered approximately by a number of people.[17] The rotations and vibrations are treated as sharply quantized states, which is probably a very good approximation. The transmission coefficient, κ, is a constant of the order of unity. For the reaction $H+H_2 \rightarrow H_2+H$, we have seen that κ is nearly one-half. However, if we distinguished a chemical reaction only when a particular form of H_2, *ortho* as an example, is converted into another particular form (*para*), this value for k' must be multiplied by an *a priori* probability of the conversion occurring. These *a priori* probabilities may be easily computed from a consideration of nuclear spin coupling; for the *ortho-para* conversion of hydrogen this factor is one-fourth. It is therefore possible to use the semi-empirical energy surfaces to calculate the rate of a simple chemical reaction.

The specific rate of reaction of a hydrogen or deuterium atom with a hydrogen, deuterium or mixed molecule is given by the expression:

$$\begin{matrix} a & b & c \\ \cdot & \cdot & \cdot \end{matrix} \qquad a+bc\rightarrow ab+c$$

$$k'=\kappa i\left(\frac{h^2}{4(2\pi)^{\frac{1}{2}}k^{\frac{1}{2}}}\right)\frac{g_{abc}\sigma_{bc}}{g_{bc}\sigma_{abc}}\left(\frac{m_a+m_b+m_c}{m_a(m_b+m_c)}\right)^{\frac{1}{2}}\frac{I_{abc}}{I_{bc}}\frac{\sinh\frac{1}{2}(h\nu_{bc}/kT)}{\sinh\frac{1}{2}(h\nu_s/kT)\sinh^2\frac{1}{2}(h\nu_\varphi/kT)}$$
$$\times\left(1-\frac{1}{24}\left(\frac{h\nu_i}{kT}\right)^2\right)T^{-\frac{1}{2}}\exp(-E_c/kT). \qquad (4)$$

[13] Pelzer and Wigner, Zeits. f. physik. Chemie **B15**, 445 (1932).
[14] E. Wigner, Zeits. f. physik. Chemie **B19**, 203 (1932).
[15] H. Eyring, J. Chem. Phys. **3**, 107 (1935).
[16] C. Eckart, Phys. Rev. **35**, 1303 (1930).
[17] Bell, Proc. Roy. Soc. **A139**, 466 (1933); Cremer and Polyani, Zeits. f. physik. Chemie **B19**, 443 (1932); Baun and Ogden, Proc. Faraday Soc. **30**, 432 (1935).

This is the expanded form of Eq. (3) for this particular case in the units cc molecules^{-1} sec.$^{-1}$. To obtain it in the units liters moles^{-1} sec.$^{-1}$ we must multiply (7) by $N^{5/2}\ 10^{-3}$ where now the masses are to be taken in atomic weight units and N is Avogadros number. Here: i=the *a priori* probability of the reaction occurring on the basis of the nuclear spin interactions. It is one except for the *ortho-para* hydrogen and the singlet-triplet to doublet (nuclear spin) deuterium conversion.

1. $H+H_2$ (*ortho*) $\rightarrow H_2$ (*para*)$+H$, $i=1/4$
2. $H+H_2$ (*para*) $\rightarrow H_2$ (*ortho*)$+H$, $i=3/4$
3. $D+D_2$ (sing.-trip.)$\rightarrow D_2$ (doub.)$+D$, $i=1/3$
4. $D+D_2$ (doub.) $\rightarrow D_2$ (sing.-trip.)$+D$, $i=2/3$

In general, i seems to be equal to the ratio of the number of nuclear states of the resultants to the sum of the initial and final states.

g_{abc} is the number of electronic states of the activated complex and this is equal to two for all of the states that we consider and is equal to g_{bc} the number of electronic states for the initial molecule plus atom.

σ_{abc} is the symmetry number of the activated state. Since the potential surface which we are considering, makes the activated complex unsymmetrical with respect to a and c, this number is equal to unity.

σ_{bc} is the symmetry number of the initial molecule bc. It is equal to two if bc is either H_2 or D_2 and unity if bc is HD.

E_c is the difference of the potential energy of the initial molecule bc from that of the activated complex abc where the zero-point energies for both states have been absorbed in the various hyperbolic sines. For the potential surface which we shall consider (20 percent additive energy), $E_c=7.63$.

I_{bc} is the moment of inertia of the initial molecule bc. It may be expressed in terms of the atomic masses and the equilibrium separation $(r_0)_{bc}$:

$$I_{bc}=\frac{m_b m_c}{m_b+m_c}(r_0)_{bc}^2.$$

I_{abc} is the moment of inertia of the activated complex. In terms of the masses of the constituents and the separations in this configuration, r_{ab}, r_{bc}:

$$I_{abc}=\frac{1}{m_a+m_b+m_c}(m_a(m_b+m_c)r_{ab}^2 + 2m_a m_c r_{ab} r_{bc}+m_c(m_b+m_a)r_{bc}^2).$$

ν_{bc} is the vibration frequency of the diatomic molecule bc. It varies inversely as the square root of the reduced mass of the molecule.

ν_ϕ= the bending frequency of the activated complex and it is doubly degenerate since the molecule can bend in two perpendicular planes with the same frequency.

ν_s is that frequency of the normal linear mode of vibration of the activated complex whose square is positive. ν_l is the other linear frequency.

The internal kinetic energy for the linear triatomic molecule in the neighborhood of the activated complex separates into two independent parts. The first part T_L is due to two independent linear modes of motion for which we shall use the coordinates r_{ab} and r_{bc} already defined by reference to Fig. 3. Here

$$T_L=(1/2M)[m_a(m_b+m_c)\dot{r}_{ab}^2 + 2m_a m_c \dot{r}_{ab}\dot{r}_{bc}+m_c(m_b+m_a)\dot{r}_{bc}^2],$$

where $M=(m_a+m_b+m_c)$ and the other m's have been defined. The second part of T_ϕ is due to a doubly degenerate bending vibration having the kinetic energy

$$T_\phi=\frac{r_{ab}^2 r_{bc}^2 m_a m_b m_c \dot{\phi}^2}{2MI_{abc}}$$ associated with each mode.

Here ϕ is the angle between r_{ab} and r_{bc}. Now the linear potential energy in the neighborhood of the activated state for 20 percent additive binding is

$$v_L=7.63+\tfrac{1}{2}f_1(r_{bc}-1.354)^2 + f_{12}(r_{bc}-1.354)(r_{ab}-0.753)+\tfrac{1}{2}f_2(r_{ab}-0.753)^2.$$

Where the r's are subtracted from the corresponding coordinate of the activated state. Angstrom units are used for the lengths. The force constants have the values

$$f_1=-14.15;\quad f_{12}=62.70\quad f_2=624.4,$$

where the units are kcal. mole^{-1} A^{-2}. Finally $\nu_\phi=\frac{1}{2}f_\phi\phi^2$ where $f_\phi=5.80$ kcal. mole^{-1} radians^{-2}.

By the usual method for small vibrations[18] we find for

$$\nu_s=(1/2\pi)(2m_am_bm_c)^{-\frac{1}{2}}\times[\alpha+(\alpha^2-4m_am_bm_cM(f_1f_2-f_{12}))^{\frac{1}{2}}]^{\frac{1}{2}},$$

$$\nu_t=(1/2\pi)(2m_am_bm_c)^{-\frac{1}{2}}\times[\alpha-(\alpha^2-4m_am_bm_cM(f_1f_2-f_{12}))^{\frac{1}{2}}]^{\frac{1}{2}},$$

where

$$\alpha\equiv m_a(m_b+m_c)f_1+m_c(m_b+m_a)f_2-2m_am_cf_{12}.$$

Here of course ν_s, ν_t and ν_0 are the linear symmetrical vibration, the imaginary frequency across the barrier and the bending frequency, respectively. We get Table I for the frequencies and for the zero-point energies and moments of inertia for the different reactions.

Wigner and Farkas[19] find from an examination of the experimental data of Farkas and Farkas for the rates of the various types of hydrogen-deuterium reactions, that for $H+H_2$

$$1/2h\nu_s=5.3 \text{ kcal. mole}^{-1},$$
$$1/2h\nu_\phi=0.75,$$

which is in very good agreement with our values given in Table I. They find that the difference of the potential energy at the activated state and the initial states, i.e., our E_c is 7.2 kcal./mole as compared with our calculated value of 7.63 using 20 percent additive energy. The reinterpretation of the results of Farkas and Farkas by Wigner and Farkas changes the activation energy from 5.5 to 7.8 kcal./mole which is now in agreement with the low temperature measurements of Geib and Harteck[20] and is to be compared with the value of 8.5 which we are using. The important features of our surface all lie well within the probable error of the best available experiments. For this reason it is of considerable interest to present our theoretical values for all the reactions over a considerable range of temperature. The calculated values were obtained before the experimental results of Farkas and Farkas and the reinterpretation of Farkas and Wigner were available and the agreement came as something of a surprise particularly since it was felt that for the zero-point energy of the activated state to be actually larger than the initial state would probably lead to wrong relative rates for some of the reactions.

Table I.

	Reaction	I_{abc} (g cm²)	$-i/2h\nu_t$ (kcal./mole)	$\frac{1}{2}h\nu_\phi$ (kcal./mole)	$\frac{1}{2}h\nu_s$ (kcal./mole)	Zero-Point Energy Activated State (kcal./mole)	Zero-Point Energy Initial State (kcal./mole)
1	$H+H_2$	3.79×10^{-40}	0.90	0.95	5.18	7.08	6.21
2	$D+D_2$	7.58	.64	.67	3.66	5.00	4.39
3	$H+DH$	4.69	.83	.86	4.57	6.29	5.38
4	$D+HD$	7.50	.68	.86	4.38	6.10	5.38
5	$H+HD$	4.92	.83	.88	4.40	6.16	5.38
6	$D+H_2$	5.45	.73	.93	5.17	7.03	6.21
7	$D+DH$	5.77	.66	.76	4.56	6.08	5.38
8	$H+D_2$	4.92	.82	.70	3.67	5.07	4.39

$\kappa=\frac{1}{2}$ for the reactions 1. $H+H_2\rightarrow H_2+H$, 2. $D+D_2\rightarrow D_2+D$, 3. $H+DH\rightarrow HD+H$, 4. $D+HD\rightarrow DH+D$. The absolute rates of these reactions are therefore calculated from Eq. (4). See Table II. Eqs. (1) and (2) are for the total reaction rates. If one is interested in the *ortho-para* conversions these rates must be multiplied by the appropriate values of i already discussed.

In reactions (4) to (8) where the zero-point energies are different in the two passes on either side of the central basin, it is more difficult to calculate the transmission coefficient. However, this factor may be evaluated if we assume that when a system passes through the nearest pass and into the basin, its chances of decomposing in the two different manners is independent of the initial state of the system. This assumption is equivalent to the relation: $\kappa_f+\kappa_r=1$. Let G_f and G_r be the reaction rates of the forward and reverse reactions except for the transmission coefficients:

$$k_f'=\kappa_fG_f \quad k_r'=\kappa_rG_r.$$

But the equilibrium constant for the reaction, K, is defined as the ratio of the rates of the forward and the reverse reactions. Therefore:

$$K=k_f'/k_r'=G_f\kappa_f/G_r\kappa_r$$

and $\kappa_f=G_rK(G_f+G_rK)^{-1}$, $\kappa_r=G_f(G_f+G_rK)^{-1}$.

Now since κ_f and κ_r separately can never exceed

[18] Whittaker, *Analytical Dynamics* (Cambridge Press, 1927), p. 127.

[19] Farkas and Wigner (reference 1b) obtained the results for $\frac{1}{2}h\nu_s$, $\frac{1}{2}h\nu_\phi$, and E_0' quoted here by using a combination of the low and high temperature measurements. The use of high temperature measurements alone would, in their opinion, indicate a somewhat different set of constants.

[20] Geib and Harteck, Zeits. f. physik. Chemie (Bodenstein Volume), 849 (1931).

TABLE II. *Reaction rates (in liter mole^{-1} sec.$^{-1}$).*

REACTION	k'	283°	300°	600°	900°	1000°
1. $H+H_2 \rightarrow H_2+H$	(H.E.T.)		7.3×10^4	7.3×10^7	9.2×10^8	1.5×10^9
	(F.&F.)				1.5×10^9	2.2×10^9
	(G.&H.)	8.5×10^4				
2. $D+D_2 \rightarrow D_2+D$	(H.E.T.)		3.0×10^4	3.5×10^7	4.4×10^8	7.6×10^8
	(F.&F.)					1.2×10^9
3. $H+DH \rightarrow HD+H$	(H.E.T.)		2.2×10^4	2.6×10^7	3.2×10^8	5.2×10^8
	(F.&F.)					6.8×10^8
4. $D+HD \rightarrow DH+D$	(H.E.T.)		2.4×10^4	2.4×10^7	2.6×10^8	4.4×10^8
	(F.&F.)					1.0×10^9
5. $H+HD \rightarrow H_2+D$	(H.E.T.)		1.1×10^4	1.8×10^7	2.6×10^8	4.5×10^8
	(F.&F.)					9.5×10^8
6. $D+H_2 \rightarrow DH+H$	(H.E.T.)		7.1×10^4	6.2×10^7	7.1×10^8	1.2×10^9
	(F.&F.)					2.5×10^9
7. $D+DH \rightarrow D_2+H$	(H.E.T.)		3.0×10^4	2.5×10^7	3.0×10^8	5.0×10^8
	(F.&F.)					7.9×10^8
8. $H+D_2 \rightarrow HD+D$	(H.E.T.)		1.5×10^4	2.8×10^7	4.3×10^8	7.4×10^8
	(F.&F.)					1.2×10^9

In the above table H.E.T. indicates the present authors, F.&F. Farkas and Farkas[18] and G.&H. Geib and Harteck.[19]

unity their sum cannot exceed 2 so that the true rates cannot exceed the calculated ones by more than a factor two due to the assumed relation $\kappa_f+\kappa_r=1$. That $\kappa_f+\kappa_r$ does not differ much from unity seems reasonably certain from an inspection of the surface. Thus we know the wave packet representing the system will be refracted like a light wave with an index of refraction depending on the total energy minus the potential energy and in this basin this will lead to repeated reflection. The same kind of factors operate to make egress random in quantum mechanics as operate in the classical case. The equilibrium constants can be evaluated independently of κ_f and κ_r from a knowledge of the initial and final states.

$$K_{H+HD}=\frac{k'_{H+HD}}{k'_{D+H_2}}=\frac{g_{H_2}\sigma_{HD}}{g_{HD}\sigma_{H_2}}\times\left(\frac{2m_D}{m_H+m_D}\right)^{\frac{1}{2}}\frac{\sinh\frac{1}{2}(h\nu_{HD}/kT)}{\sinh\frac{1}{2}(h\nu_{H_2}/kT)},$$

$$K_{D+DH}=\frac{k'_{D+DH}}{k'_{H+D_2}}=\frac{g_{D_2}\sigma_{HD}}{g_{HD}\sigma_{D_2}}\times\left(\frac{2m_H}{m_H+m_D}\right)^{\frac{1}{2}}\frac{\sinh\frac{1}{2}(h\nu_{HD}/kT)}{\sinh\frac{1}{2}(h\nu_{D_2}/kT)}.$$

The transmission coefficients are then found from the above relations. They are functions of the temperature since the zero-point energy at the two activated states are different. The transmission factors and the equilibrium constants are:

T	K_{H+HD}	K_{D+DH}	κ_{H+HD}	κ_{D+H_2}	κ_{D+DH}	κ_{H+D_2}
300°	0.144	2.147	0.192	0.808	0.819	0.181
600°	.287	.929	.332	.668	.673	.328
900°	.364	.719	.383	.618	.621	.379
1000°	.378	.677	.396	.604	.621	.379
∞	.577	.408				

We wish to express our appreciation to the American Philosophical Society for financial assistance.

The Absolute Rates of Reaction of Hydrogen with the Halogens

A. WHEELER, B. TOPLEY AND H. EYRING, *Frick Chemistry Laboratory, Princeton University*

(Received December 30, 1935)

In this paper we apply the statistical-mechanical method which has only recently been developed for reaction rates to three new groups of reactions. These are the reactions of I_2, Cl and Br with the various kinds of hydrogen molecules. In the first type ($I_2+H_2\rightarrow 2HI$) symmetry properties enable one to divide the six internal modes of vibrations for the four coplanar atoms into three sets with one, two and three modes of vibration in each so that in obtaining the frequency nothing greater than a cubic is solved. This treatment of the frequencies will apply to a very broad class of reactions. The potential surfaces probably yield too high a zero-point energy for the activated state. In spite of this result they give the right relative rates for the various isotopic reactions because mass enters very strongly into what in the past has been thought of as the collision factor. The study of isotopic reactions in conjunction with the new theory of rates gives a detailed knowledge of the potential in the activated state and can be carried much farther than has been done in this preliminary treatment. The treatment has been carried far enough however to show its general applicability to these types of processes.

INTRODUCTION

IN the present paper we carry through the calculations for the absolute rates of the following reactions:

$$H_2+I_2\rightarrow 2HI \quad (1)$$

$$D_2+I_2\rightarrow 2DI \quad (2)$$

$$H_2+Cl\rightarrow H+HCl \quad (3)$$

$$D_2+Cl\rightarrow D+DCl \quad (4)$$

$$DH+Cl\rightarrow D+HCl \quad (5)$$

$$HD+Cl\rightarrow H+DCl \quad (6)$$

$$H_2+Br\rightarrow H+HBr \quad (7)$$

$$D_2+Br\rightarrow D+DBr \quad (8)$$

$$DH+Br\rightarrow D+HBr \quad (9)$$

$$HD+Br\rightarrow H+DBr \quad (10)$$

These reactions can be divided into three groups (each of which is characterized by the halogen involved). For each group a single potential energy surface suffices to give the absolute reaction rate for all members of the group. The best surfaces available at the present time are the so-called semiempirical surfaces, the construction of which has been described elsewhere.[1]

The preliminary calculations for the present paper led to the crystallization of a point of view of treating reaction rates which has been presented in a previous paper.[2]

We are here concerned with chemical processes for which the slow step corresponds to passage across the potential barrier separating reactants and final products. The atomic configurations formed at the moment of passage across the potential barrier we call the activated complex. If the potential energy for the activated configurations is known statistical mechanics suffices to fix the concentration of the activated complex and gives the rate at which the complex decomposes. We now proceed to a consideration of the individual cases.

THE REACTION OF HYDROGEN WITH IODINE

In constructing our potential energy surface we use the lowest root of the equation[1,3]

$$E=A+B+C \pm(\tfrac{1}{2}((\alpha-\beta)^2+(\alpha-\gamma)^2+(\beta-\gamma)^2))^{\frac{1}{2}}, \quad (11)$$

where in the case of four atoms each letter stands for the sum of two terms indicated by the same letters but with the subscripts 1 and 2 respectively. (See Fig. 1.) Thus $A=A_1+A_2$, $\alpha=\alpha_1+\alpha_2$, etc. Further $(A_1+\alpha_1)$ is the potential energy between two isolated atoms in this case, H and H as a function of the distance between them, with a corresponding meaning for the other sums.

[1] H. Eyring and M. Polanyi, Zeits. f. physik. Chemie **B12**, 279 (1931); H. Eyring, J. Am. Chem. Soc. **53**, 2537 (1931); H. Ekstein and M. Polanyi, Zeits. f. physik. Chemie **B15**, 334 (1932). For more details and a variety of applications see subsequent papers of these authors.

[2] H. Eyring, J. Chem. Phys. **3**, 107 (1935).

[3] F. London, *Probleme der Modernen Physik* (Sommerfeld-Festschrift) (S. Hirzel, Leipzig, 1928), p. 104; Zeits. f. Elektrochemie **35**, 552 (1929).

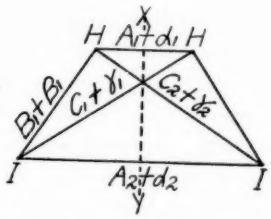

FIG. 1. Activated configuration.

For this reaction we take the additive binding corresponding to the latin letters as 14 percent and the exchange or nonadditive binding corresponding to the greek letters as 86 percent of the total. We shall find that to obtain exact agreement with experiment a somewhat different percentage is required but our purpose here is not to obtain numerical agreement (which is in fact readily obtained as we shall see) but to illustrate the principles involved and to find what information regarding the potential surface can be obtained by a comparison with experiment. In this way suggestive results are obtained which should be helpful in guiding further investigations by both experiment and theory.

In constructing the Morse[4] curves

$$E=D'[\exp(-2a(r-r_0)-2\exp(-a(r-r_0))$$

the following constants were used for the H to H bond: $r_0=0.74$; $a=1.94$; $D'=102.4+6.2$; while for the I to I bond $r_0=2.66$; $a=1.86$ and $D'=35.39+0.30$. Here r_0 is the distance between the atoms at the minimum of potential. D' is equal to the heat of dissociation plus the zero-point energy. $a=0.1227\omega_0(\mu/D')^{\frac{1}{2}}$ where the constant 0.1227 is such that the frequency ω_0 and the energy D' are to be expressed in cm^{-1}. The reduced mass of the oscillator μ is to be taken in atomic weight units.

We find using Eq. (11) for the potential energy that the activated state corresponds to the four atoms lying in a plane as indicated in Fig. 1. The atomic distances in the activated state are: for H to H we find $r_1=0.97$A; for I to I we find $r_2=2.95$A; and for the nearest H to I distance $r_3'=1.75$A. The distances r_1, r_2 and r_3' suffice to fix the activated configuration since it is planar and symmetrical with respect to the line $X-Y$. However, to specify completely the position of four atoms we must specify twelve coordinates. Since the activated complex is non-linear we have three rotational degrees of freedom in addition to the three translations of the molecule as a whole. This leaves six internal coordinates to be specified. If the activated complex were an ordinary molecule we would expect six vibration frequencies which could be found by the standard method for finding normal coordinates,[5] using the potential function (11). Now we apply this method in the present case and find five normal frequencies and a sixth normal coordinate having a reasonable though low frequency except that it is multiplied by $(-1)^{\frac{1}{2}}$. This arises of course from the fact that the force constant along this normal coordinate is negative instead of positive, i.e., for this type of motion the system is in unstable equilibrium (it is at the top of a potential hill) whereas for the other five motions (normal coordinates) it is stable, i.e., any displacement from the activated configuration increases the potential energy.

Using statistical mechanics we can therefore write for the concentration of activated complexes, which lie at the top of the barrier and in a distance dq_n measured normal to it and which have momenta lying between p_n and p_n+dp_n the expression:

$$\exp(-E_0/kT)\frac{(2\pi m^*kT)^{\frac{1}{2}}}{h^3}\frac{8\pi^2(8\pi^3A^*B^*C^*)^{\frac{1}{2}}(kT)^{\frac{1}{2}}}{h^3}\prod_{i=1}^{5}\left(1-\exp\left(-\frac{h\nu_i^*}{kT}\right)\right)^{-1}$$
$$\cdot\left[\exp\left(-\frac{p_n^2}{2m_nkT}\right)\left(1-\frac{1}{8}\left(\frac{h\nu_n}{kT}\right)^2\left(1-\frac{p_n^2}{3m_nkT}\right)\right)\right]dp_ndq_n(H_2)(I_2)\left\{\frac{(2\pi m_1kT)^{\frac{1}{2}}}{h^3}\frac{(2\pi m_2kT)^{\frac{1}{2}}}{h^3}\right.$$
$$\left.\cdot\frac{8\pi^2I_1kT}{h^2}\frac{8\pi^2I_2kT}{h^2}(1-\exp(-h\nu_1/kT))^{-1}(1-\exp(-h\nu_2/kT))^{-1}\right\}^{-1}. \quad (12)$$

[4] P. Morse, Phys. Rev. **34**, 57 (1929).

[5] Whittaker, *Analytical Dynamics* (Cambridge Press, 1927), p. 171.

Here (H_2), m_1, I_1 and ν_1, are the concentration, mass, moment of inertia and frequency of hydrogen, respectively, while for the I_2 molecule we use (I_2) for concentration and the subscript 2 for the other quantities. The asterisk indicates the corresponding quantities for the activated complex. The subscript n indicates the degree of freedom normal to the potential energy barrier, i.e., the degree of freedom for which the square of the frequency is negative. For very flat barriers we can take $\nu_n=0$ in which case the quantity in 12 enclosed in square brackets reduces to the classical expression. The quantum-mechanical correction term arising from the curvature of the potential barrier $\nu_n\neq 0$ as given is due to Wigner.[6] In it corrections involving higher than the second power of h are neglected. For barriers of very large curvature it will be necessary to take a more accurate account of tunneling by some method such as that used by Eckart.[7] This correction term is of course the analogous quantity for negative curvatures that zero-point energy is for positive curvatures. As more information accumulates we will no doubt be able to improve our partition function for the activated state in other particulars. $p_n/m_n dq_n$ is the number of times per second (a frequency) that the particles in the length dq_n having velocities p_n/m_n are emptied across the barrier. We now multiply expression (12) by $p_n/m_n dq_n$ to get the rate at which activated complexes with momenta lying between p_n and p_n+dp_n pass over the barrier. Integrating for all positive velocities across the barrier, i.e., from $p_n=0$ to ∞ we get for the total rate of reaction:

$$k_1'(H_2)(I_2)=\frac{\kappa(2\pi m^*kT)^{\frac{1}{2}}}{h^3}\frac{8\pi^2(8\pi^3A^*B^*C^*)^{\frac{1}{2}}}{h^3}(kT)^{\frac{1}{2}}\prod_{i=1}^{5}\left(1-\exp\left(-\frac{h\nu_i^*}{kT}\right)\right)^{-1}$$
$$\cdot\left[\frac{kT}{h}\left(1-\frac{1}{24}\left(\frac{h\nu_n}{kT}\right)^2\right)\right]\exp\left(-\frac{E_0}{kT}\right)(H_2)(I_2)\left\{\frac{(2\pi m_1kT)^{\frac{1}{2}}}{h^3}\frac{(2\pi m_2kT)^{\frac{1}{2}}}{h^3}\right.$$
$$\left.\cdot\frac{8\pi^2I_1kT}{h^2}\frac{8\pi^2I_2kT}{h^2}\left(1-\exp\left(-\frac{h\nu_1}{kT}\right)\right)^{-1}\left(1-\exp\left(-\frac{h\nu_2}{kT}\right)\right)^{-1}\right\}^{-1}; \quad (13)$$

here k_1' is the specific reaction rate and is in cc molecules^{-1} sec.$^{-1}$. To get k_1' in cc moles^{-1} sec.$^{-1}$ we must multiply by Avogadro's number N. The transmission coefficient, κ_1, is the fraction of activated complexes which having crossed the barrier do not return, and

$$\frac{kT}{h}\left(1-\frac{1}{24}\left(\frac{h\nu_n}{kT}\right)^2\right)=\int_0^\infty\frac{1}{h}\exp\left(-\frac{p_n^2}{2m_nkT}\right)\left(1-\frac{1}{8}\left(\frac{h\nu_n}{kT}\right)^2\left(1-\frac{p_n^2}{3m_nkT}\right)\right)\frac{p_ndp_n}{m_n}.$$

In order to find the normal coordinates it is necessary to separate the kinetic energy for the six internal coordinates from the six coordinates for translation and rotation. We are therefore interested in finding 6 types of independent motion each of which leaves the center of gravity undisplaced and gives no net angular momentum about the center of gravity. The following set of displacements indicated diagrammatically in Fig. 2 fulfill these conditions. In motion (1) the cross indicates a downward displacement while the circle indicates an upward one. The other motions all correspond to displacements in the plane of the molecule. The plane of the activated complex is of course a plane of symmetry. In addition the plane normal to this and bisecting the H−H and I−I bonds is also a symmetry plane. We shall speak of the latter as the plane $X-Y$ (see Fig. 1). The requirements of nonrotation and nondisplacement of the system as a

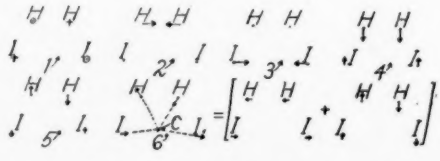

FIG. 2. Six orthogonal motions which can be used to express the kinetic energy of four atoms in a plane with a plane of symmetry perpendicular to it. Motion 6 is resolved into its horizontal and vertical components.

[6] E. Wigner, Zeits. f. physik. Chemie **B19**, 203 (1932).
[7] C. Eckart, Phys. Rev. **35**, 1303 (1930).

whole together with the specification of the motion of some one particle suffices to specify each of the six modes of motion in Fig. 2. We can classify these modes of motion into three groups on the basis of reflection in the two symmetry planes. Thus reflection in the plane of the molecule changes the sign of the displacement of motion (1) and leaves all the rest unchanged. Reflection in the plane $X-Y$ changes the sign of the displacements of 5 and 6 and leaves all the others unchanged. We thus have the three groups (A) motion 1; (B) motions 2, 3, 4 and (C) motions (5) and (6).

Now the expression for the potential and for the kinetic energy T (expressed in terms of these displacements and velocities of displacement from equilibrium) must be unchanged by either of these two reflections in the symmetry planes. This is only possible if in the quadratic expressions for T and V there are no cross terms between any two of the three groups of motions. Since further the process of finding normal coordinates is simply one of finding a transformation which eliminates the cross terms simultaneously in T and V we know that (1) must be a normal mode of vibration, that three others will be formed from linear combinations of the motion of group (B) and finally that the other two will be a linear combination of group (C). This type of question has been frequently considered.[8]

Group A

For the small displacement 1 we can conveniently take as our coordinate the relative angular displacement φ about the axis $X-Y$ of the H—H oscillator with respect to the oscillator I—I. The kinetic energy is then

$$T_A=\tfrac{1}{2}\frac{I_1I_2}{I_1+I_2}\dot{\varphi}^2 \qquad (14)$$

and the potential energy is

$$V_A=\tfrac{1}{2}k\varphi^2 \qquad (15)$$

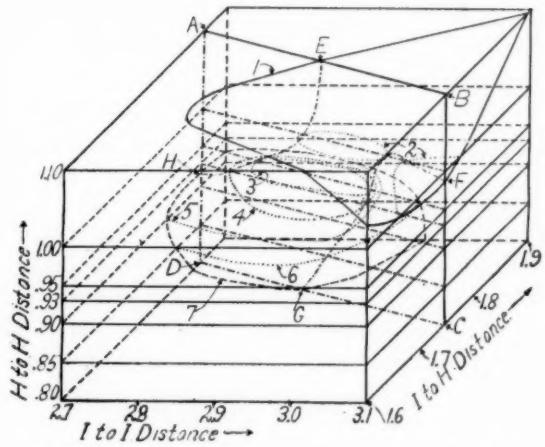

FIG. 3. Equipotential energy surface corresponding to 96 kcal. for the planar-symmetrical complex (see Fig. 1) for (H_2I_2). The sections numbered 1 to 7 lie in the horizontal planes for which the H to H distance has the seven values 1.10, 1.00, etc., to 0.80 given on the vertical axis. The hour-glass-like section *EHFG* lies in the vertical plane *ABCD*.

where I_1 and I_2 are the moments of inertia of the oscillators H—H and I—I, respectively, at the equilibrium distances already specified for the activated state. The potential function (11) gives $k=39.4$ kcal. per mole per rad.$^{-2}$. We then find in the usual way[5]

$$V_\perp=\frac{1}{2\pi}\left(\frac{k(I_1+I_2)}{I_1I_2}\right)^{\frac{1}{2}}=994\ \text{cm}^{-1} \qquad (16)$$

for $H_2+I_2\leftarrow$ while for $D_2+I_2\rightarrow$ this frequency is 700 cm^{-1}.

Group B

If for the symmetrical configurations indicated in Fig. 1 we make a three-dimensional plot of the equipotential surface corresponding to 96 kcal. as given by Eq. (11) with 14 percent additive binding we get Fig. 3. The H to H distance r_1 is plotted vertically, the I to I distance r_2 from left to right and the shortest H to I distance r_3' from front to back. The intersection of the equipotential surface with the "visible" surface of the parallelopiped is indicated by heavy lines as are all other visible intersections. "Invisible" intersections with the surface of the parallelopiped are indicated by simple broken lines except in the case of the plane *A B C D*. All invisible intersections with this plane are indicated by dot-dash lines. The intersection of

[8] Dennison, Phil. Mag. **1**, 195 (1926); Astrophys. J. **62**, 84 (1926); Brester, Zeits. f. Physik **24**, 337 (1924); Placzek, *Handbuch der Radiologie*, Vol. 6, second edition (Marx, Leipzig, 1934); Wigner, Nach. Göttingen (1930); E. B. Wilson, Jr., Phys. Rev. **45**, 706 (1934); Manneback, *Calcul et Identification des Vibrations des Molécules*, editions E. D. K. (132 rue Féronstrée, Liège).

A B C D with the equipotential surface *E F G H* reveals the latter as a somewhat distorted hour glass. The reaction $H_2+I_2\rightarrow 2$ HI corresponds to the streaming of mass points from the lower-far-left corner up through the neck of the hour glass to the upper-front-right corner. The dotted curves are the various horizontal sections of the equipotential surface. In obtaining Fig. 3 many points were calculated but there are still slight uncertainties in some of the cross sections. The mechanical problem is to find how the mass point vibrates at the neck of the hour glass. There will be two vibrations normal to the neck and a translation along it. This latter motion corresponds to passing over the energy barrier which in three-atom reactions is more simply though not more definitely indicated as the crossing of an energy barrier plotted in three dimensions. To plot the analogous surface here would require a fourth dimension. The three asymmetric motions lie in a space orthogonal to that plotted in Fig. 3.

The kinetic energy of the three symmetric motions is

$$T_B=\frac{1}{2}\left(\frac{m_H}{2}\dot{r}_1^2+\frac{m_I}{2}\dot{r}_2^2+\frac{2m_Hm_I}{m_H+m_I}\dot{r}_3^2\right). \quad (17)$$

The three separate terms are the kinetic energies for motions 2, 3 and 4 in order as indicated in Fig. 2. Hence $\frac{1}{2}m_H$ is the reduced mass for the oscillator H_2 and r_1 is the distance between the H atoms; $\frac{1}{2}m_I$ and r_2 are the reduced mass and distance between atoms respectively for the molecule I_2. r_3 is the distance between the centers of gravity of the H_2 and the I_2 molecules and $2m_Hm_I/(m_H+m_I)$ is the reduced mass for the oscillator composed of an H_2 molecule as one particle vibrating with respect to the I_2 as the other particle. (r_3 should not be confused with r_3'. Fig. 3 would not be particularly different in appearance if we had plotted r_3 instead of r_3'. The actual choice was simply a matter of convenience.) To get the normal modes we require in addition the potential energy V_B as a function of the distances r_1, r_2 and r_3. The direction cosines of the line L lying along the axis of the bottle neck were determined as accurately as possible by an inspection of Fig. 3. Then by constructing the 96 kcal. equipotential ellipse normal to L as well as other ellipses for the same equipotential surface but tilted slightly with respect to L it was possible to locate this axis more exactly. The potential function V_B is then written as

$$V_B=\tfrac{1}{2}k_1s_1^2+\tfrac{1}{2}k_2s_2^2+\tfrac{1}{2}k_3s_3^2 \quad (18)$$

where s_1 and s_2 are the distances measured along the major and minor axes, respectively, of the ellipse and s_3 is the distance measured along the axis L of the hour glass. The values found were $k_1=30$, $k_2=150$, $k_3=-65$ in kcal. per mole per A^2.

The equations found for the r coordinates in terms of the s's are

$$\begin{aligned} r_1&=0.3971s_1+0.4189s_2+0.8164s_3,\\ r_2&=-0.9102s_1+0.0676s_2+0.4082s_3,\\ r_3&=-0.1158s_1+0.9054s_2-0.4082s_3. \end{aligned} \quad (19)$$

Since this transformation is unitary the matrix for the inverse transformation is found by simply interchanging rows and columns. $T(s_1s_2s_3)$ is found by substituting Eq. (19) (after taking the time derivative) in (17). We thus form $L=T-V$, and after finding the three Lagrangian equations $(d/dt)(\partial L/\partial\dot{s}_i)-\partial L/si$ we make the usual substitutions $s_i=A_ie^{-i\lambda t}$. Finally we solve the resulting secular equation. When we take the mass of the hydrogen atoms equal to 1 we get the three frequencies 86, 1280, and $965\cdot(-1)^{\frac{1}{2}}$ in cm^{-1}. With the mass of hydrogen taken equal to 2 these frequencies are 86, 915, and $678\cdot(-1)^{\frac{1}{2}}$.

Group C

From symmetry and other simple considerations it is clear that the first four types of motion in Fig. 2 are orthogonal to each other and also orthogonal to 5 and 6. Motions 5 and 6 are not orthogonal to each other. The direction of motion of all atoms in (6) is toward or away from the center of gravity C.

The kinetic energy for the vibration of group (C) is

$$\begin{aligned} T_C=&m_H\left(1+\frac{r_1^2m_H}{r_2^2m_I}\right)\dot{y}^2+2\sin\alpha\, m_H\\ &\times\left\{1-\left(\frac{r_1m_H}{r_2m_I}\right)^2\right\}\dot{y}\dot{q}+m_H\left(1+\frac{m_H\cos^2\alpha}{m_I\cos^2\beta}\right)\dot{q}^2. \end{aligned} \quad (20)$$

Here m_I and m_H are the mass of an iodine and hydrogen atom, respectively. y is the sum of the vertical displacements of an H and the nearest I atom for the motion 5. q is the displacement of an H from the minimum along the line joining it with the center of gravity. α is the angle which the path of an H atom in motion (6) makes with the horizontal and β is the corresponding angle for the I atom. The potential energy is written as

$$V_c = \tfrac{1}{2}(350)y^2 + \tfrac{1}{2}(400)q^2 + 350yq. \quad (21)$$

Where as before the force constants 350 and 400 are expressed in the units kcal. per mole per A^2.

The frequencies obtained for light hydrogen are 1400 and 1730 cm^{-1}, respectively; while for deuterium the values were 990 and 1225 cm^{-1}.

The values for the three moments of inertia for the activated complex with two H atoms is 552.8, 4.1 and 556.9 and with two D atoms is 553.2, 8.2 and 561.4 in units of atomic weights A^2. The moment of inertia used for H_2 was 0.2738 and for D_2 was 0.5476 and for I_2 was 449.1.

The difference in energy between the initial state on our surface corresponding to H_2+I_2 (as well as for D_2+I_2) and the activated state (this of course ignores zero-point energies in both states) was found to be $35.7+108.6-96=48.3$. The zero-point energies in the initial state for H_2+I_2 is $6.2+0.3=6.5$ kcal., while for the activated state we find 7.8 for the sum of the zero-point energies for the five vibrations. For the initial state of D_2+I_2 we have the zero-point energy $4.4+0.3=4.7$ and for the activated state the value is 5.56. If the zero-point energy in the activated state had been zero we see that for H_2+I_2 the activation energy at the absolute zero would be $E_0=48.3-6.9=41.4$ in approximate agreement with experiment. When we take into account zero-point energy of the activated state we get 49.6 kcal. Thus since 14 percent additive binding has been found to give the experimental activation energy for a wide variety of reactions when the zero-point energy in the activated state is ignored, approximately 20 percent will be required to give the experimental values when account is taken of the activated zero-point energy. We shall not recalculate our surface for this reaction at this time but shall use 20 percent in the other reactions considered.

We now compare our calculated results with those of Bodenstein.[9] If we use our calculated frequencies and moments of inertia in Eq. (13) but take $E_0'=35{,}500$ kcal. which gives agreement between theory and experiment for 700°K we get Table I. Where $E_0'=E_0-\epsilon_{act.}+\epsilon_{init.}$ and where

TABLE I.

$T°$	log $k_{obs.}$	log $k_{calc.}$	log $(k_{calc.}/k_{obs.})$
575	−0.880	− 0.61	+ 0.27
700	1.808	1.808	0
781	3.126	2.98	− .14

$\epsilon_{act.}$ and $\epsilon_{init.}$ are the sums of the zero-point energies in the activated and initial states, respectively. Only the extremes of temperature are considered since the intermediate values add nothing to the check.

If we now arbitrarily divide our group (C) frequencies by two and fit experiment at 700° by taking $E_0'=38{,}260$ leaving unchanged all the other calculated frequencies and the moments of inertia we find: (see Table II). Finally if we fit

TABLE II.

$T°$	log $k_{calc.}$	log $(k_{calc.}/k_{obs.})$
575	−0.693	+0.187
700	1.808	0
781	3.025	− .10

experiment at 700° by taking $\nu_n=0$; $E_0'=39{,}700$ and taking 180 and 1000 cm^{-1} for the group (C) frequencies keeping the other frequencies and moments of inertia unchanged we obtain the values given in Table III.

TABLE III.

575	−0.85	+0.03
700	1.808	0
781	3.09	−0.036

Thus the calculated potential surface with 14 percent additive deviates from the true one first by giving too high an activation energy and secondly by giving frequencies somewhat too

[9] Bodenstein, Zeits. f. physik. Chemie **13**, 56 (1894); **22**, 1 (1897); **29**, 295 (1898); Kassel, *Kinetics of Homogeneous Gas Reactions* (Chemical Catalog Co. 1932), p. 154; Hinshelwood, *Kinetics of Chemical Change* (Oxford Press, 1933), p. 72.

large. By simply increasing the percentage additive binding a surface would be obtained which would give a very satisfactory account of experiment.[10] It should be clear that if by the use of the experimental data for the H_2+I_2 reaction we accurately determine the frequencies, activation energy and moments of inertia to be used in (13) then with our theory we should be able to predict exactly the other two reactions $DH+I_2 \rightarrow DI+HI$ and $D_2+I_2 \rightarrow 2DI$ which use the same potential surface.

If we use our theoretical frequencies and moments of inertia for the reaction D_2+H_2 and choose $E_0'=35{,}500$ as before we find this rate is slower than that for H_2+I_2 by the ratios 2.6, 2.34 and 2.26 at the three temperatures 575, 700 and 781°. Since our calculated frequencies are probably too stiff we expect the observed ratios will be somewhat larger than this. Experimental information on this ratio will be valuable in determining in what way our calculated potential surface deviates from reality and so indicate how our method of calculation can be improved in the general case.

Pressure Effects

The partition functions used in calculating k_1' are such that k_1' is not strictly the specific reaction rate except at low pressures, i.e., where activities are equal to concentrations. However, at all pressures[11] we can write

$$k_1' = \kappa K^* \frac{kT}{h}\left(1-\frac{1}{24}\left(\frac{h\nu_n}{kT}\right)^2\right),$$

where
$$K^* = \frac{a^*}{a_1 a_2 \cdots} = \frac{c^* \alpha^*}{c_1 \alpha_1 c_2 \alpha_2 \cdots}. \qquad (21a)$$

Here K^* is the equilibrium constant between reactants and the activated complex where the partition function for the latter by definition is normalized to unity (one unit cell) in the degree of freedom normal to the barrier. a^*, c^* and α^* are the activity, concentration and activity coefficient for the activated complex and the letters in the denominator of (21a) have the same significance for the various reactants. Now the specific reaction rate constant when multiplied by the concentration of reactants must give the rate of reaction (i.e., the concentration of activated complexes multiplied by the reciprocal of their mean life). Hence this constant is clearly $k_1'\alpha_1\alpha_2/\alpha^*$. Thus the specific reaction rate constant depends on the pressure as Kistiakowsky[12] finds and the theoretical problem is the familiar one of taking account of the virial coefficients and of the finite volumes from which each particular molecule or complex excludes other molecules. These two effects are usually treated together and involve adding to the partition function for translation the factor obtained by integrating over a potential function due to the other molecules. Now the excluded volume varies with the violence of collision but in analogy to a zero-point energy one might suggest as a zero-point volume for a gas the volume from which a molecule excludes other molecules approaching it with zero velocity. Unfortunately such a concept for volume is less sharply defined than for energy. The excluded volume is not a property of a single molecule but depends on the pair colliding. In spite of a certain unavoidable arbitrariness of definition Evans and Polanyi choose to take as one factor in α_i the expression $\exp(-pV_i/kT)$ where V_i is the excluded volume for the molecule i. There can be no real objection to such a treatment provided one introduces another factor A_i such that $\alpha_i = A_i \exp(-pV_i/kT)$ where we know how to calculate α_i and also α^* at least in principle. The two factors in α_i are in fact seen to

[10] We wish to correct an error in an earlier paper (Eyring, J. Am. Chem. Soc. **53**, 2546 (1931)). An arithmetical mistake in calculating the a in the Morse curve for I_2 led to a calculated activation energy for the reaction $H_2+I_2 \rightarrow 2HI$ of 28 kcal. for 10 percent additive binding whereas with the correct a the value is considerably greater than 48 kcal. After this correction is made the conclusions in that paper remain unchanged in the light of our present calculations with the higher percentage of additive binding. This was also pointed out at the Washington meeting of the American Society in 1932 by A. Sherman and H. Eyring in an unpublished paper showing the general validity of a fixed percentage additive binding for calculating reaction rates. The question of directed valence for this and the other hydrogen halogen reactions has been extensively investigated in a thesis by A. Wheeler. Putting the angle dependence into (11) which comes from treating the valence electrons of the I atoms as being in p states increased the activation energy by around 4 kcal. for the H_2+I_2 reactions. The activated configuration became slightly nearer a linear one. There are no important changes in the general properties of the surface calculated in this way.

[11] W. F. K. Wynne-Jones and H. Eyring, J. Chem. Phys. **3**, 492 (1935); Evans and Polanyi, Trans. Faraday Soc. **21**, 875 (1935).

[12] Kistiakowsky, J. Am. Chem. Soc. **50**, 2315 (1928).

be conceptually related to the "internal pressure" and "excluded volume" terms in van der Waals equation. Reactions in condensed phases involve the α's in this same way and have been discussed at length elsewhere.[11] Kistiakowsky's considerations on the effect of pressure on the decomposition of HI should be extended in the light of the present theory to take account of α^* as well as the other α's. In this, of course, the general theory proceeds exactly as Brönsted[13] does in solution.

The Reaction of Chlorine Atoms with Hydrogen Molecules

For the HCl Morse curve we use $D'=105.5$; $a=1.79$, $r_0=1.282$, $\omega_0=2840$. For the H_2 molecule the same Morse curve was used as in the preceding reaction. Eq. (11) is then used for calculating the potential energy in the usual way. The activated state corresponds to a linear configuration $\underset{m_1}{X}\leftarrow r_1\rightarrow\underset{m_3}{Y}\leftarrow r_2\rightarrow\underset{m_2}{Cl}$ with $r_1=1.40$A and $r_2=1.30$A. In this configuration which serves to define the masses m and distances r, the letters X and Y may stand for either hydrogen or deuterium. The kinetic energy associated with these two coordinates is

$$T_L=\tfrac{1}{2}\frac{m_1(m_2+m_3)}{M}\dot{r}_1^2+\tfrac{1}{2}\frac{m_2(m_1+m_3)}{M}\dot{r}_2^2+\frac{m_1m_2}{M}\dot{r}_1\dot{r}_2, \quad (22)$$

where M is the sum of the three masses. The potential energy

$$V_L=\tfrac{1}{2}k_1r_1^2+\tfrac{1}{2}k_2r_2^2 \quad (23)$$

where $k_1=-40$ and $k_2=550$. The units are kcal. mole^{-1} A^{-2}. The barrier is so nearly normal to r_1 that no cross terms need be introduced into the potential. The usual method for calculating the frequencies gives:

$$\nu_\pm=\frac{1}{2\pi}[A^{-1}(B+C\pm((B+C)^2-2MAk_1k_2)^{\frac{1}{2}})]^{\frac{1}{2}}, \quad (24)$$

where $A=2m_1m_2m_3$; $B=m_1(m_2+m_3)$ $_2$; $C=m_2(m_1+m_3)k_1$. For each of the two c generate bending vibrations we have the kinet energy

$$T_\varphi=\frac{r_1^2r_2^2m_1m_2m_3\dot{\varphi}^2}{2I_3M}, \quad (25)$$

where φ is the angle between r_1 and r_2, and

$$I_3=m_1r_1^2+m_2r_2^2-\frac{(m_1r_1-m_2r_2)^2}{M} \quad (26)$$

the moment of inertia of the linear triatomic molecule. The potential energy is $V_\varphi=\frac{1}{2}f_\varphi\varphi^2$. This gives us the frequency

$$\nu_\varphi=\frac{1}{2\pi}\left(\frac{f_\varphi I_3M}{r_1^2r_2^2m_1m_2m_3}\right)^{\frac{1}{2}}. \quad (27)$$

We find for the force constant $f_\varphi=7.56$ kcal. mole^{-1} rad.$^{-2}$. The moments of inertia and frequencies for the various molecules are given in Table IV. The difference in potential energy for the initial and for the activated state (which of course neglects the zero-point energy in both states) is $E_0'=11.6$ kcal. for this reaction. In obtaining this value and the other quantities in IV the additive binding has been taken as 20 percent of the total for each diatomic molecule.

Table IV.

System	ν_φ	I	ν_+	ν_-
H−H−Cl	551	8.55	2496	720 i
H−D−Cl	415	9.94	1800	705 i
D−H−Cl	523	15.11	2496	520 i
D−D−Cl	386	16.33	1769	406 i

The equation for the specific rate for a reaction of the type XY+Cl→X+Y Cl where X and Y may each be either hydrogen or deuterium is:

$$k'=\sigma_1\left(\frac{M}{m_2(m_1+m_2)}\right)^{\frac{1}{2}}\frac{I_3}{I_1T^{\frac{1}{2}}}(6.65\times10^{13})\times\left(1-\exp\left(-\frac{h\nu}{kT}\right)\right)\left(1-\exp\left(-\frac{h\nu_\varphi}{kT}\right)\right)^{-2}\times\left(1-\exp\left(-\frac{h\nu_+}{kT}\right)\right)^{-1}\left(1-\frac{1}{24}\left(\frac{h\nu_-}{kT}\right)^2\right)\times\exp\left(-\frac{E_0}{kT}\right). \quad (28)$$

[13] Brönsted, Zeits. f. physik. Chemie **102**, 109 (1922); **115**, 337 (1925).

In the above expression σ_1 is the symmetry number for H_2 and is equal to two, while ν is the vibration frequency for this molecule.

Rodebush and Klingelhoeffer[14] have measured the rate of this reaction by introducing Cl atoms into H_2. At the temperatures of 0° and 25°C they give as the probability of reaction per collision 1.4×10^{-5} and 3.3×10^{-5}, respectively. Multiplying these quantities by the number of collisions at unit concentrations, using their collision diameters, we obtain for the specific reaction rates at the two temperatures 3.3×10^9 and 8.2×10^9 in units of cc mole^{-1} sec.$^{-1}$. Using the calculated half-quanta with the calculated E_0' we find $E_0=11.6+5.1-6.2=10.5$ kcal. for reaction (3) where exactly as in the H_2+I_2 reaction $E_0=$ the activation energy at the absolute zero and $E_0=E_0'+$zero-point energy in the activated state —zero-point energy in the normal state. Rodebush and Klingelhoeffer find an activation energy of 6 kcal. A slight increase in the additive binding would, of course, give exact agreement but this would have little effect on our frequencies. Instead of recalculating our surface with a slightly larger percentage additive binding we use our theoretical frequencies and moments of inertia in (28), and take $E_0'=7.0$. This gives the experimental rate at 0°C. For 25° the equation then gives 7.1×10^9. If we take our $\nu_-=0$ (i.e., neglect the tunnel effect) and fit at 0° we require $E_0'=6.75$. This equation then gives 9.8×10^9 at 25° for the specific rate.

Using $E_0'=7.0$ and the calculated frequencies we get for the ratio of the rates for $H_2+Cl\rightarrow H+HCl$ to $D_2+Cl\rightarrow D+DCl$ at 0° and 25° the values 5.6 and 3.3, respectively. Rollefson[15] gives for the ratios of the *over-all* rates of combination of Cl with H_2 and with D_2 when in each case CO is present the values 13.4 at 0° and 9.75 at 32°C. If we are justified in assuming that Rollefson was measuring the ratio of the rates for H_2+Cl and D_2+Cl we must conclude that our frequencies in the activated state are a little too large, i.e., the curvatures of our surface at the activated state are a little too great. Reaction rates (5) and (6) follow immediately from the calculated frequencies and moments of inertia. Since there are at present no experiments with which to compare them we shall not discuss them further at this time.

The Reaction of Bromine Atoms with Hydrogen Molecules

For the HBr Morse curve we use $D'=89.9$, $a=1.83$, $r_0=1.42$, $\omega_0'=2603$. We use 20 percent additive binding and proceed exactly as in the preceding case except that Br takes the place of Cl. We use the same definitions. The activated state corresponds to $r_1=1.5$ $r_2=1.42$.

$$V_L=\tfrac{1}{2}k_1r_1^2+\tfrac{1}{2}k_2r_2^2, \qquad (29)$$

$k_1=-45$; $k_2=500$ in kcal. mole^{-1} A^{-2} and $\nu_\varphi=\tfrac{1}{2}k_\varphi\varphi^2$. Here $k_\varphi=7.56$ kcal. mole^{-1} rad.$^{-2}$. The frequencies and moments of inertia are now given in Table V. As before the frequencies are in the units cm^{-1} and the moments of inertia are in atomic weights A^2.

Table V.

System	ν_+	ν_-	ν_φ	I
H−H−Br	2340	760 i	460	10.34
H−D−Br	1670	760 i	350	12.15
D−H−Br	2340	540 i	430	18.43
D−D−Br	1670	540 i	320	20.19

In Table VI we give the observed specific rates and ratios of rates taken from the work of Bach, Bonhoeffer and Moelwyn-Hughes[16] and of Bodenstein and Lutkemeyer.[17] As yet unpublished data of Dr. Nelson Trenner of this laboratory give for the photochemical combination of Br_2 with H_2 and with D_2 the ratio

$$\frac{k(H_2+Br)}{k(D_2+Br)}=9.7 \text{ at } 538°K.$$

Twenty percent additive binding yields a calculated value of $E_0'=25.1$ which then gives for $E_0=25.1+4.63-6.2=23.5$ where 4.63 is the calculated zero-point energy in the activated state. Bodenstein and Lutkemeyer give 17.6 for the activation energy while Bach, Bonhoeffer and Moelwyn-Hughes find 17.7 kcal. These values are not directly comparable with E_0 but as we see below our activation energy is too high. This can of course be corrected by taking a slightly larger percentage additive binding. In construct-

[14] Rodebush and Klingelhoeffer, J. Am. Chem. Soc. **55**, 130 (1933).
[15] G. K. Rollefson, J. Chem. Phys. **2**, 144 (1934).
[16] Bach, Bonhoeffer and Moelwyn-Hughes, Zeits. f. physik. Chemie **B27**, 71 (1934).
[17] Bodenstein and Lutkemeyer, Zeits. f. physik. Chemie **114**, 208 (1924).

TABLE VI.

T	499°K		574.5°K		612°K	
	Obs.	Calc.	Obs.	Calc.	Obs.	Calc.
$k(H_2+Br)$	1.16×10^6	1.01×10^6	1.25×10^7	1.25×10^7	3.01×10^7	3.46×10^7
$\frac{k(H_2+Br)}{k(D_2+Br)}$	7.15	4.19	5.4	2.91	4.8	2.5

ing Table VI the frequencies and moments of inertia for the two reactions were taken from Table V and E_0' was taken as 20.45 in order to obtain agreement for the middle temperature. This value is directly comparable with the calculated value of 25.1 above. Rates for (7) and (8) at other temperatures as well as for (9) and (10) are readily obtained from Eq. (28) and Table V.

The foregoing considerations show clearly that the new theory of absolute reaction rates with reasonable potential energy surfaces will agree perfectly with the experimental findings. Conversely with sufficiently good experimental rates we can get an accurate picture of the potential surface in the neighborhood of the activated state using the general theory. Morris and Pease[18] have recently reviewed the experimental data for the reactions of hydrogen with the halogens and proposed tentative activation energies. Our potential surfaces for H_2+I_2 give the rather surprising result that the total zero-point energy in the activated state exceeds that for the initial states. The available experimental results suggest that these calculated zero-point energies of the activated states are probably a little too large. It is noteworthy, however, in spite of this apparent shortcoming that these surfaces still indicate that hydrogen is considerably more reactive than deuterium in agreement with experiment. New accurate experiments should point the way to improvements in the general methods of calculating potential energy surfaces.

We wish to thank Dr. William Altar for helpful discussion.

[18] Morris and Pease, J. Chem. Phys. 3, 796 (1935).

MARCH, 1936 JOURNAL OF CHEMICAL PHYSICS VOLUME 4

The Heitler-London Repulsive State of Hydrogen

HUBERT M. JAMES, ALBERT SPRAGUE COOLIDGE AND RICHARD D. PRESENT, *Harvard University and Purdue University*

(Received November 25, 1935)

A variational method has been used in the study of the $1s\sigma 2p\sigma\ ^3\Sigma_u$ state of H_2. Two independent computations with formally different functions gave, for a nuclear separation of 1.5 a_H, energies which agreed to within 0.03 ev and functions with a root-mean-square fractional difference of about 2 percent. A study of the way in which the computed energies converged to a limit, as the complexity of the varied functions was increased, indicates that the interaction energy of the atoms at this distance is $+5.145\pm0.02$ ev. Computations were also made for nuclear separations of 1.6 a_H and 1.87 a_H. A potential curve passed through points thus determined and approaching the Heitler-London curve asymptotically for large nuclear separations is believed to be accurate to 0.2 ev for nuclear separations greater than 1.35 a_H. This curve is compared with the results of previous computations and the curve constructed by Finkelnburg and Weizel to account for the variation with wave-length of the excitation potential of the continuous spectrum. Discussion of the disagreement with the results of Finkelnburg and Weizel is deferred to a later paper.

IN two previous papers,[1, 2] the authors have described a method for constructing wave functions for the lower states of the H_2 molecule, based upon the variation principle, and adapted from the work of Hylleraas upon the He atom. The states heretofore discussed have been the attractive states $^1\Sigma_g$ (the ground state), $^1\Sigma_u$ (the B state), and $^3\Sigma_g$ (the upper state for the continuous spectrum, according to Winans and

[1] H. M. James and A. S. Coolidge, J. Chem. Phys. 1, 825 (1933).
[2] R. D. Present, J. Chem. Phys. 3, 122 (1935).

Stueckelberg[3]). In all these cases, the results could be checked by comparing the energy as calculated from the wave function with that yielded by a study of the vibration terms in the spectrum. It is of interest to apply the method to a repulsive state, the most easily treated one being the $^3\Sigma_u$ state predicted by Heitler and London (the lower state for the continuous spectrum). Here, however, we have no adequate experimental check; our only empirical information about this state is due to Finkelnburg and Weizel,[4] who have roughly located a portion of its potential energy curve by studying the excitation potential of various wave-lengths in the continuous spectrum, with the aid of the Franck-Condon principle. The success of our method must therefore be judged by internal evidence, such as the rapidity of convergence to a limit of energies computed using functions of increasing complexity, and the degree to which the limit approached is independent of the arbitrary parameters introduced. In the present paper we communicate the results of our computations and compare them with those of previous, more approximate methods of attack, reserving for the following paper a discussion of the numerous problems that arise when we attempt to make a careful comparison between these results and those obtained by Finkelnburg and Weizel. Since we have already fully described our method, it is unnecessary to give the details here; we have, however, thought it worth while to discuss and illustrate the estimation of the limits of convergence somewhat more fully than in the previous papers, as certain new aspects of this question appeared during the present work.

The calculations were made by using the same basic material as in the other papers. If the nuclei are designated by a and b, the electrons by 1 and 2, and the distances between them in Bohr radii a_H are denoted by the customary symbols, then the coordinates are

$$\lambda_1=(r_{1a}+r_{1b})/R, \quad \lambda_2=(r_{2a}+r_{2b})/R,$$
$$\mu_1=(r_{1a}-r_{1b})/R, \quad \mu_2=(r_{2a}-r_{2b})/R,$$
$$\rho=2r_{12}/R.$$

The wave function is then

$$\psi=\sum_{mnjkp} C_{mnjkp}[m\delta_1 n\delta_2 jkp], \quad j+k \text{ odd},$$

where $[m\delta_1 n\delta_2 jkp]$ stands for

$$(1/2\pi)\{e^{-\delta_1\lambda_1-\delta_2\lambda_2}\lambda_1{}^m\lambda_2{}^n\mu_1{}^j\mu_2{}^k - e^{-\delta_2\lambda_1-\delta_1\lambda_2}\lambda_1{}^n\lambda_2{}^m\mu_1{}^k\mu_2{}^j\}\rho^p.$$

The material at hand permitted us to compute with $\delta_1=\delta_2=0.75$ and with $\delta_1=0.5$, $\delta_2=1$. Table I gives the results obtained for the internuclear distance $R=1.5a_H$ with several selections of terms in the series. Each function, designated by a capital letter at the top of the table, contains those terms which are marked by stars under the designating letter and opposite the abbreviations at the left. (These abbreviations have the form $[mnjkp]$, the values of δ_1 and δ_2 being understood.) At the bottom of the table are given the corresponding calculated energies, in units of 27.08 ev. In the case of the best functions obtained with each choice of δ's there is also given the limit of convergence, estimated as discussed later.

The agreement of the two parallel calculations is remarkably satisfactory. Functions E and G give energies differing by 0.01 ev, and may be accepted as good approximations to the best function which can be constructed without explicitly introducing r_{12}. (The addition to G of eight more terms with $p=0$ improved the energy by less than 0.02 ev.) This best function is evidently the one which would be obtained as an exact solution of a wave equation in which the term $1/r_{12}$, a function of the elliptical coordinates λ_1, μ_1, λ_2, μ_2, and $(\varphi_2-\varphi_1)$, is replaced by its average value over $(\varphi_2-\varphi_1)$ for every λ_1, μ_1, λ_2, μ_2. When E and G, respectively, are converted into F and H by applying a correction for dependence upon r_{12}, a somewhat greater discrepancy makes its appearance; but this is removed entirely, within the probable error, when the appropriate allowances are made for convergence of the series. The calculation with different δ's is undoubtedly to be preferred, as it allows explicitly for the promotion of one electron which must take place as the nuclei are brought near each other and the molecular wave function approaches the $1s2p$ function of the helium atom. The superiority of the function with two δ's is

[3] J. G. Winans and E. C. G. Stueckelberg, Proc. Nat. Acad. Sci. **14**, 867 (1928).
[4] W. Finkelnburg and W. Weizel, Zeits. f. Physik **68**, 577 (1931).

TABLE I.

TERMS	$\delta_1=\delta_2=0.75$ A	B	C	D	E	F	$\delta_1=0.5\delta_2=1$ G	H
[00100]		*		*	*	*	*	*
[01100]	*	*	*	*	*	*	*	*
[02100]					*	*		
[10100]	*	*	*	*	*	*	*	*
[11100]	*	*	*	*	*	*	*	*
[12100]					*	*		
[20100]			*	*	*	*		
[21100]			*	*	*	*		
[00120]	*	*	*	*	*	*	*	*
[01120]							*	*
[10120]	*	*	*	*	*	*		
[00300]					*	*	*	*
[01300]					*	*		
[00101]								*
[10101]						*		*
[11101]						*		
energy	−0.7967	−0.7972	−0.7983	−0.8012	−0.8064	−0.8080	−0.8067	−0.80906
limit						−0.812		−0.8100
uncertainty						±0.003		±0.0007

In addition to the terms shown, a number of other terms were tried out and discarded; these were [00211] in the case $\delta_1=\delta_2=0.75$, and [02100], [20100], [00010], [10010], [11010], [10120], [11120], [01300], [01101], [11101], and [10121] for $\delta_1=0.5$, $\delta_2=1$.

manifested by the more regular convergence and the smaller number of terms required to get a satisfactory approximation.

The importance of the r_{12} terms is small, as is to be expected from the triplet character of the state. Because of the antisymmetry to exchange of the space coordinates of the electrons the terms in the wave function which do not explicitly involve r_{12} vanish to the first order with r_{12}. The terms with $p=1$ vanish to the second order, and may thus be expected to produce a lowering of the computed energy of the order of that given by the $p=2$ terms in singlet functions, which also vanish with r_{12} to the second order. In fact, in our treatments of a $^3\Sigma_g$ and a $^3\Sigma_u$ state of this molecule the $p=1$ terms gave improvements of 0.06 ev in each case, as against improvements of 0.07 ev and 0.05 ev, respectively, given by terms with $p=2$ in treatments of $^1\Sigma_g$ and $^1\Sigma_u$ states.

In the case of attractive states, it has heretofore always been found that when a series converges regularly and rapidly upon a limit, this limit is in excellent agreement with experiment; we are hence in all probability justified in concluding that the results obtained by correcting function H for convergence are very nearly right. Strong internal corroboratory evidence is furnished by the agreement with function F. However, it must be admitted as possible that the functions used cannot approximate indefinitely closely to the true functions or that the analysis of convergence has not been exhaustive, so that the true value of the energy lies appreciably lower than estimated, and only by chance do the two functions give energies which are in error by the same amount. Were this true, it would still be exceedingly unlikely that the errors in the functions themselves would be everywhere the same, since they differ from each other not only in the parameters δ but also in the coefficients. A detailed agreement between them must be taken to indicate their individual agreement with a third limiting function, the one which we desire. We have accordingly determined the coefficients in F and H (given in Table II) and have computed the values of the two functions for forty different configurations of the electrons, well distributed through the region within which $\lambda_1, \lambda_2 \leq 2$. With the exception of two points near nodal surfaces, where small absolute differences become relatively large, the maximum relative difference $(F-H)/H$ was 5 percent, and its root-mean-square average was

TABLE II.

R in aH	1.5	1.5	1.6	1.87
δ_1, δ_2	0.75, 0.75	0.5, 1	0.5, 1	0.5, 1
TOTAL ENERGY, (atomic units)	−0.8080	−0.80906	−0.83097	−0.87472
REPULSION ENERGY (ev)	5.20	5.17	4.58	3.39
COEFFICIENTS OF TERMS BELOW				
[00100]	1.21236	1.548772	1.897818	2.416480
[01100]	.01928	−0.027247	−0.159414	−0.373883
[02100]	−.02644			
[10100]	.86174	0.204526	0.017095	−0.342534
[11100]	−.45434	−0.048833	−0.034078	0.014003
[12100]	.06103			
[20100]	.12237			
[21100]	−.01610			
[00120]	.36873	0.683718	0.728560	0.801804
[01120]		0.039157	−0.020635	−0.135245
[10120]	.28495			
[00300]	.27807	0.205257	0.208275	0.205674
[01300]	−.03385			
[00101]		0.248869	0.237395	0.134036
[10101]	.12211	−0.017416	−0.017510	0.001903
[11101]	−.02542			

2 percent. This figure was obtained by evaluating $\Sigma(F-H)^2/\Sigma H^2$ over the forty points, in order to avoid the integrations required in computing $\int(F-H)^2dV/\int H^2dV$, the root-mean-square relative difference of the functions. It is possible that the integral would come out somewhat greater, because of the contributions from remote regions (larger values of λ_1, or λ_2). As the energy does not depend much upon the function in these regions, it is to be expected that approximate functions obtained by minimizing the energy will be subject to larger errors there.

By reasoning similar to Eckart's,[5] if we assume that there is no coherence between the errors in the two functions, and take the apparent convergence limit as the true energy, we can estimate the mean discrepancy from the errors in the computed energies. It comes out somewhat greater than 2 percent, in agreement with the above. We have thus an additional check on the correctness of our results.

To extend our information about the repulsive state, we have made computations for other values of R. To judge by analogy with the ground state, the values $\delta_1=0.5$, $\delta=1$ should be good for a considerable variation in R. Table II shows the energy computed for three separations, using these values of δ and the same nine terms of the series as are contained in function H; the coefficients are also given. No special estimate of convergence has been made for the other separations; doubtless the allowance for it when $R=1.87$ should be increased somewhat over that for $R=1.5$, or additional terms in the series included, if the greatest possible accuracy is required, because the values of δ become less appropriate as R increases. For $R>2$, we shall have to use different δ's. This work is now in progress.

Fig. 1 will make possible a comparison of our work with that in the literature. We have drawn a curve passing through the points representing our corrected value at $R=1.5$, the same distance below the uncorrected point at $R=1.6$, somewhat more below that at $R=1.87$, and approaching asymptotically from below the Heitler-London curve as calculated by Sugiura's[6] method. Pending the investigation of the region $2<R<4$, we believe this may be accepted as lying within 0.2 ev of the correct potential curve over the whole range, and much nearer for the smaller values of R. We have also included the results of Hylleraas[7] and MacDonald.[8] Those of Hylleraas (with which MacDonald's closely

[5] C. Eckart, Phys. Rev. **36**, 878 (1930).

[6] Y. Sugiura, Zeits. f. Physik **45**, 484 (1927).

[7] E. A. Hylleraas, Zeits. f. Physik **71**, 739 (1931).

[8] J. K. L. MacDonald, Proc. Roy. Soc. **A136**, 528 (1932).

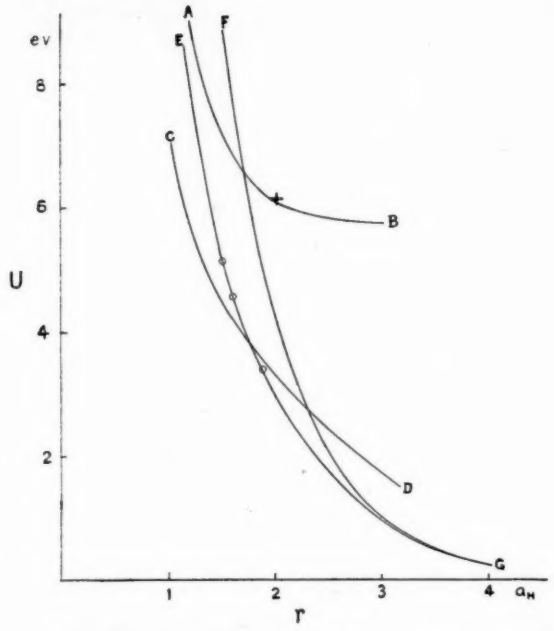

FIG. 1. Energy of the $1s\sigma 2p\sigma\ ^3\Sigma_u$ state of H_2. *AB*, computation of Hylleraas; *CD*, estimate of Finkelnburg and Weizel; *FG*, Heitler-London method; *EG*, estimate of the present authors; +, computation of MacDonald: 0, computation of the authors.

agree) lie above the H-L curve at $R=2$, but below it at $R=1.5$. Evidently both methods are subject to large errors in this region, the H-L method being much better for larger R, as is well understood, while those of Hylleraas and MacDonald, involving the use of H_2^+ functions as a basis of approximation, work best at smaller separations and for more highly excited molecular states.

The "experimental" curve of Finkelnburg and Weizel is also shown. It is very far indeed from confirming our computations. We do not believe, however, that this proves our results to be in error. We shall show in the following paper that it is possible to make very plausible assumptions by which our theoretical curve may be brought into harmony with what Finkelnburg and Weizel actually observed.

On the Choice of Parameters δ

The choice of values for the exponents δ_1, δ_2 is in principle arbitrary; in practice it is a matter of convenience. There is, to be sure, one choice of δ's which, for any given selection of series terms, will give a lower energy than any other. But upon adding more terms, the optimum δ's will in general be found to change, slowly at first, but increasingly erratically as the number of terms becomes greater. On the other hand, the improvement obtainable by varying the δ's goes rapidly down with increasing number of terms; consequently, although the best δ's for a very complex function may be quite different from those for a simple function, the error produced by using the latter values instead of the former will be very small. This is, of course, because when many terms are available it is possible to compensate errors in the δ's by readjustments in the coefficients, C_{mnjkp}.

In practice, it is necessary to use δ's lying within a certain appropriate range. As set forth in the next paragraph, an unfortunate choice of δ's results in slow and irregular convergence on the limiting energy. The choice of δ's may be made through a preliminary investigation with a simple, generally a one-term, function. This need require no great accuracy, as the resulting δ's will not, in general, be just the best ones for the more complex functions to be used later, but this discrepancy will be of small importance. The one-term function $(10100)=(1/2\pi)(e^{-\delta_1\lambda_1}\lambda_1\mu_1 e^{-\delta_2\lambda_2} - e^{-\delta_1\lambda_2}\lambda_2\mu_2 e^{-\delta_2\lambda_1})$ evidently represents a model in which the electrons occupy two orbits, an inner "one-quantum" nodeless orbit, and an outer "two-quantum" orbit with a node in the median plane. The effect on the outer electron of promotion and the partial shielding of the nuclei by the inner electron is here represented (with $\delta_1=0.5$, $\delta_2=1$) not only by a diminution in the exponent of the outer orbit, but by the factor λ_1, which operates to displace the maximum density outwards. The general significance of the δ's is thus made clear. As a matter of fact, the particular values here used were those which had been found most appropriate for the term [10000] of the state $1s\sigma 2s\sigma\ ^3\Sigma_g$. Somewhat different values would doubtless have been chosen if the present calculation had been the first undertaken, but they could hardly have led to a more successful convergence.

On Estimating Convergence Limits

When the δ's are favorably chosen convergence has, in all calculations so far undertaken, been quite regular. By this, we mean that the improvement obtained by adding any given term to the function is found to decrease system-

TABLE III. *Energies obtained with various functions.* For each entry, the function used contains the term indicated at the top in addition to the combination indicated at the left. The last figure may be uncertain to several units.

	0	2	3	4	5	6	7	8	9	10
(1)	−0.74788	−0.78307	−0.74886	−0.77013	−0.76224	−0.75723	−0.76968			
(2)	− .78307		− .78350	− .80271	− .79739	− .78392	− .78388			
(3)	− .78350			− .80348	− .79819	− .78481	− .78493			
(4)	− .80348				− .80359	− .80457	− .80458	−0.80442	−0.80364	−0.80525
(5)	− .80359					− .80462	− .80463			
(6)	− .80462						− .80465			
(7)	− .80465									
(7′)	− .80458							− .80553	− .80516	− .80526
(8′)	− .80553								− .80611	− .80620
(9′)	− .80611									− .80642

atically as we increase the number of terms already present in the combination to which it is added. (It must be clearly understood that when we speak of "adding" a term to a function, we mean simply that the given term is added to the list of terms from which the function is formed. The new function will not be the sum of the given term and the previous function, because when the best possible combinations of the two sets of terms are made, the coefficients will not preserve their values, or even their ratios. As a matter of fact, we have not even determined the coefficients except in the case of the best functions found.) This regularity is a great help in estimating the possible improvements from omitted terms. If, at any stage in building up a function, one or more terms are found to be of negligible value, it can be confidently predicted that they will never become more valuable as the complexity of the function increases, and they may be thrown out once for all.

In the present calculation with $\delta_1=\delta_2=0.75$, this regularity of convergence did not appear, a fact which we ascribe to the obvious unsuitability of the choice of δ's. Table I shows a marked example of "cooperation" between several terms which together give more improvement than the sum of their individual contributions. Considering the first four functions, it will be seen that A is improved by 0.0005 on addition of [00100] to form B, by 0.0016 on addition of [20100] and [21100] to give C, and by 0.0045, more than twice the sum of the individual improvements, when all three terms are put in to give the function D. As a result of this lack of regularity, it was impossible to form any really satisfactory estimate of the convergence limit in this case.

When the δ's were taken as 0.5 and 1, no such irregularity was noted. As this is a typical case of the application of our method, we shall present a fairly detailed description of the process of determining the best simple function and estimating the allowance for convergence.

The terms not involving ρ were first numbered in the following manner, arbitrarily, except that a few of the terms expected to be most important were put first:

1	[10100]	6	[10010]	11	[11010]
2	[00100]	7	[00010]	12	[02100]
3	[11100]	8	[00300]	13	[01120]
4	[00120]	9	[20100]	14	[11120]
5	[10120]	10	[01100]	15	[01300]

A function containing a set of these terms will be indicated by a sum of the corresponding numbers, and the following abbreviations will be employed:

$$(n)=1+\cdots+n\,;\ (n')=(n)-5-6\,;\ (n'')=(n')-7.$$

In Table III there will be found the energies associated with functions containing such sequences, plus one other term. Examination of this table will show how consistently one finds the importance of a particular term in a function unchanged or decreased on the addition of another term or terms, particularly if several functions are already present. It will be noted that the most essential terms are 1, 2, and 4, and that the function (7′) is practically as good as (7). This observation was the basis for omitting further consideration of terms 5 and 6. It will be noted also that 7 seems to be unimportant when 10 is present. It was indeed found that (10″) gave the energy −0.80632; this function was accordingly taken as the basis in the further investigations. The negligibility of 9 was also noted, (10″)−9 giving an energy of −0.80619, but at this stage in the work it was more convenient to retain this term.

The usefulness of the functions 11, 12, 13, 14, and 15 was next tested by adding them singly to (10″). The results:

$$(10'')+11\sim-0.80650\,;\quad (10'')+12\sim-0.80648\,;$$
$$(10'')+13\sim-0.80683\,;\quad (10'')+14\sim-0.80632\,;$$
$$(10'')+15\sim-0.80632.$$

The retention of 13 was thus indicated, and the function (4)+8+10+13∼−0.80670 was chosen as the basis for further work. In obtaining this function the neglect of eight terms had involved losses totalling 0.00064∼0.017 ev; the complete

fifteen-term function would thus in all probability have given an energy differing from -0.80670 by less than this amount.

Examination of the relative importance of the terms in the following sets, where just one index varies, will show how rapidly the importance of a term falls with the increase of one of the indices, especially when this rises above 1: 2, 1, 9; 1, 3; 4, 5; 7, 6; 8, 15; 2, 10, 12; 4, 13; 3, 14; 8, 15. A very minor exception seems to be offered by the term 11, which was itself negligible.

Inspection of these results leads us to the following estimates of the improvements available on addition of remaining terms in the indicated sequences:

$[0n100]\sim 0.00005$; $[n1100]+[1n100]\sim 0.00015$; $[n0120]\sim 0.00002$; $[mn120]\sim 0.00000$; $[0n120]\sim 0.00010$; $[0n300]\sim 0.00000$; $[mn300]\sim 0.00005$; $[n1010]+[1n010]\sim 0.00005$; $[n0010]\sim 0.00010$; $[m03n0]\sim 0.00000$; $[003n0]\sim 0.00020$; $[00n00]\sim 0.00015$; $[mnj00]\sim 0.00005$; $[001n0]\sim 0.00015$; $[011n0]\sim 0.00010$; $[mn1j0]\sim 0.00005$.

Adding to these amounts the quantities neglected in the construction of the simple function, we obtain $0.00186\sim 0.050$ ev. This amount should be a very safe upper limit for the improvement obtainable from the addition of an indefinite number of terms not depending on ρ, and in view of the usual nonadditivity of small improvements 0.03 ev would appear to be a safe estimate of the change to be expected.

To the seven-term function not involving ρ five terms in ρ were next added: $[00101]$, $[10101]$, $[01101]$, $[11101]$, $[10121]$. Of these only the first two proved to be worth keeping, the resulting nine-term function giving an energy of -0.80906, while the complete twelve-term function gave -0.80918. The improvement available from addition of further terms in ρ was estimated to be not more than 0.01 ev.

In the study of the basic state of H_2 it was found that the convergence on addition of terms not involving ρ was much more rapid if there were already present in the function terms which did depend on ρ. (It will be noted that this is not simply a special case of "regular" convergence, since two different limits are involved.) Though in this state the r_{12} terms are much less important than in the basic state, it is to be expected that a similar effect will exist here. In view of this we have estimated that the convergence limit is probably less than 0.03 ev below the energy of our best function, -0.80906, and can be said to be -0.8100 ± 0.0007 with considerable assurance.

MARCH, 1936 JOURNAL OF CHEMICAL PHYSICS VOLUME 4

A Study of the Franck-Condon Principle

ALBERT SPRAGUE COOLIDGE, HUBERT M. JAMES AND RICHARD D. PRESENT, *Harvard University and Purdue University*

(Received November 26, 1935)

The validity of the Franck-Condon principle has been investigated in connection with its application to the calculation of spectral intensities in the continuous radiation due to the transitions between the $1s\sigma 2s\sigma\ {}^3\Sigma_g$ and the $1s\sigma 2p\sigma\ {}^3\Sigma_u$ states of H_2. For the latter state, a potential curve was constructed on the basis of the authors' theoretical calculations. For the former state, a curve was computed from spectral data by Dunham's method. Accurate wave functions for both states were determined by mechanical integration with the differential analyzer. Transition probabilities from the first four vibrational levels of the stable state were determined by mechanical integration, both for the case that the electric moment matrix element is constant (as assumed in the Franck-Condon method) and for the case that it is a linear function of the nuclear separation. In addition integrals were determined which permitted the calculation of the probability of excitation of the several vibrational levels by electron impact from the ground state, upon the basis of an extension of the Franck-Condon method. The spectral intensities so obtained are compared with those given by several forms of approximate calculation, and the discrepancies critically discussed. Comparisons are also made with the experimental work of Smith and of Finkelnburg and Weizel. It is concluded that the Franck-Condon principle leads to results definitely incompatible with their observations. Indications are found that other transitions than the one treated in this work are contributing appreciably to the radiation observed by Smith. An analysis of the spectrum observed by Finkelnburg and Weizel leads to a critical discussion of the method used by them in deducing the potential curve of the repulsive state, from which is drawn the conclusion that this curve is without quantitative significance.

Introduction

IN the preceding paper[1] a sharp disagreement was found to exist between the theoretical potential curve for the Heitler-London repulsive state of H_2 and that deduced by Finkelnburg and Weizel,[2] who applied a rough form of the Franck-Condon principle in interpreting their observations on the excitation of the continuous hydrogen spectrum. Our purpose in the present paper is to subject this principle to a careful scrutiny, investigating the fundamental assumption and comparing the crude form commonly used with more rigorous approximations. Our results will then enable us to make a critical analysis of the procedure of Finkelnburg and Weizel, and to obtain a satisfactory correlation between our computed curve and their experimental results.

The continuous near ultraviolet spectrum of hydrogen is produced by transitions from the various quantized vibrational levels of the $1s\sigma 2s\sigma\ ^3\Sigma_g$ electronic state to the continuous levels of the $1s\sigma 2p\sigma\ ^3\Sigma_u$ state. (See Fig. 1.) The population of the upper state is maintained by electron-impact excitation from the ground state, of which only the lowest vibrational level is usually present in important amount, while the resulting distribution among the vibrational levels of the upper state depends upon the velocity distribution of the exciting electrons. Where the latter is known, as in the experiments of Finkelnburg and Weizel, a theoretical prediction of relative spectral intensities can be carried out, provided we have knowledge of the potential curves and vibrational wave functions of the three electronic states involved, and make use of the Frank-Condon principle for both excitation and radiation probabilities. A much simpler case to treat is that where the radiation comes from a single vibrational level, so that only radiation probabilities need to be considered. An example may be furnished by the work of Smith[3] on the spectrum from H_2 in the presence of excess He, which he believes to quench all radiation except that from the lowest vibrational level.

Of the three electronic states concerned, the ground state is accurately known, both experimentally and theoretically. The upper state, $^3\Sigma_g$, may be determined with considerable precision, as it is the lower state of several prominent and well-known band systems. With the aid of the information about the repulsive state yielded by the calculations of the previous paper, we are in a position to make critical tests of the Franck-Condon principle, by finding out how far the spectral intensities calculated with its use agree with the observations of Finkelnburg and Weizel and of Smith.

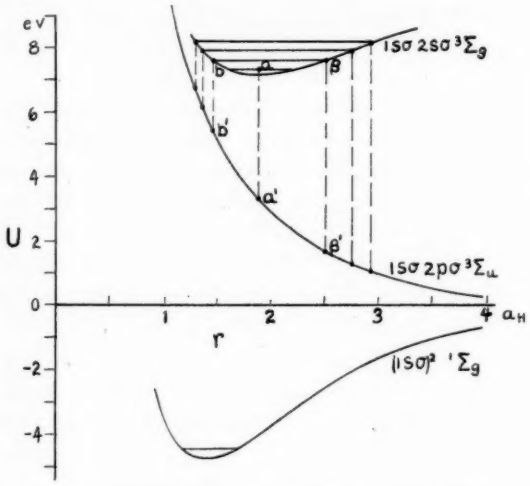

FIG. 1. $U(r)$ curves and vibrational levels for H_2.

Of the electronic states involved, the ground state is the only one for whose potential curve and vibrational wave functions simple analytical expressions were used. For the excited states, the determination of the wave functions and the evaluation of the transition probabilities were effected by mechanical means. In accomplishing this, we have been fortunate in commanding the powerful assistance of the differential analyzer of Massachusetts Institute of Technology, which the engineering department kindly made available to us.

The Franck-Condon Principle

The Franck-Condon principle applies to the calculation of transition probabilities between molecular states belonging to different electronic levels. The fundamental assumption of both the

[1] H. M. James, A. S. Coolidge and R. D. Present, preceding paper.
[2] W. Finkelnburg and W. Weizel, Zeits. f. Physik **68**, 577 (1931).
[3] N. D. Smith, Phys. Rev. **49**, 345 (1936).

classical and the wave-mechanical forms of this principle is that in changes of electronic states the accompanying changes in the vibrational states of the nuclei depend only on the character of the nuclear motions in the two states. In classical terms, the small mass of the electrons is presumed to prevent their determining to an appreciable extent what happens to the heavy nuclei, except as they provide the potential fields in which the nuclei move in each state. In terms of wave mechanics, the transition probabilities depend upon the matrix elements between the given states of the electronic contributions to the electric moment, and the essence of the principle is the assumption that in calculating these matrix elements we need consider only an integration over the coordinates of the nuclei. It is supposed that the integration over the electronic coordinates would give a result which is independent of the positions and motions of the nuclei (at least within the range of nuclear coordinates where the nuclear part of the wave functions is appreciable) and which therefore need not be evaluated if only relative transition probabilities are desired.

In order to formulate this more specifically, let us start with the quantum-mechanical expression for the energy radiated in spontaneous transitions between two quantized states a, a' of a molecule. The energy, per second, per molecule present in the upper state, is[4]

$$A_{aa'}=4(2\pi\nu)^4/3c^3\times|\mathbf{D}_{aa'}|^2, \qquad (1)$$

where ν is the frequency radiated, and $\mathbf{D}_{aa'}=\int\psi_a\mathbf{D}\psi_{a'}d\tau$ is the matrix element between a and a' of the variable part of the electric moment. We must assume that the complete wave function for either state may be adequately represented as the product of two factors, one describing the state of the nuclei, while the other, referring to the electrons, contains the nuclear coordinates only as parameters. This approximation amounts to treating the nuclei as though they moved in a force-field derived from a potential; it is sufficiently accurate for our purpose, even with so light a molecule as H_2. Then the electric moment with which we are concerned is that with respect to the center of the internuclear axis, and only the electrons contribute to it.

Let us consider a diatomic molecule in a Σ state; we represent the positions of the nuclei by their separation r and the polar angles φ, θ, while the unspecified electronic coordinates (relative to the center of gravity and the figure axis) are designated $r_1, r_2, \cdots r_n$. We may then write[5]

$$\psi_a=\psi_{e,\,v,\,K,\,M}=F_e(r;r_1,r_2,\cdots r_n)\times R_{evK}(r)r^{-1}P_{KM}(\varphi,\theta). \qquad (2)$$

Here, e, v, K, M are quantum numbers; F_e is the electronic factor, which does not involve the angles; P_{KM} is a surface harmonic. R_{evK}, the radial or vibrational function, is conveniently defined in connection with the factor r^{-1}, as this simplifies future operations; it is a solution of the Schrödinger equation

$$R''-K(K+1)r^{-2}R+8\pi^2\mu h^{-2}(E-U_e(r))R=0. \qquad (3)$$

where $U_e(r)$ is the potential due to nuclear and electronic interactions, and E is a proper energy value. Now, if we multiply the product of two such ψ's by any vector function such as $\mathbf{D}$, which is centrally symmetrical in the r_i, and integrate over r and the r_i, holding the angles fixed, the Σ symmetry insures that the resulting vector will have a component only along the figure axis. Designating the angle between this axis and the x-direction as θ, we obtain

$$(\mathbf{D}_{evKM,\,e'v'K'M'})_z=\int\int\cos\theta\sin\theta d\theta d\varphi P_{KM}(\varphi,\theta)P_{K'M'}(\varphi,\theta)\times\Big|\int dr R_{evK}(r)R_{e'v'K'}(r)\int\int\cdots\int dr_1dr_2\cdots dr_n\mathbf{D}(r_1,r_2,\cdots r_n,\phi,\theta)\times F_e(r;r_1,r_2,\cdots r_n)F_{e'}(r;r_1\cdots)\Big|. \qquad (4)$$

The y- and z-components will differ only by angle factors in the first integral; in any case, this integral vanishes unless $K=K'\pm1$.

Now it has been shown by Gibson, Rice and Bayliss[6] that the remainder of this integral is practically independent of K. We shall not at-

[4] P. A. M. Dirac, *Quantum Mechanics* (1930), p. 232.

[5] M. Born and R. Oppenheimer, Ann. d. Physik **84**, 457 (1927).

[6] G. E. Gibson, O. K. Rice and N. S. Bayliss, Phys. Rev. **44**, 193 (1933).

tempt to resolve the radiation from the different rotational levels, but shall consider only the total radiation for each vibrational transition. We shall also suppose that in the cases to be studied the distribution of radiating molecules among the rotational states is the same for each vibrational state. Then the total effect of the weighting factors arising from the angle integrations will be the same for each v, and we may write

$$I_{ev,\,e'v'}=N_vA_{ev,\,e'v'}$$
$$=CN_v\nu^4[\int drR_{ev}(r)R_{e'v'}(r)D_{ee'}(r)]^2, \quad (5)$$

where

$$D_{ee'}(r)=|\iiint\cdots\int dr_1dr_2\cdots dr_n$$
$$\times\mathbf{D}(r_1, r_2, \cdots r_n, \phi, \theta)F_e(r; r_1r_2\cdots r_n)$$
$$\times F_{e'}(r; r_1, r_2, \cdots r_n)|, \quad (6)$$

N_v is the total population of the vth level, and C is an unknown constant.

The Franck-Condon principle rests on the assumption that $D_{ee'}(r)$ varies so slowly, $R_{ev}(r)R_{e'v'}(r)$ so rapidly, with r, that the former factor may be replaced by an average value, taken in front of the integral sign, and absorbed in the constant C. The problem of comparing transitions between different vibrational states of the same pair of electronic states is thus reduced to that of evaluating the overlap integral of the vibrational wave functions. In the absence of any specific information about the nature of the quantity $D_{ee'}(r)$, this assumption is recommended primarily by its convenience. It should be most satisfactory in cases in which at least one of the sets of vibrational wave functions concerned is concentrated into a small range of r, as with heavy molecules with strong binding and low vibrational quantum numbers. It is least likely to work in a case like H_2, where even in the lowest vibrational levels the wave function has a considerable range in r; this is, therefore, an especially favorable opportunity to test the validity of the assumption.

Even with the aid of the Franck-Condon assumption one must have information about the vibrational wave functions in order to calculate transition probabilities. In the absence of such information, additional assumptions must be introduced. The most common one (adopted by Finkelnburg and Weizel) is equivalent to replacing each wave function by a constant times a δ function at the classical turning point, or by two such functions if there are two such points (stable molecules), except that levels with $v=0$ are represented by a single δ-type function at the equilibrium point. Transitions are thus possible only between states having the same turning points (counting the equilibrium distance as the turning point of the ground state). Another approximation, due to Condon,[7] treats one wave function (specifically, that of a repulsive state) like a δ function, while retaining the true form of the other (stable state). The overlap integral is therefore simply the value of the discrete wave function at the turning point of the state in the continuum, and the distribution of radiation intensity can be found from the square of this function by projecting it upon the vertical energy axis by means of the repulsive potential curve, and multiplying by the proper frequency factor.

Eq. (5) gives the intensity of each line in a discrete spectrum arising from transitions between two stable states. When one state lies in the continuum, we require, not the energy per line, I, but the energy per unit of spectral width, which we shall call I_λ when measured on the wave-length scale and I_ν when measured on the frequency scale. We may regard this as obtained on multiplying I by the (infinite) number of adjacent states associated with radiation which lies in the band of width $d\lambda$ or $d\nu$. Thus, $Idn=I_\lambda d\lambda=I_\nu d\nu$. It is easy to show by the method of artificial quantization that corresponding to Eq. (1) we have in this case

$$A_\nu=4(2\pi\nu)^4(2\mu)^{\frac{1}{2}}/3E^{\frac{1}{2}}c^3\times|D_{aa'}|^2, \quad (7)$$

$$A_\lambda=4(2\pi)^4c^2(2\mu)^{\frac{1}{2}}/3E^{\frac{1}{2}}\lambda^6\times|D_{aa'}|^2. \quad (8)$$

Here E is the energy above dissociation of the state in the continuum, and $D_{aa'}$ is the matrix element of D between a normalized discrete function a and a function a' in the continuum so normalized that the radial factor R reduces to a sine wave with amplitude 1 at large distances. The final expression for the energy radiated in transitions from the quantized state e, v to the band of continuous levels of the elec-

[7] E. U. Condon, Phys. Rev. **32**, 858 (1928).

tronic state e', whose energies lie close to E', so as to fill a spectral interval of width $d\lambda$, is found to be

$$(I_\lambda)_{ev,\ e'E'} = CN_v\nu^6E'^{-4} \times[\int drR_{ev}(r)R_{e'E'}(r)D_{ev'}(r)]^2. \quad (9)$$

The corresponding Franck-Condon expression is

$$(I_\lambda)_{ev,\ e'E'} = C'N_v\nu^6E'^{-4}M^2_{ev,\ e'E'}, \quad (10)$$

where M is the overlap integral $\int drR_{ev}(r)R_{e'E'}(r)$.

The Franck-Condon principle may be extended to the calculation of probabilities of excitation by electron impact, the reasoning being closely similar.[8] It would lead us to expect the changes in rotational state of a molecule with change of electronic state to be small, and to be essentially independent of the changes in vibrational state. Applying a more careful treatment to these latter transitions one finds a probability proportional to

$$[\int G_{ee'}(r)R_{ev}(r)R_{e'v'}(r)dr]^2,$$

where $G_{ee'}$ is the matrix element of the perturbing function between the electronic states e and e'. In the case of a singlet-triplet transition, this depends on the energy of the exciting electrons, V, in a way which may be taken as proportional to the excess of this energy over a certain critical value, V_v (the excitation potential of the vth vibrational level) provided this excess is not too large.[9] If we now assume that $G_{ee'}$ is so slowly varying a function of r that it may be taken outside the integral sign, we obtain an approximation corresponding to the Franck-Condon approximation in the treatment of radiative transitions. We can then write for the excitation probability

$$F_{ev,\ e'v'} = K(V-V_v)M^2_{ev,\ e'v'}. \quad (11)$$

If the interesting transitions all take place from the rotational levels of a single vibrational state, the distribution among the rotational states of each final vibrational state will be essentially the same; in treating radiative transitions arising from such a distribution one might then employ Eqs. (9) or (10).

[8] N. F. Mott and H. S. W. Massey, *The Theory of Atomic Collisions* (1933), p. 209.

[9] See, for instance, the computations on the excitation of the transition $(1s\sigma)^2\ {}^1\Sigma_g - 1s\sigma 2p\sigma\ {}^3\Sigma_u$ by H. S. W. Massey and C. B. O. Mohr, Proc. Roy. Soc. **A135**, 258 (1932) or the observations on singlet-triplet excitations in Hg by W. Schaffernicht, Zeits. f. Physik **62**, 106 (1930).

Location of Potential Curves

For the $1s\sigma 2s\sigma\ {}^3\Sigma_g$ potential curve it would possibly have been sufficiently accurate to use a Morse curve, for which the exact wave functions are known. However, since the use of the integrating machine made it possible to determine accurate wave functions for any potential, it seemed worth while to attempt to improve upon the Morse approximation, finding a curve which would give energy levels (rotational and vibrational) in somewhat better agreement with experiment.

As a starting point, we have taken the elaborate analysis of Dunham,[10] who has assumed a potential curve represented by $U(\xi)=a_0\xi^2(1+a_1\xi+a_2\xi^2+\cdots+a_6\xi^6)$; $\xi=(r-r_e)/r_e$, r_e being the equilibrium value of r. In terms of the 8 constants in this expression Dunham derives other constants Y_{lj} such that the term value of the Kth rotational, vth vibrational state can be expressed as $F_{vK}=\Sigma_{lj}Y_{lj}(v+\frac{1}{2})^l K^j(K+1)^j$. Our problem was first, to find a set of Y's which would fit the observed term values, and second, to deduce the corresponding constants in the potential function.

Now, Richardson and Davidson[11] have found that the term values for this state can be satisfactorily expressed, for not too large values of v and K, by the finite series

$$F_{vK}=2594.30v-70.43v^2+0.90v^3+0.04v^4 +[33.386-1.6497v+0.0212v^2](K+\tfrac{1}{2})^2.$$

This series was obtained in a form suitable for use with the old quantum theory. Upon conversion to an expression involving $v+\frac{1}{2}$ and $K(K+1)$ instead of v and $(K+\frac{1}{2})^2$, we obtain seven of the desired Y's: Y_{10}, Y_{20}, Y_{30}, Y_{40}, Y_{11}, Y_{21}, and Y_{31}. Since there are eight parameters in the potential function to be determined another condition is needed; this was chosen as the requirement that the ratios of successive a_n's should not change erratically. This somewhat indefinite condition was sufficient to fix an approximate value for a_6, and it was found that

[10] J. L. Dunham, Phys. Rev. **41**, 721 (1932).

[11] O. W. Richardson and P. M. Davidson, Proc. Roy. Soc. **A125**, 23 (1929).

neither the other a's nor the value of $U(\xi)$ in the important range was more than slightly sensitive to the choice of a_6.

By a method of successive approximations we have determined the following potential curve, which according to Dunham's formulas would give accurately the seven Y's adapted from Richardson and Davidson:

$$\omega_e = 2664.88 \text{ cm}^{-1},\ B_e = 34.2228 \text{ cm}^{-1},\ r_e = 0.986\text{A},$$
$$U(\xi) = 6.400\xi^2(1 - 1.6333\xi + 1.9397\xi^2 - 2.147\xi^3 + 2.491\xi^4 - 3.076\xi^5 + 3.3\xi^6) \text{ ev.}$$

It should be noted that the term values associated with this potential curve are not necessarily just those given by the 7-term equation of Richardson and Davidson, for Dunham's formulas assign small but not vanishing values to the higher Y's.[12] Richardson and Davidson, using the Bohr theory formulas relating term values to the parameters appearing in $U(\xi)$, obtained $U(\xi) = 6.24\xi^2[1 - 1.6375\xi + 1.943\xi^2 - 2.15\xi^3 + 2.5\xi^4]$. The close agreement of our values with theirs is somewhat surprising when one considers the differences in the methods of quantization, especially since the quantum condition employed in deriving their formulas was $\oint p dq = vh$ rather than $\oint p dq = (v + \frac{1}{2})h$, so that the zero-point vibrational energy was neglected.

A potential function in the form of a finite polynomial can be a good approximation only for small values of ξ. For large positive ξ the true function approaches a limiting value asymptotically and rapidly. An infinite series (for example, the series expansion of $e^{-\xi}$) can reproduce this behavior, but any finite series must, as ξ increases, eventually become dominated by the term of highest degree, increasing or decreasing rapidly. In order to estimate the error in our function caused by omission of the higher terms, we have compared it with another series in which a_6 was chosen as zero and the other coefficients selected so as to reproduce the seven Y's when substituted in Dunham's equations. This procedure is open to the objection that a series terminating with a_5, a negative quantity, does not satisfy Dunham's boundary conditions; it is safe to assume, however, that for small values of ξ where the function is found to be but slightly sensitive to the value of a_6 the error due to omitting higher terms is even slighter. In view of the regular alternating values of the coefficients, it is apparent that if the series were extended its value for small positive ξ would be found below that of the series terminating with ξ^6, and above that ending with ξ^5. The values of these series are shown in Table I for various values of ξ, under the respective headings U_6 and U_5. For comparison, we have also computed $U_M = 3.029(1 - e^{-1.471\xi})^2$, the potential curve constructed as suggested by Morse.[13] It will be seen that for ξ up to 0.3 or 0.4, U_6 and U_5 agree with each other better than with U_M, and may be taken to be an improvement upon U_M. For larger ξ, U_6 is definitely too high, U_5 too low, the mean being, however, still below U_M. As the best compromise, we have taken for our potential curve for $\xi < 0.5$ the mean of U_6 and U_5, the first being assigned three times the weight of the second. Above $\xi = 0.5$ we have extrapolated a curve following the general course of U_M but falling gently below it. For negative ξ the sharp rise in U limits the range of interest to small values, where U_6 may be confidently accepted. The fact that it does not reproduce the singularity which the true function must have at $\xi = -1$ is of no practical importance, as the wave function is there wholly negligible in any case.

Our work with the ground state involved only

TABLE I. *Potential curves for* $^3\Sigma_g$. $U(\xi)$ *in ev.*

ξ	U_M	U_5	U_6
−0.3	0.932	1.011	1.010
−0.2	0.354	0.366	0.365
−0.1	0.076	0.076	0.076
0.0	0.000	0.000	0.000
0.1	0.055	0.055	0.055
0.2	0.192	0.189	0.189
0.3	0.377	0.369	0.370
0.4	0.588	0.569	0.579
0.5	0.803	0.754	0.818
0.6	1.024	0.845	1.133

[12] Since this work was carried out, Sandeman [Proc. Roy. Soc. Edinburgh **55**, 49 (1935)] has published an account of an essentially similar investigation. His treatment differs from ours in that he made a new analysis of the spectral term values and employed six Y's to determine a series ending with a_4. In applying Dunham's formulas he made certain (probably good) approximations. His potential curve differs from ours in lying nearer to the Morse curve for $\xi < 0.3$ and diverging from it for smaller ξ than does ours. He also gives an interesting discussion of the uncertainties involved in applying this method.

[13] P. M. Morse, Phys. Rev. **34**, 57 (1929).

the lowest vibrational level. The potential curve therefore did not have to be accurately known over more than a small range, within which we assume it to be given by the Morse function

$$U=4.723(1-e^{-1.024\xi})^2,$$

with $r_e=1.4a_H$.

For the repulsive state we constructed two potential curves (Fig. 2), between which we believe the true curve must lie for $r>1.5a_H$. The upper curve passes through the three computed energies[1] at $r=1.5$, 1.6, and $1.87a_H$, with the same small allowance for convergence as was carefully estimated for $r=1.5a_H$. It coincides with the Heitler-London curve for $r=3$, and in the intermediate portion is interpolated in as flat a curve as looks plausible. The lower curve passes through our computed points at $r=1.5$ and 1.6, which we believe to be quite accurate, and through the Heitler-London point at $R=4$. At $r=3$ the curve is below the Heitler-London curve by an amount equal to 30 percent of the interaction energy. This seems a safe outside limit for the error in the Heitler-London method at this distance, in view of the fact that for the ground state it gives the interaction energy with an error of only 32 percent at the much smaller distance $r=1.5$. The most probable curve, as given in the previous paper, lies between these two curves, nearer the lower one for small r and nearer the upper one for large r. For $r<1.5a_H$ in each case we have used the curve as given there.

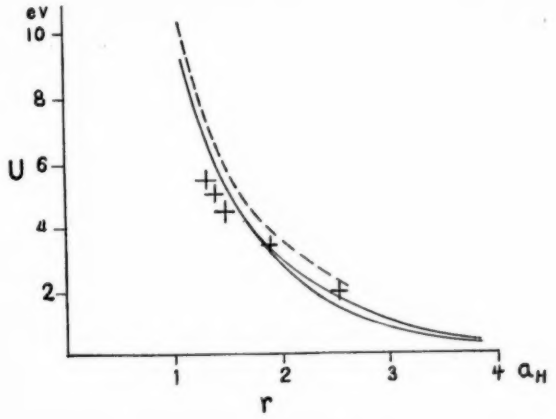

FIG. 2. $U(r)$ curves for the Heitler-London repulsive state. Solid lines are the potential curves used in this work. + indicates a point obtained by the construction of Finkelnburg and Weizel. Broken line is approximately the potential curve needed to give agreement with observation if the Franck-Condon approximation is used.

USE OF THE DIFFERENTIAL ANALYZER

The work of finding the wave functions belonging to potential curves of the excited states, and of evaluating the normalization, overlap and other integrals, was performed with the differential analyzer. The machine (for a description of which see the paper by Bush[14]) is capable of turning out progressively the solution of an ordinary differential equation which follows from the arbitrary starting conditions to which the machine is initially set; at the same time it can evaluate definite integrals involving the solution being generated. In our case it was desired to find the wave functions as solutions of the equation

$$R''+(E-U(r))R=0,$$

or

$$R'=-\int(E-U)Rdr. \tag{12}$$

In this equation, $U(r)$ is one of the potential curves already described, and was introduced into the machine in the form of a carefully prepared graph, the scale being so chosen that the constant factor in the Schrödinger equation reduced to unity. Simultaneously, it was desired to determine one or more of the integrals $\int R^2dr$, $\int RSdr$, $\int R^2Sdr$, and $\int RSrdr$, over the range of r covered, S being a second function of r, introduced graphically. The machine was therefore set up as shown in Fig. 3, in the notation of Bush. (Scales, gear ratios, and directions of rotation have been omitted.)

INVESTIGATION OF THE $1s\sigma 2s\sigma\ ^3\Sigma_g$ STATE

Our first concern was to control the potential curve calculated for the $^3\Sigma_g$ state by verifying that its proper energy levels are such that their separations are in agreement with experimental data. This step also furnished the wave functions required for further work. The proper energy is the value of E such that the solution of the differential equation obtained by starting with the correct initial conditions either to the left

[14] V. Bush, J. Frank. Inst. **212**, 447 (1931).

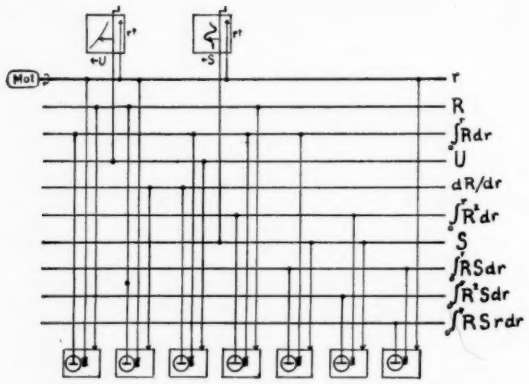

FIG. 3. Connections for the differential analyzer.

or to the right of the "classically accessible region" (i.e., the region where $E-U$ is positive) will increase rapidly to a point of inflection at the first turning-point ($E-U=0$), oscillate through $v+1$ maxima and minima to a second point of inflection at the second turning point, and thereafter decrease steadily, approaching the axis asymptotically if working toward the right, touching it at the origin if toward the left. This last steady decrease was never actually obtained. In the terminal region, the integration is the opposite of self-correcting, and the magnification of errors in the energy setting, in the operation of the machine itself, or in following the potential curve inevitably causes the function sooner or later to diverge violently, either above the axis or below. It was possible, however, to determine the proper energy with sufficient precision as the mean of two slightly different values, the wave functions corresponding to which were in very close agreement over the initial range and the classical range, but eventually diverged, becoming infinite in opposite senses. The same proper energy resulted from runs in the opposite direction.

Since the zero-point vibrational energy is not experimentally known we were forced to find it by a process of trial and error, obtaining $E=0.170$ ev for $v=0$. This may be confidently accepted, as that portion of the potential curve which is of importance in determining the lowest wave function lies close to the position of equilibrium, where there can hardly be any serious error in the curve. For $v=1$, we found E greater by an amount in very good agreement with the experimental value for the separation of these two levels, but this was not the case for $v=2$ and $v=3$. Since the energy separations are known directly from experiment, while the potential curve rested upon an involved process of construction, it appeared logical to attempt to modify the curve in such a way that it would more closely reproduce the observed energy levels. We found that such a curve could be produced by depressing the original curve slightly in the region $1.25<\xi<1.4$, and elevating it in the region $1.4<\xi<1.65$, the change nowhere exceeding 0.02 ev.

On comparing the wave functions laid down from the two directions (discarding, of course, the terminal portions vitiated by incipient divergence) we observed the same sort of systematic differences as were noted in preliminary tests of the machine, a gradual increase in amplitude and a slight displacement in the positions of the nodes and loops in the direction toward which the machine was operating. We were informed that the machine could in general be trusted to one percent, and that the drift in the amplitude of an oscillating function was a recognized exception. The functions finally adopted were constructed by a process which can be roughly described as averaging the results of runs in both directions over the classical region where the effects of incipient divergence were neglible, and slightly modifying the initial, nonclassical portions of the runs in each direction so as to fit them smoothly to the central portion. As the magnitude of the adjustments seldom exceeded one percent of the maximum value of the functions, it does not seem worth while to go further into details.

The correctness of a potential curve cannot be established solely by showing that it reproduces observed vibrational energy levels. Corresponding to a given set of such levels there can be an infinite series of potential curves, derived from each other by a distortion in the general nature of a horizontal shear. The correct curve can be selected only by considering rotational energy as well. As a further check on our adjusted potential curve, and on its wave functions, we have used the latter to compute values of B_v, the coefficient of $K(K+1)$ in the term-value series, for comparison with experiment, accord-

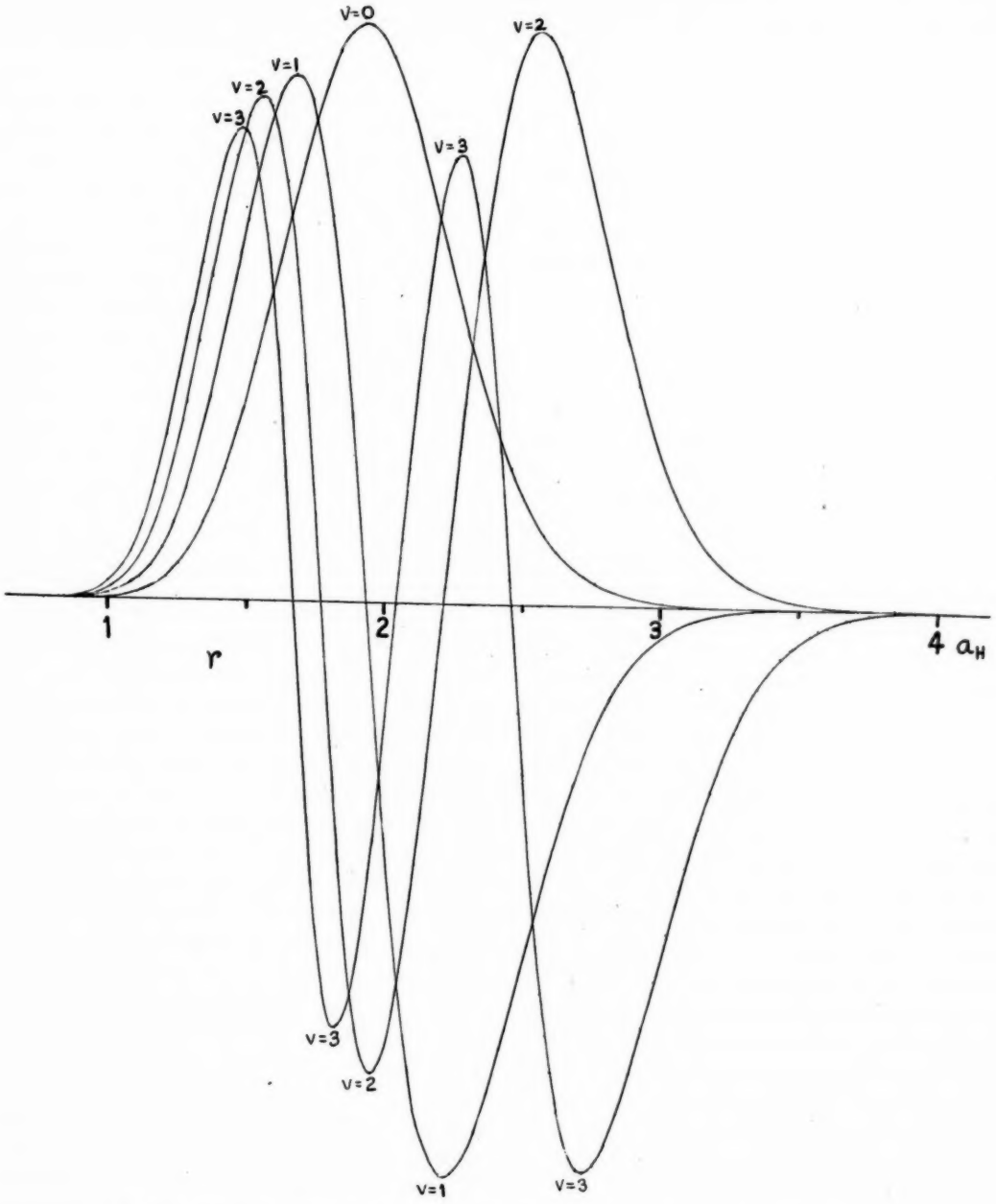

FIG. 4. Wave functions for the $1s\sigma 2s\sigma\ ^3\Sigma_g$ state. For normalization see the text.

ing to the formula

$$B_v = (h^2/8\pi^2\mu) \int R^2 r^{-2} dr / \int R^2 dr. \qquad (13)$$

(This was accomplished by setting the machine to produce $\int R^2 S dr$ with $S = 1/r^2$. Appropriate corrections for the slight modifications made on the wave function were applied in computing this and other integrals.) For the three lowest levels the average error was 0.15 percent, each result being correct to within the accuracy with which the machine records. For $v = 3$, our result was 1.2 percent too large, indicating that our

potential curve rose a little too steeply for large r. The agreement was, however, regarded as satisfactory for our purposes, and no further adjustments of the curve were attempted.

The wave functions for the four lowest levels are accurately reproduced in Fig. 4, where they have been brought to have approximately the same maximum amplitude. To normalize these functions comparably they should be multiplied by the following factors:

$v=0$, 1.000; $v=1$, 1.143; $v=2$, 1.202; $v=3$, 1.227.

In connection with the analysis of the work of Finkelnburg and Weizel we have required the relative values of the overlap integrals $\int R_v S dr$, where R_v is the vth radial function of the $^3\Sigma_g$ state and S is the radial function of the zeroth vibrational level of the $^1\Sigma_g$ ground state. For S we used the solution for the Morse potential of the ground state, which was known analytically. This was plotted and introduced in the course of the integrations which gave the $^3\Sigma_g$ wave functions. We found for the overlap integrals, when $v=0, 1, 2, 3$, the ratios $1.00 : 1.06_3 : 0.98_5 : 0.78_8$. The large value for $v=0$ is at first surprising, in view of the relative positions of the potential curves (Fig. 1). The equilibrium points of the two states differ by about $0.5a_H$, and the classically accessible regions for the lower states overlap but little. According to the crudest form of the Franck-Condon principle one would expect excitation to the upper $v=0$ level to be much less frequent than that to the three higher levels. The result which we have found arises in part from the rather high probability of this light molecule getting into the classically inaccessible region, and in part from the effect of the negative loops in the functions for $v\neq 0$, both of these being factors which are neglected in using the δ function approximations.

Investigation of the Repulsive State

In running the machine to produce wave functions associated with the repulsive potential curve, we had naturally always to proceed toward the right, as there is no outer boundary condition to start from. This did not produce any serious errors, however, as the rapid increase in errors noticed when working with the attractive state was due to the large negative value taken on by $(E-U)$ beyond the second turning point, and in this case $E-U$ remains positive, when once the classical region is entered. The systematic increase in amplitude was, of course, present; the effect was quite small, and was partially overcome by an appropriate correction. No allowance was made for the displacement of the positions of the nodes and loops.

We have already seen that it is convenient to take functions with unit limiting amplitude. In order to avoid lengthy integrations into the region where U is negligible, we have made use of the Wentzel-Brillouin-Kramers approximation, according to which the wave function may be regarded as a sine-curve with amplitude everywhere proportional to $(E-U)^{-\frac{1}{4}}$, in the region where $E-U$ changes slowly in proportion to the wave-length. Tests showed that, beyond the third or fourth loop, the heights of successive maxima of our functions obeyed this relation within the limit of error, when proper allowance for the secular increase due to machine error was made. It was therefore easy to determine the factor required to normalize each run to unit limiting amplitude. Four typical functions, computed for the higher of our repulsive potential curves, are plotted in Fig. 5, where they have been given the same maximum amplitude.

Simultaneously with the generation of R, the wave function of the repulsive state, we evaluated the integrals $M=\int RSdr$ and $L=\int RSrdr$. These integrals, in which S is one of the vibrational wave functions of the $^3\Sigma_g$ state, were needed for the proposed calculation of radiative transition probabilities. For the case $v=0$, they were determined over a range of energies E of the lower state, and for both modifications of the potential curve, in order to study the ultimate effect of modifying this curve. For other values of v we have employed only the upper curve, for reasons to appear later. The values obtained, reduced to functions normalized as described, are given in Tables II and III.

The ratio L/M, which is a sort of average value of r, is seen to be roughly equal to the turning point of the corresponding function on the $^3\Sigma_u$ curve; this relation might be useful in developing an approximate treatment of the theory of radiation in the case that $D_{ee'}(r)$ is not constant, but can be expanded in powers of r.

Approximate Forms of the Franck-Condon Computation

A study of the various current approximations to the complete Franck-Condon computation has been carried out in order to throw some light on the extent to which one may rely on the more easily applied procedures. Here we shall not be concerned with the legitimacy of the fundamental Franck-Condon approximation, but rather with the further simplifications which are so commonly made. H_2 is a particularly satisfactory system on which to make such a test, because of the small mass of the nuclei.

Table II. *Integrals L and M, upper* $^3\Sigma_u$ *potential curve.*

E (ev) above dissociated atoms	L	M	L/M	Turning Point
		$v=0$		
1.305	1.06	.42	2.52	2.76
1.740	3.40	1.41	2.41	2.49
2.175	6.72	2.97	2.27	2.29
2.610	10.16	4.76	2.14	2.12
3.045	11.74	5.84	2.01	1.97
3.480	11.18	5.93	1.89	1.84
3.914	9.30	5.27	1.77	1.73
4.349	6.75	4.09	1.65	1.64
4.784	4.30	2.80	1.54	1.56
		$v=1$		
1.305	− 4.17	−1.57	2.66	2.76
1.740	− 9.65	−3.85	2.50	2.49
2.175	−12.47	−5.28	2.36	2.29
2.610	−10.44	−4.70	2.22	2.12
3.045	− 3.90	−1.87	2.08	1.97
3.480	+ 3.07	+1.55	1.98	1.84
3.914	+ 7.50	+4.05	1.85	1.73
4.349	+ 8.53	+4.91	1.74	1.64
4.784	+ 7.14	+4.42	1.62	1.56
5.219	+ 5.11	+3.42	1.50	1.49
		$v=2$		
1.740	+13.38	+5.15	2.60	2.49
2.175	+ 7.83	+3.20	2.45	2.29
2.610	− 2.61	−1.12	2.35	2.12
3.045	− 8.83	−4.05	2.18	1.97
3.480	− 7.27	−3.54	2.05	1.84
3.914	− 1.07	− .57	1.89	1.73
4.349	+ 4.48	+2.46	1.82	1.64
4.784	+ 6.90	+4.12	1.67	1.56
5.219	+ 6.82	+4.30	1.59	1.49
		$v=3$		
1.740	− 7.56	−2.82	2.68	2.49
2.175	5.68	+2.20	2.58	2.29
2.610	9.52	+3.97	2.40	2.12
3.045	1.29	.58	2.23	1.97
3.480	− 6.79	−3.17	2.14	1.84
3.914	− 7.18	−3.58	2.01	1.73
4.349	− 2.06	−1.11	1.86	1.64
4.784	3.15	1.76	1.79	1.56
5.219	6.06	3.63	1.67	1.49
5.654	6.17	4.01	1.54	1.43

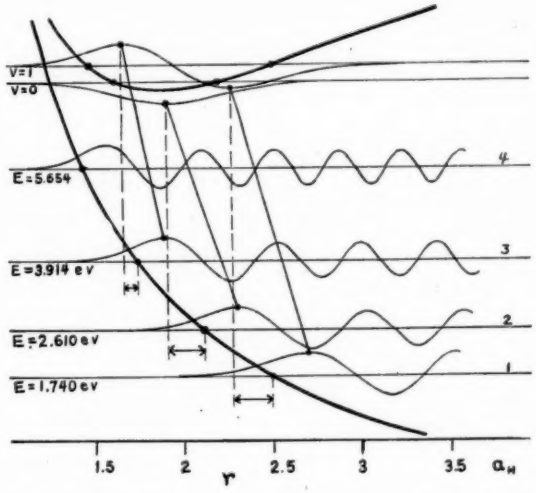

Fig. 5. Potential curves and typical wave functions for $1s\sigma 2s\sigma\ ^3\Sigma_g$ (upper) and $1s\sigma 2p\sigma\ ^3\Sigma_u$ (lower). Solid lines indicate transitions giving approximately the maximum radiation intensity. Arrows indicate discrepancies between locations of turning points of lower functions and maxima of upper functions.

The vibrational quanta are large in the discrete states, and in the interesting states of the continuum the oscillations of the radial function have a relatively great wave-length. The conditions are thus particularly unfavorable for the application of the classical concepts which lead one to the simpler forms of the Franck-Condon principle, and the errors associated with them in this case may be taken as a rough upper limit for all cases.

In Table IV and Fig. 6 we have summarized the results of six methods of computing the continuous spectra associated with the four lowest vibrational levels of the $1s\sigma 2s\sigma\ ^3\Sigma_g$ state. In each case the potential function for this state was represented by our best curve, while

Table III. *Integrals L and M, lower* $^3\Sigma_u$ *potential curve.*

E (ev)	L	M	L/M	Turning Point
		$v=0$		
1.305	2.48	1.02	2.44	2.76
1.740	5.31	2.31	2.30	2.49
2.175	8.12	3.72	2.18	2.29
2.610	10.32	4.98	2.07	2.12
3.045	10.87	5.54	1.96	1.97
3.480	10.13	5.48	1.85	1.84
3.914	8.25	4.73	1.74	1.73
4.349	5.73	3.53	1.63	1.64
4.784	4.06	2.64	1.54	1.56

TABLE IV. *Values of* λ *for maximum* I_λ.

F, complete Franck-Condon computation; *T*, correlation of turning points; *M*, correlation of maxima; *O*, maximum overlapping; *M–T*, correlation of maximum of discrete function with turning point in continuum; *R*, treatment of radial function in continuum as a δ function at the turning point.

v	*F*	*T*	*M*	*O*	*M–T*	*R*
0	2620	3160*	3608	3029	3010	2700
1	3280	5600	4923	3751	3650	3230
	2180	2090	2518	2294	2290	2220
2	3710	6850	6246	4336	4270	3550
	2540		2825	2592	2500	2450
	†	1870	2110	†	1970	†
3	3940	8600	——	4588	4820	
	2710		2992	2786	2580	
	2150		2272	2168	2070	
		1720	1881	†	1790	

* Corresponds to minimum in $U(r)$.
† Outside range computed.

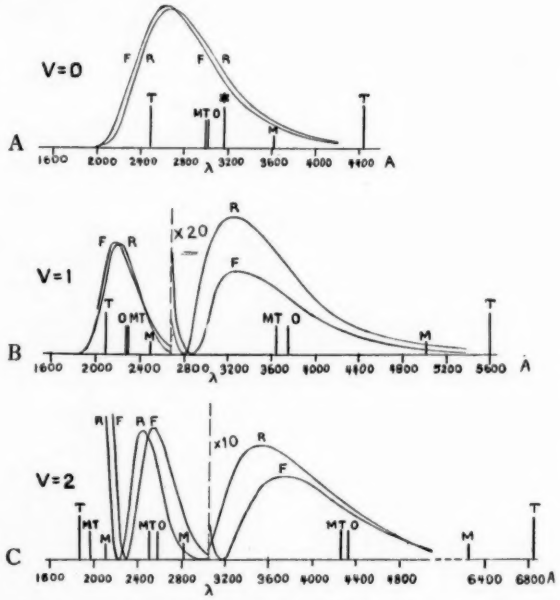

FIG. 6. Predictions of continuous spectra according to various methods. Vertical lines indicate positions of maxima of intensity. Note indicated changes of vertical scale.

the repulsive state was represented by the upper of the two approximate curves of Fig. 2. Method *F* is the complete Franck-Condon computation obtained when the integrals *M* of Table II are inserted into Eq. (10). (In Fig. 5 we have illustrated the relation of the wave functions involved in the transitions of maximum intensity, according to this method. State 2 is the corresponding end state for transitions from the $v=0$ level, while states 1 and 3 are similarly related to the $v=1$ level.) Method *R* is the reflection method used by Condon[7] and by Winans and Stueckelberg.[15] Method *O* results if the factor ν^6 in Eq. (10) is neglected. We have not computed the entire spectrum by this method, but have merely located the positions of maximum I_λ, which correspond essentially to maximum overlapping of the wave functions. The other methods give only the wave-lengths of maximum intensity. Method *T* is that of correlating turning points, as discussed in the introduction. (It will be recalled that for $v=0$ the minimum of $U(r)$ is used instead of the turning point. The corresponding entries in Fig. 6 and Table IV are marked with an asterisk, and the following discussion of the method does not apply to them. In Fig. 6, we have also included the two maxima which would be indicated if one were not to modify this method for $v=0$.) In method *M* the maximum intensity is supposed to be associated with transitions between states whose wave function have the maxima of their terminal loops at the same r, Method $M-T$, on the other hand, correlates the maximum of the discrete wave function with the turning point of the state in the continuum.

We now examine the approximations underlying the various methods, taking method *F* as the standard of perfection. Method *T* is the most commonly used and the most highly simplified. In arriving at this method it is customary to neglect the dependence of the intensity on ν, and to consider that in evaluating the overlap integral *M* one may neglect all save the terminal loops of the wave functions. Insofar as this is permissible, the arrangement giving maximum overlapping will be very nearly that for which the maxima of the terminal loops coincide. On this basis it is the method *M* which recommends itself; the utility of method *T* will depend on the turning points having the same relation to the maxima in the two states.

Now, the distance between turning point and maximum of any function depends primarily upon the slope of the potential curve in the vicinity. To this approximation, it varies in a sense opposite to the slope, and passes through an infinity with change of sign when the slope is

[15] J. G. Winans and E. C. G. Stueckelberg, Proc. Nat. Acad. Sci. **14**, 867 (1928).

reversed. Where the two potential curves have similar slope (long wave radiation in our case) method T will nearly coincide with method M. As the slopes begin to differ, the discrepancy will increase, becoming very large near the minimum of $U(r)$ and thereafter (short wave side) being large and in the opposite direction. Thus, when method T is used to predict transitions from a stable potential curve, the results obtained from the two sides will differ considerably in character. In our case the long wave maxima come out too far to long waves, the short wave maxima too far to short waves. Method M, on the other hand, gives maxima consistently too far to the long wave side. (Note the slanting lines of Fig. 5.)

This systematic error is in part due to the neglect of the ν^6 factor, which will always bring it about that the transitions giving greatest intensity involve greater energy changes than those corresponding to the maximum of the overlap integral. Method O, which has no features to recommend its general use, has been included merely to illustrate this effect. The difference between methods F and O decreases rapidly with the slope of the repulsive potential curve, and is accordingly small for the short wave radiation.

The residual discrepancy (difference between methods O and M) is essentially due to neglect of nonterminal loops of the wave functions. It seems to be generally believed that the shorter wave-length and smaller amplitude of these loops is so marked that they contribute negligibly to the overlap integral. Comparison of Fig. 5 with figures occurring in the literature of the Franck-Condon method will indicate that the rapidity of decrease of the amplitude is easily overestimated. (This decrease in amplitude is independent of the masses of the nuclei where the first approximation of the W. B. K. method is valid. Note, however, that the heavier the nuclei the nearer to the turning point does this approximation hold.)

TABLE V. $\int R_{ev}R_{e'E}dr$, *integrated over n loops of* $R_{e'E}$.

	$E=2.610$			$E=3.480$		$E=4.349$		
	$v=0$	$v=1$	$v=2$	$v=1$	$v=3$	$v=0$	$v=1$	$v=2$
$n=1$	4.96	−5.56	−1.60	−.30	−1.36	5.79	4.07	.84
2	4.74	−4.58	−1.04	2.26	−2.44	3.48	6.15	1.91
3	4.76	−4.71	−1.13	1.38	−4.21	4.26	4.29	3.48
4		−4.70	−1.13	1.58	−2.65	4.05	5.11	1.86
5				1.55	−3.33	4.10	4.86	2.69
6					−3.12	4.09	4.92	2.39
7					−3.18		4.91	2.48
8					−3.17			2.46

The way in which the integral $\int_0^r R_{ev}R_{e'E}dr$ depends on the range of integration is illustrated in Table V, where there will be found the values in typical cases of these integrals taken over the first n loops of the wave function of the upper repulsive curve. In each case the upper limit of the important range of integration is fixed by the rapid decrease of the discrete wave function. In the examples given as many as five loops of $R_{e'E}$ make important contributions to the integral, while if higher values of E or v had been considered even more would have been effective. For $E=3.480$, $v=3$ both the third and fourth loops have greater effect on the value of the integral than the first, while for $E=4.349$, $v=2$ the fifth loop is as important as the first. It appears from this that the effect of nonterminal loops may be very complicated.

It is clear, however, that when the terminal loops have their maxima coinciding, the overlap integral can still be increased by a shift of the function in the continuum which reduces any cancellation due to contributions from the other loops. When both functions have nodes to the right of their terminal maxima (potential curves have slopes of the same sign), this can be accomplished by a displacement in that direction which tends to bring together the nodes of the two functions, so far as is compatible with the different widths of the loops. This will be to the right or the left, according as the terminal loop of the function in the continuum is narrower or wider than that of the discrete function. When the first nodes lie on opposite sides of the main loops (potential curves have slopes of different sign), the shift should be such as to separate the nodes. In our problem, the two cases apply to the radiation bands of longest and shortest wave-length, respectively, except for $v=0$. Since the wave functions of the repulsive curve have the narrower loops, they should in both cases be shifted to larger values of r, thus producing radiation of higher energy (as predicted by method O) than that corresponding to matching of the maxima (method M). Evidently the same relation holds for the

single band of $v=0$ and for the intermediate bands of $v=2, 3, \cdots$.

Increase in the slope of the potential curves, by suppressing the nonterminal loops, may diminish the difference between method M and method O. It will, however, increase the difference between method O and method F; there is accordingly no situation in which method M may be expected to give very closely the results of method F.

Method $M-T$ is a modification of method M which will in part correct for neglect of the ν^6 factor and the nonterminal loops. The very close agreement of method $M-T$ with method O indicates that the result is in this case very nearly an accurate correction for the latter of these omissions. With method M, method $M-T$ shares the advantage of giving an estimate of the position of all the maxima of intensity, while method T can deal only with the two extreme maxima of intensity. The advantage in accuracy over M has been pointed out, and the greater simplicity of application is desirable, particularly when an inverse application of the method (determination of an unknown potential curve) is to be made. It is certainly the best of the correlation methods, and even in this difficult case gives fairly satisfactory results.

Method R, in which the function in the continuum is treated like a properly normalized δ function located at the turning point, appears to be very satisfactory, despite the difficulty of setting up a formal justification for it. Though we have not found it necessary to introduce such an approximation in discussing them, methods M, T, and $M-T$ give results that would be obtained if the correct wave functions were replaced by properly located δ functions. Now it is clear from Fig. 5 that the width of the terminal loop of the function in the continuum is by no means negligible as compared with that of the loops of the discrete functions. Only when the repulsive potential curve is extraordinarily steep would it appear reasonable to replace this function by a δ function at the turning point. The similarity in the results given by method O and method $M-T$, as displayed in Table IV, may be taken to indicate that under a wide range of conditions this approximation is a satisfactory one which includes a correction for the neglect of the nonterminal loops. Then, taking the correct function for the discrete state and introducing the dependence of the radiation intensity on ν one obtains method R as a generalization of and improvement on method $M-T$, which takes account approximately of all factors in the situation.

We must, however, discuss the normalization of the equivalent δ function. Let the repulsive potential curve be treated as a straight line over the region in which R_1 and R_2, solutions for the energies E_1 and E_2, respectively, deviate appreciably from the W. B. K. solutions. Let r_1 and r_2 be equal distances from the respective turning points; then within this region $R_1(r_1)$ will bear a constant ratio to $R_2(r_2)$. We now apply the first W. B. K. approximation for $r>r_1$, r_2. Between r_1 and ∞, R_1 will decrease in amplitude by the factor $[(E_1-U(r_1))/(E_1-U(\infty))]^{\frac{1}{4}}$, while between r_2 and ∞, R_2 will decrease by a factor $[(E_2-U(r_2))/(E_2-U(\infty))]^{\frac{1}{4}}=[(E_1-U(r_1))/(E_2-U(\infty))]^{\frac{1}{4}}$. If both have unit amplitude at ∞, then $R_1(r_1)/R_2(r_2)=[(E_1-U(\infty))/(E_2-U(\infty))]^{\frac{1}{4}}$. The areas of terminal loops will thus bear this ratio to each other, and so should the δ functions used to replace them. Or we may use equal δ functions, omitting the factor $E^{-\frac{1}{4}}$ from Eq. (10). This is indeed what has been done by Condon and by Winans and Stueckelberg, though they give no justification for it. When the curvature of the potential curve is appreciable the terminal loops will have different breadths; one may expect that the narrower loops should be replaced by δ functions normalized to smaller quantities.

In Fig. 6 the relative intensities predicted by methods F and R have no significance; within each figure the two intensity distributions were brought to the same maximum intensity. The positions of the maxima agree quite satisfactorily, and the general character of the intensity distributions is very similar. There is, however, a tendency of method R to give too large an intensity for large λ, in accordance with our remark on variation of the normalization of the equivalent δ function with change in the slope of the potential curve. The tendency of the distributions predicted by method R to shift toward small λ with increasing v, as compared with those given by the complete computation, is to be

noticed. It appears to be associated with the changing effect of the nonterminal loops of the function in the continuum with decreasing breadth of the loops of the other function. In general these results seem to encourage the use of the method R, since the errors evident here are markedly smaller than those which arise from the fundamental Franck-Condon assumption in this case, as we shall show in the next division of this paper.

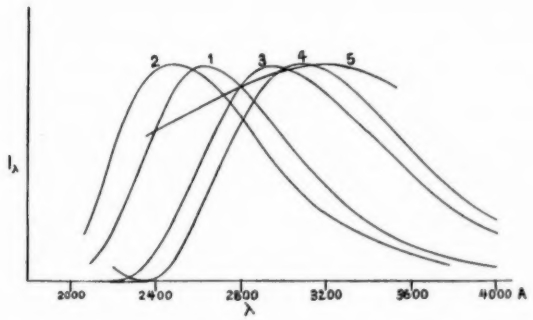

FIG. 7. I_λ, computed and observed. 1, upper repulsive potential curve, Franck-Condon approximation; 2, lower curve, Franck-Condon approximation; 3, upper curve, $\xi=-0.410$; 4, upper curve, $\xi=-0.434$; 5, Smith's observations. The relative intensities of the distributions are not significant.

COMPARISON WITH SMITH'S WORK

We have a possible basis for a comparison between calculated and observed spectral intensities in the recent work of Smith,[3] who has measured the hydrogen discharge spectrum both from pure gas and in the presence of a large excess of helium.[16] The helium was expected to restrict the radiation to that coming from the lowest vibrational level of the upper state or states involved, removing substantially all excited vibrational energy by inelastic collisions before radiation could occur. Under similar conditions, it could be verified that the many-line spectrum was restricted to the lines associated with initial levels with $v=0$. The presence of helium caused a marked change in the intensity distribution of the continuous spectrum, the maximum being shifted in the long wave direction by some 700A. This supports Smith's interpretation of the effect of the added helium, at least qualitatively, for it will be shown later that, according to our calculations, the radiations from the higher vibrational levels must have their principal maxima at shorter wave-lengths than that from the $v=0$ level. We seem justified in concluding that Smith's technique is effective in limiting the radiation to that from the lowest vibrational levels of the various electronic states.

Now, there is no reason to suppose that Smith's spectrum was obtained wholly from the special electronic transition treated by our calculations. We must enquire whether we may expect the existence of any region in which this particular radiation is so predominant as to justify a comparison with our calculated distribution. By reference to Fig. 7, it will be seen that the calculated I_λ curve for the $1s\sigma 2s\sigma\ ^3\Sigma_g \rightarrow 1s\sigma 2p\sigma\ ^3\Sigma_u$ transition has a sharp maximum near 2500A or 2600A (according to which potential curve is used in computing). Other transitions might originate on more highly excited stable states, and go either to the same or to more highly excited repulsive states. From the latter class of transitions, no radiation of shorter wave-length than 3646A can arise; no stable level of the system could have an energy greater than of $H+H^+$, while the repulsive state must have at least the energy of a normal and a two-quantum excited atom, so that the energy radiated is limited to Rh/4. Such radiations fall outside the range of Smith's observations.[17] Radiations due to transitions of the former class should lie well to the short wave side of the maximum for our transition. The next lowest known state which can combine with $1s\sigma 2p\sigma\ ^3\Sigma_u$ is $1s\sigma 3d\sigma\ ^3\Sigma_g$, which lies about 2.1 ev higher. As

[16] Smith's measurements were based on comparison with the carbon arc, which was assumed to have the spectrum characteristic of a black body at 3810°K. Until a better standard is available, it will be impossible to estimate the error due to this assumption, but it seems very unlikely that it can be sufficient to alter the general character of the conclusions which we shall reach.

[17] The appearance of these continua may be responsible for the observations of Chalonge [Ann. de physique 1, 123 (1934)], who found that when the pressure of H_2 in the discharge was made very low the radiation with $\lambda > 3600$A was enhanced with respect to the rest of the spectrum. This enhancement took place under just those conditions in which the Balmer lines began to appear on his plates, indicating the production of excited H, as must be expected in connection with the radiation of these continua. Chalonge's interpretation of his observations, based on changes in the relative proportions of the radiations from the vibrational levels of the $1s\sigma 2s\sigma\ ^3\Sigma_g$ state, is clearly incompatible with Smith's observations and our calculations.

an orientating calculation, we have computed the spectrum produced by transitions from this state, using the Franck-Condon principle and representing the potential curve of the upper state by simply raising that for $1s\sigma 2p\sigma\ ^3\Sigma_g$ by 2 ev. The resulting I_λ has a maximum at 1900A, and at 2650A amounts to less than 5 percent of its maximum value. This distribution is probably too far toward the red; the true potential curve for $1s\sigma 3d\sigma\ ^3\Sigma_g$ has a greater equilibrium distance than that which we have used, and an allowance for this would increase the energy of the radiation. It is hardly possible that continuous radiations from H_2^+ or He_2 would be present, as they require too high an excitation energy.

The spectrum predicted to be observed under Smith's conditions, on the basis of the Franck-Condon principle, is therefore essentially that due to the transition here considered, slightly reenforced on the short wave side, and with slight shifting of the maximum toward higher energy. Any contamination from higher vibrational levels must operate in the same direction. It will be seen that Smith's results (curve 5, Fig. 7) are in striking disagreement with this prediction. It should be emphasized that there is no possibility of relocating the potential curve in any manner consistent with our theoretical knowledge about it, so as to remove this disagreement. We regard this as proof that in this case the Franck-Condon principle is in disagreement with experiment, and that it is necessary to take into account the way in which $D_{ee'}$ depends upon r.

We propose to carry out a theoretical determination of this dependence. Pending the completion of this laborious task, we have been able to obtain a rough idea of the effects to be expected. With the aid of the integrals M and L of Table II, we can compute the spectrum corresponding to an electric moment function of the form $D_{ee'}(r)=C(1+\xi r)$, where ξ is a constant chosen to make the position of the maximum for $v=0$ agree with experiment. This linear moment function is nothing more than a first approximation to the real function, useful in the range of r which contributes most heavily to the overlap integral corresponding to the maximum I_λ, where it should have approximately the correct relative slope. Little significance must be attached to its value in other regions, especially beyond the r where it changes sign. In Fig. 7, curves 3 and 4, we show I_λ for $v=0$, computed from the upper potential curve with two values of ξ; that for $\xi=-0.434$ has a maximum in fair agreement with Smith's curve. If the radiation from the higher electronic states is similarly shifted to the red, we have a plausible explanation of the form of this curve. Thus, we can again calculate the radiation from $1s\sigma 3d\sigma\ ^3\Sigma_g$, assuming that for this transition the value of $D_{ee'}$ is the same as for $1s\sigma 2s\sigma\ ^3\Sigma_g$; with $\xi=-0.434$ we obtain a maximum at 2100A, decreasing to 10 percent at 2700A. Owing to the ν^6 factor, this more energetic radiation would be so intense that a population of the three-quantum level less than a tenth of that of the two-quantum level would explain the relative intensities found by Smith at 3200A and at 2400A.

The Work of Finkelnburg and Weizel

The attempt to reproduce theoretically the results of Finkelnburg and Weizel meets with serious difficulties, due principally to the uncertainties involved in interpreting their observations. Using the method of Lau and Reichenheim,[18] they have photographed the spectrum of the hydrogen discharge in such a way that a horizontal displacement on their plates corresponds to a change in wave-length, a vertical displacement to a change in the energy of the exciting electrons, V. Unfortunately for us, the purpose in hand did not require them to calibrate or photometer their plates; they merely noted the position of the fairly sharp boundary of the region of perceptible blackening, thus obtaining the apparent excitation potential of each wave-length. Actually, of course, this gives, not the theoretical critical potential for each λ but a threshold potential, sufficiently in excess of the critical to produce an unknown, just perceptible, finite intensity of radiation I_λ which depends upon the sensitivity-curve of the plates, the dispersion of the quartz prism, and the geometry of the spectrograph. A possible though improbable assumption is that the critical I_λ was the same at all wave-lengths. The minimum of their $V-\lambda$

[18] E. Lau and O. Reichenheim, Naturwiss. **18**, 86 (1930).

curve would then represent the most intense radiation from $v=0$, which should be the first to appear when the exciting potential is raised. Finkelnburg and Weizel's points are so irregular that the minimum cannot be accurately located; it seems to fall between 3000A and 3200A, in approximate agreement with Smith's curve, which is an argument in favor of the assumption of uniform perceptible intensity. We regard this as additional evidence that the Franck-Condon principle is invalid, since this principle requires a maximum I_λ between 2500A and 2600A. The discrepancy is much too great to be explicable as a result of any reasonable variation of the minimum perceptible intensity.

As a basis for the consideration of the continuum excited by electrons homogeneous in velocity, let us imagine a three-dimensional model, in which V and λ are laid out as Cartesian coordinates in a basal plane, above which a dome-shaped surface is so constructed that at each point its height is proportional to I_λ for the corresponding V, λ. The intersection of the dome with the basal plane will trace the locus of the true critical potential. Planes parallel to the base will intersect the dome to give curves which may be projected upon the base to form a family of contour lines. Upon the assumption of uniform perceptible intensity, Finkelnburg and Weizel's curve should be one of these contour lines. Upon a different assumption, it should cut across the contour lines systematically.

In order to illustrate the structure of the continuum observed under the experimental conditions of Finkelnburg and Weizel we have constructed such a model, using the upper potential curve for the $1s\sigma 2p\sigma\ ^3\Sigma_u$ state. We have employed the linear moment function, taking $\xi=-0.434$ in order to bring the maximum I_λ for $v=0$ to $\lambda=3100$A; the resulting approximation should be at least qualitatively reliable for $\lambda>2700$A. The first step was to compute the spectrum from each of the first four vibrational levels separately, using Eq. (10). These spectra are shown in Fig. 8. Fig. 9 shows, for comparison, the same spectra computed with $\xi=0$. The most striking effect of the assumption of linear moment is the great reduction of the relative intensity of the short wave maxima. As was indicated in the discussion of Smith's work, this reduction

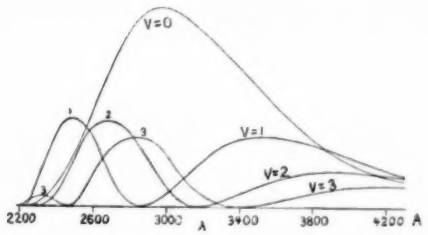

FIG. 8. I_λ predicted, taking $\xi=-0.434$.

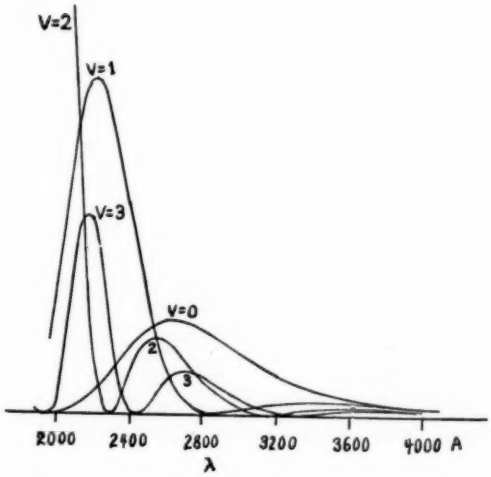

FIG. 9. I_λ predicted by Franck-Condon approximation.

is probably excessive, arising from the spurious vanishing of $D_{ee'}$ at $r=2.3a_H$. We next computed the population of each vibrational level by Eq. (11), taking $M_{ev,\ e'v'}$ between the levels in question and the lowest level of the ground state. Upon superposing the intensities of the radiations from different levels, we obtained the total intensity at each V and λ. Fig. 10 shows cross sections of the resulting surface, for three values of V, the contributions from each v being indicated. Fig. 11 shows the contour lines, drawn solid, while the broken lines cut across them in such a way as to pass through values of I_λ everywhere proportional to the dispersion of quartz, as Finkelnburg and Weizel's curve should do if their perceptible intensity varied with λ only because of the variation in dispersion.

Although Finkelnburg and Weizel's curve is a relation between V and λ, we cannot introduce it immediately into Fig. 11, because the absolute

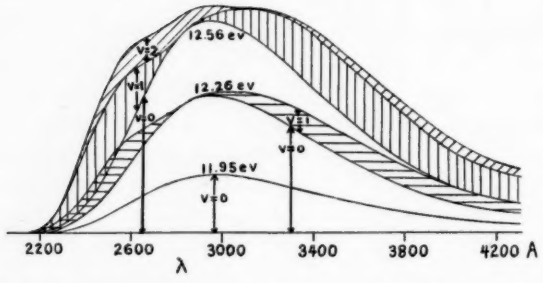

FIG. 10. Composition of radiation emitted for various exciting potentials. I_λ is plotted.

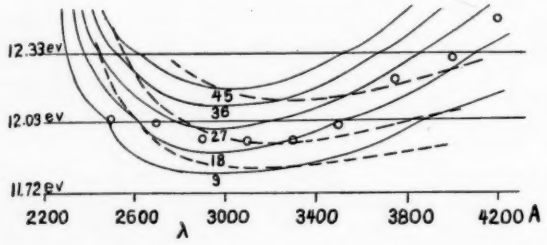

FIG. 11. Contours of I_λ. Solid lines are computed by using $\xi=-0.434$. Broken lines are contours of I_λ times the dispersion of quartz. Circles are observed points of Finkelnburg and Weizel.

value of V in their experiments is not well known. They estimate that their minimum comes at $V=11.86$ ev, with a possible error of 0.2 ev, but believe that the relative position of their points is much more accurately known. We find it preferable to place their minimum at 11.95 ev, or 0.23 ev above the theoretical critical potential $V_k=11.72$, the value determined by the position of our potential curves. Points representing their observations as thus interpreted are shown as circles in Fig. 11.

The assumption of linear moment, coupled with that of constant perceptible intensity, thus leads to satisfactory agreement, the circles falling nicely between the contours marked 18 and 27 except on the extreme left, where we have already stated that the calculated intensities must be expected to be too low, the contour lines therefore too high, because of the vanishing of our approximation for $D_{ee'}(r)$. It is therefore possible to regard Finkelnburg and Weizel's curve as the locus of constant I_λ, having that value which is excited by 0.23 ev excess potential in the region of the maximum radiation from $v=0$. It is clear that other hypotheses concerning the perceptible intensity and the electric moment function could be combined in such a way as to give perhaps equally plausible interpretations. But it seems to be definitely established that the Franck-Condon assumption of constant moment is incompatible with the experiments of Finkelnburg and Weizel. We have determined roughly the relocation of the potential curve which would remove this incompatibility. We find that the broken curve of Fig. 2, in connection with the Franck-Condon assumption and method R, gives an intensity contour agreeing very well with the $V-\lambda$ curve of Finkelnburg and Weizel. Such a position of the potential curve, however, would be in definite contradiction to the Heitler-London computations, as well as our own, and cannot be regarded as a possibility.

With the above results in mind we can now pass to a discussion of the method used by Finkelnburg and Weizel in locating their potential curve. If there had been observable structure in the continuous spectrum, so that a given part of the radiation could have been associated with transitions from a particular vibrational level, they could have followed the method devised by Kuhn,[19] which is based on the simplest form of the Franck-Condon principle, method T. Points on the repulsive curve would then have been obtained thus: The spectrum arising from transitions from the level $v=1$, say, would have two principal maxima of intensity. The corresponding turning points in the known upper state, b and β would be first located on the energy diagram, Fig. 1. Then, measuring down from b to b' a distance corresponding to the energy of the photons at the maximum with greater λ, and from β to β' a distance corresponding to the energy at the other maximum, two points on the lower potential curve would be located. Since the absence of structure in the spectrum prevented such a procedure, Finkelnburg and Weizel were forced to take as the most strongly radiated wavelengths those which first became observable when the energies of the exciting electrons exceeded that necessary to produce the first visible radiation (excitation of $v=0$) by the vibrational energies of the upper states. Their further procedure was then that sketched above.

A tacit assumption inherent in this method is

[19] H. Kuhn, Zeits. f. Physik **63**, 458 (1930).

that the radiation due to transitions from each level becomes observable when the exciting potential exceeds the necessary minimum by the same amount. The second, and more fundamental assumption, is that there is little overlapping of the radiation from different v's, so that the appearance of each such radiation at the proper exciting potential will not be obscured by off-maximum radiation from the lower v's. Figs. 8 and 9 will show how far from the truth this probably is.

It will be noted that in the interesting long-wave region the maxima for $v=1$ and $v=2$ are relatively weak, and occur well within the region to which $v=0$ contributes strongly. Radiation from these levels will thus be obscured by that from $v=0$ unless they are much more strongly excited, which is not the case. In Fig. 10 the curve for $V=11.95$ is a cross section corresponding to the minimum energy of excitation which gives observable radiation. The minimum observable intensity is thus 23 in the arbitrary units used. To fix the wave-length associated with radiation from $v=1$, Finkelnburg and Weizel then noted the λ at which radiation of this intensity appeared, when the exciting potential was raised by 0.31 ev (the difference in energy between $v=1$ and $v=0$), thus reaching 12.26 ev on our scale. According to our figure this would be 3850A; only 30 percent of this radiation comes from the $v=1$ level. Similarly, only about 13 percent of the radiation associated by Finkelnburg and Weizel with the $v=2$ level appears to come from that level. That the wave-lengths selected in this way are within some 400A of the corresponding computed maxima thus appears to be merely a coincidence. Nor is this agreement a measure of the accuracy of the procedure of Finkelnburg and Weizel, for as has already been shown, the form of the Franck-Condon principle used by Finkelnburg and Weizel involves even more serious approximations. It seems, then, that the construction of Finkelnburg and Weizel cannot be depended on and that as yet we possess no method of determining a repulsive potential curve by observations on a continuous spectrum in which there is no analyzable structure.

Experimental studies of the H_2 continuum free from those factors which complicate the interpretation of the results of Smith and of Finkelnburg and Weizel are much to be desired. Controlled excitation of H_2 in the presence of an excess of He should yield a spectrum arising only from transitions from a single vibrational level of the $1s\sigma 2s\sigma\ {}^3\Sigma_g$ state, which could be compared with a theoretical prediction free from the complication of an assumed excitation function. This spectrum might be obtained by a modification of the method of Lau and Reichenheim, or by excitation with electrons emitted from a hot equipotential cathode. The Lau-Reichenheim method would also yield results of great value if the plates were properly calibrated, for the assumption of a linear excitation function seems to be a good approximation over a fair range of V. A complete theoretical treatment of the $1s\sigma 2s\sigma\ {}^3\Sigma_g - 1s\sigma 2p\sigma\ {}^3\Sigma_u$ continuum, free from arbitrary assumptions about the quantity $D_{ee'}(r)$, is now under way. We hope that experimental results of comparable precision may soon become available.

In conclusion we wish again to express our indebtedness to the Electrical Engineering Department of the Massachusetts Institute of Technology for the use of the differential analyzer, and to thank Professor S. H. Caldwell and Professor P. M. Morse for advice concerning its operation. We are also indebted to Professor O. Oldenberg and Dr. N. D. Smith for helpful discussions of the experimental aspects of the problem.

The Decomposition of Ethylamine and Diethylhydrazine

H. AUSTIN TAYLOR AND JOHN G. DITMAN,* *New York University*

(Received December 21, 1935)

The decomposition of ethylamine has been reinvestigated in the light of criticism of earlier work. The reaction has been shown to occur by a bimolecular no volume change decomposition into symmetrical diethylhydrazine and hydrogen followed by the decomposition of the hydrazine by a chain mechanism which is first order. The mechanism is shown to account for the induction period and its rapid variation with temperature and pressure, as well as accounting satisfactorily for apparent discrepancies and inconsistencies found by previous workers.

IN a previous study of the decomposition of ethylamine[1] it was found that the course the reaction followed was apparently homogeneous and unimolecular. As a result of further work on dimethylamine[2] doubt was cast on this seeming simplicity of reaction as "probably fortuitous due to a mutual compensation of several reactions." Later in the same year Schumacher and Wiig[3] published the results of an investigation of the ethylamine decomposition at lower pressures and concluded that the reaction was heterogeneous and complex, probably involving a chain mechanism. This latter conclusion was drawn from the erratic nature of the decomposition, the effect of added gases notably water vapor and air, the effect of a change in surface and from the reaction products which were found to be mainly hydrogen, methane and nitrogen, with small amounts of unsaturated hydrocarbons and some basic material. This tremendous divergence of observation alone would call for further study. Schumacher offers no explanation. Unfortunately the evidence presented is not consistent as indicated by his inability to reproduce a temperature coefficient. Sickman and Rice[4] also conclude from a study of the decomposition of propylamine at low pressures that the reaction probably has a chain mechanism though again no detailed mechanism is offered.

The fundamental point of difference between this later work and the earlier work by Taylor appears to lie in the existence of an induction period, never observed by him, found by Sickman and Rice only at lower pressures (5 mm) and by Schumacher and Wiig especially at lower temperatures and lower pressures but markedly erratic, showing little consistency or reproducibility.

The presence of an induction period caused by an initial acceleration of the rate of a reaction has so frequently been regarded, either as an annoying complication in an otherwise apparently simple reaction and hence to be disregarded as innocuously as possible for subsequent quantitative treatment, or gratuitously, as an indication of the presence of a chain mechanism, that it was deemed advisable to study this case in more detail in an endeavor to reconcile the conflicting results mentioned. Although it has not been found possible to elucidate the mechanism completely, numerous observations have been made, which, pointing to the same conclusions, leave no doubt as to the main steps involved and offer an explanation of the apparent inconsistencies so far observed.

The mechanism postulated is, for the main part, the following:

$$2C_2H_5NH_2 \rightarrow C_2H_5NH-NHC_2H_5+H_2$$
$$C_2H_5NH-NHC_2H_5 \rightarrow N_2+H_2+2C_2H_5.$$

It seems advisable to justify this scheme qualitatively before discussing the quantitative results. In the first place, on allowing ethylamine vapor at pressures from 400 to 500 mm, to remain at 300°C, some 200° below the temperature at which a noticeable pressure increase occurs, a pressure decrease was observed. This was traced to the condensation in the capillaries joining the reaction vessel and manometer, of

* Abstract from a thesis presented in partial fulfillment of the requirements for the degree of Doctor of Philosophy at New York University, June 1935.

[1] H. Austin Taylor, J. Phys. Chem. **34**, 2761 (1930).

[2] H. Austin Taylor, J. Phys. Chem. **36**, 1960 (1932).

[3] H. J. Schumacher and E. O. Wiig, Zeits. f. physik. Chemie **A162**, 419 (1932).

[4] D. V. Sickman and O. K. Rice, J. Am. Chem. Soc. **57**, 22 (1935).

some higher boiling material formed in the early stages of reaction. The condensation was completely eliminated by heating the capillaries to 85°C under which circumstances no pressure change was noted even after several days. The occurrence of a reaction at so low a temperature precluded the possibility of the condensate being a polymer of an unsaturated hydrocarbon as a product of the decomposition proper and the significance of the temperature necessary to prevent condensation is apparent since the boiling point of symmetrical diethylhydrazine is given as 84° to 86°C.

Analyses of the gases in the reaction system at the end of the induction period showed a large excess of hydrogen over the nitrogen and hydrocarbon and several times the percentage of hydrogen found by Schumacher in the final products of decomposition. Taken in conjunction with the above-mentioned evidence for a reaction at low temperature involving no change in volume, this elimination of hydrogen necessitates the first step postulated. To prove definitely the presence of diethylhydrazine samples of liquid products were condensed in dynamic decompositions of ethylamine which showed fractions boiling at 84° to 86°C. This liquid had reducing properties, showing easy reduction of ammoniacal silver nitrate and difficult reduction of Fehling's solution, properties characteristic of the hydrazine. Samples of liquid ethylamine sealed in bomb tubes and heated at 300°C for a period of a few hours likewise showed the same product. In fact it was found possible to produce a relatively pure sample of the hydrazine by allowing ethylamine vapor to circulate rapidly through a small furnace at 250° to 300° in a closed system. The furnace temperature as well as the time of contact is sufficiently low that subsequent decomposition of the hydrazine is reduced to a minimum and the extent of reaction may be judged by the hydrogen pressure developed. Fig. 1 illustrates a convenient form of the apparatus.

In the hope of obtaining kinetic measurements of this, the primary reaction, samples of ethylamine vapor sealed in small tubes were heated at 400°C in a lead bath for various lengths of time and titrated with iodine to determine the amounts of diethylhydrazine produced. The results showed a qualitative increase in concentration of the hydrazine with time of heating but quantitatively were not consistent. This was traced by titrations of known samples of amine and hydrazine to an indefiniteness in the endpoint of the iodine titration, apparently a function of the amine content.

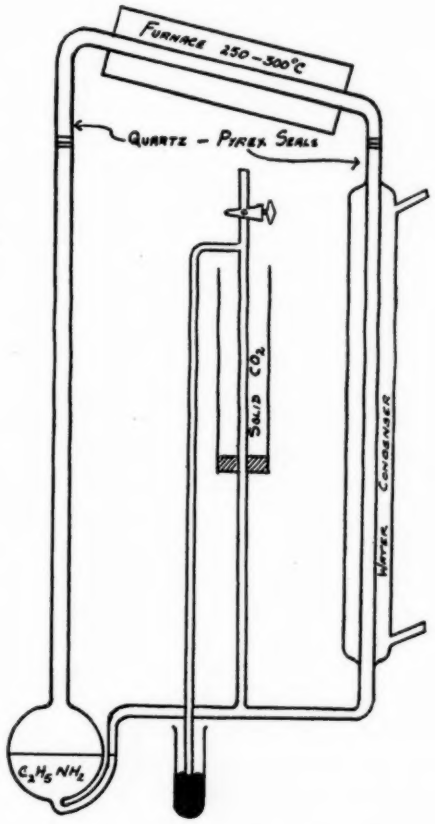

FIG. 1. Apparatus for production of diethylhydrazine from ethylamine.

With the foregoing results as complete evidence of the first stage of ethylamine decomposition, the fact that it involves no change in the number of molecules would be responsible for an induction period in a rate measurement in terms of pressure change. That it alone is responsible was shown by a separate study of the decomposition of diethylhydrazine. This latter proceeds at measurable speed in the temperature range 500° to 540°C, the same as that for ethylamine and under no circumstances was found to give an induction period. However, if air or oxygen had been in contact with the hydrazine

previous to its admission to the reaction flask, or if air was present even in very small amounts in the reaction flask upon admitting the hydrazine, the decomposition was immeasurably rapid at 500° and could only be measured conveniently around 300°C. This phenomenon is readily explicable by the easy oxidation of the hydrazines to the corresponding azo compounds.[5] There is no reason to believe that azoethane would differ greatly from azomethane in its decomposition and should therefore decompose easily around 300°C to yield nitrogen and ethyl radicals. A sample of diethylhydrazine containing a small amount of air would therefore resemble a system undergoing decomposition induced by ethyl radicals at the temperature necessary merely to produce the radicals thermally. Once contamination by air had been observed as indicated by the fast decomposition, it was found only necessary to freeze the diethylhydrazine in solid carbon dioxide and evacuate the system thoroughly, after which the normal rate of decomposition at the higher temperatures again obtained.

The decomposition of diethylhydrazine must therefore be a chain reaction and for that reason the second equation given above in the mechanism postulated has been left in terms of ethyl radicals. Were these to combine to give butane the over-all reaction would be

$$C_2H_5NH-NHC_2H_5 \rightarrow N_2+H_2+C_4H_{10}$$

corresponding to a 200 percent pressure increase. Actually as is shown later butane is found but naturally under the conditions of the experiments in quite small amounts. The reactions of free ethyl radicals either alone or in presence of free hydrogen have been well studied[6] and lead to the expectation of finding methane as the principal product with more or less unsaturated hydrocarbon in a polymerized form depending on the amount of hydrogen present. The pressure increase observed for the complete reaction of decomposition of either ethylamine or diethylhydrazine is consistent with this view. What the individual steps in the hydrazine chains are cannot be specified. Suffice that the over-all reaction is of first order but shows a variation with pressure that has come to be associated with a chain mechanism and a variation with temperature that is not strictly of the Arrhenius type. Further discussion is deferred until the observed data have been presented.

Experimental

The rates of decomposition of ethylamine and diethylhydrazine were measured by following the rate of pressure change manometrically. The reaction vessel was of fused quartz, the rest of the apparatus being Pyrex. Evacuation was obtained through a Langmuir mercury vapor pump backed by an oil pump, although samples could also be drawn off the system by means of a Töpler pump. The connecting capillaries between reaction vessel and manometer were heated to 90°C in all experiments for the reason stated above.

Since earlier work had indicated the necessity of using highly purified materials special care was taken in this regard. The purification of ethylamine is a very difficult task with the result that many commercial samples on the market labeled pure may contain as much as 2 percent ammonia as well as secondary amine. This was true of the Eastman Kodak sample which was the starting material. The purification followed the method of Pohland and Mehl[7] being virtually a fractional distillation in vacuum between the temperatures of solid carbon dioxide and solid carbon disulphide. The vapor pressure of the purified product measured at 0.4°C was 273 mm in agreement with their values.

The diethylhydrazine was prepared by the Thiele[8] method adapted for the ethyl derivative in place of the methyl in the original. Diformylhydrazine is ethylated with diethylsulphate and then hydrolized with concentrated hydrochloric acid. The hydrazine is distilled from an alkaline solution and repeatedly fractionated from barium oxide until dry.

[5] No mention of azoethane is found in the literature. It seems highly probable that this is due to the easy oxidation of the diethylhydrazine. Chromic acid which is satisfactory for the methyl derivative causes complete destructive oxidation of the ethyl compound and azoethane can only be produced by use of a very mild oxidizing agent.

[6] H. S. Taylor and D. G. Hill, J. Am. Chem. Soc. **51**, 2922 (1929).

[7] E. Pohland and W. Mehl, Zeits. f. physik. Chemie **A164**, 48 (1933).

[8] Thiele, Ber. **42**, 2576 (1909).

TABLE I.

Temperature 482°C				Temperature 490°C						Temperature 500°C				
Initial Pressure (mm)	224.5	258	299	Initial Pressure (mm)	33	37.5	58	69	105	Initial Pressure (mm)	79.5	89	107	123
Time (min.)	Pressure Increase (mm)			Time (min.)	Pressure Increase (mm)					Time (min.)	Pressure Increase (mm)			
2	0.5	0.5	1.0	4	—	0.5	0.5	1.5	4.0	1	1.0	1.0	1.0	2.5
5	2.0	2.5	3.0	6	—	1.0	1.5	2.5	7.0	2	2.5	2.5	3.5	8.0
10	4.5	5.5	8.0	8	0.5	1.5	2.0	4.0	10.0	3	4.0	4.0	7.0	13.0
20	10.0	13.0	20.5	10	1.5	2.5	3.0	5.5	13.5	4	5.5	7.0	10.0	18.0
30	19.5	24.0	35.0	12	2.0	3.5	4.5	7.5	17.0	5	7.5	9.0	13.5	22.5
40	33.0	39.0	57.0	14	2.5	4.0	6.0	10.0	21.0	10	17.5	21.5	30.0	46.5
50	46.5	55.0	81.0	16	3.0	5.0	7.0	12.5	24.5	20	38.0	46.5	60.0	85.0
60	62.0	73.0	103.0	18	4.0	6.0	8.5	15.5	28.5	30	53.5	65.0	83.0	106.0
70	79.0	92.0	127.0	20	4.5	7.0	10.0	18.5	32.5	40	64.0	74.5	100.5	121.0
80	93.0	109.0	149.5	25	7.0	10.0	14.5	26.0	42.5	50	70.5	82.0	114.5	131.5
90	109.0	126.0	167.5	30	9.0	12.5	19.0	32.0	51.0	60	75.5	87.5	124.0	138.5
100	124.0	143.0	186.5	35	11.5	15.0	23.0	36.5	59.0					
110	136.5	157.0	203.5	40	14.0	18.0	27.0	40.5	66.0					
130	160.0	184.0	229.5	50	18.5	23.0	33.0	46.0	78.0					
150	179.0	205.0	248.0	60	22.0	27.0	37.0	49.5	87.5					
180	201.5	231.0	270.0											

RESULTS AND DISCUSSION

Ethylamine

The point of prime importance in the case of ethylamine is the complete reproducibility with relative ease of the reaction rate, including the induction period, when due care is taken in the use of pure material with the exclusion particularly of all traces of oxygen. It was at one time suspected during the course of the work, that reaction products strongly adsorbed on the reaction vessel walls were responsible for some observed inconsistencies which were only removed after at least twelve hours pumping. This was finally traced to a poorly fitting stopcock allowing an access of air to the ethylamine reservoir. This corrected, reproducible results were obtainable after a comparatively short evacuation of one or two hours at 10^{-4} to 10^{-5} mm.

Since interest centered on the induction period static runs were made at 482°, 490° and 500°C at pressures from 25 to 300 mm. The pressure increase at the endpoint was fairly consistent ranging generally between 125 and 130 percent. A few cases where the value was as low as 100 percent seem exceptional, though all the values are of little importance since they depend so much on the hydrocarbon equilibrium obtaining in the secondary reactions. Actual values of the pressure increase at corresponding times are given in Table I for the three temperatures studied and initial ethylamine pressures indicated. Fig. 2 illustrates the results at 490° and shows qualitatively the variation of the induction period with pressure.

Kontorova and Neumann[9] and more recently Semenoff[10] have attempted to account theoretically for the auto-accelerating rates of numerous reactions, the former on the basis of the formation of a specific intermediate, the latter by chain reactions. In the former treatment it is concluded that the formation of an intermediate without a volume change followed by its decomposition with a volume change will not give an induction period of measurable duration, when the order of the two reactions is the same. It is not proved that if the reactions are of different order the same conclusion holds. It is obvious that if the order of the two reactions is the same the ratio of the rates alone need be considered, whilst if the orders are different, the initial concentration as well as the ratio of rates must be taken into account. Semenoff finds that in numerous cases an auto-accelerating rate may be expressed by a logarithmic relation, similar to that used by Garner[11] and his co-workers in the decomposition of solid explosives, which appears suggestive of a chain reaction. The application to the data herein

[9] T. A. Kontorova and M. B. Neumann, Physik. Zeits. Sowjetunion **4**, 818 (1933).
[10] N. N. Semenoff, Acta Physiocochim. U. R. S. S. **1**, 113 (1934).
[11] Garner, J. Chem. Soc. 1393 (1933).

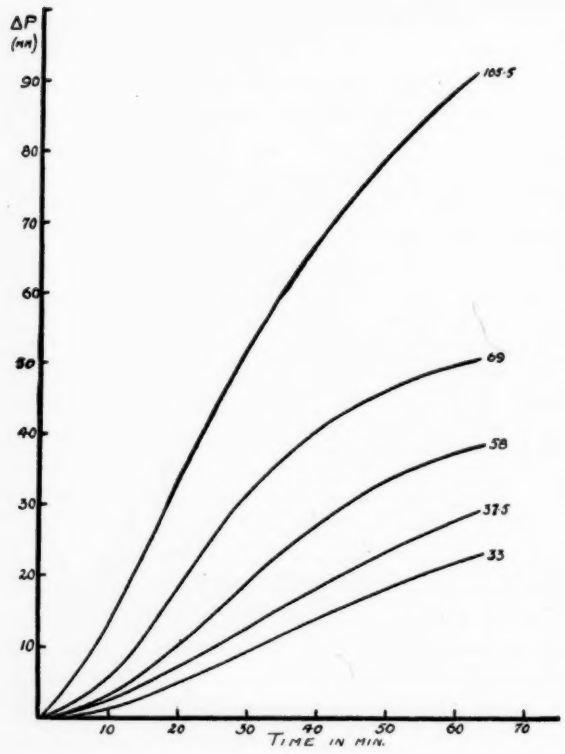

FIG. 2. Rates of pressure change of ethylamine at 490°C.

proves of little value and need not be given, especially since in any case, it could not be used as proof that the induction period has its origin in a chain mechanism.

On the other hand if the mechanism of the ethylamine reaction here postulated is correct, at least an approximate idea of the order of the initial reaction may be obtained from the limiting slope of the plot of pressure change against time, at zero time. The order is found to be two as shown by the constancy of the values obtained by dividing the limiting slope by the square of the initial concentration. The values are expressed in concentration units of moles per liter and time in seconds in Table II.

TABLE II.

TEMPERATURE 482°C INITIAL PRESSURE	$k \times 10^3$	TEMPERATURE 490°C INITIAL PRESSURE	$k \times 10^2$
224.5	2.96	33	2.20
258	3.33	37.5	2.25
299	3.16	58	1.90
		69	3.33
		105	4.50

The constancy of these values is all that may be expected in view of the inevitable error in taking slopes at zero time which is precisely that region of the reaction where experimental determinations are most difficult. It is for this reason that similar values are not given for the data at 500°C where the induction period is very short and hence the curvature of the rate curve is very great. That the values may not be used to calculate a temperature coefficient for the first reaction is obvious since the very existence of a slope signifies that a pressure increase, that is the second reaction, has already occurred to a small extent. The conclusion is inescapable however, that the formation of diethylhydrazine is of second order.

According to the proposed mechanism, at the point of inflection of the curve of the pressure change against time the rate of production of the hydrazine is equal to its rate of decomposition. Since the formation is shown to be the more rapid reaction this means that the ethylamine concentration will have become negligible at this point and hence the rest of the curve may be treated as corresponding solely to the hydrazine decomposition. Taking the point of inflection as the origin of the remainder of the curve the fractional life of the final reaction may be estimated for the various temperatures and pressures studied. These data are presented in Table III as the time in minutes for one-quarter of the total pressure change.

TABLE III.

TEMPERATURE 482°C INITIAL PRESSURE	$t_{1/4}$	TEMPERATURE 490°C INITIAL PRESSURE	$t_{1/4}$	TEMPERATURE 500°C INITIAL PRESSURE	$t_{1/4}$
224.5	35	33	15	79.5	14
		37.5	15	89	13
258	33	58	13	107	12
		69	10		
299	29	105	15	123	8

The values show a marked decrease with increase of pressure, a variation frequently found in chain reactions, but not so great as would be expected for a bimolecular reaction. The reaction appears to be much more nearly first than second order. Unfortunately the pressure ranges studied at the three temperatures do not overlap so that an accurate determination of the energy of

activation from the temperature coefficient at some constant pressure cannot be made. However by plotting the logarithms of the reciprocal times, that is a quantity proportional to the velocity constant, against the logarithm of the pressure the curves may be extrapolated, assuming they are parallel over a short pressure range and hence an approximate temperature coefficient at a fixed pressure determined. The average value so found for the energy of activation is 38,000 calories. These values will be referred to later for comparison with the results on the hydrazine alone.

The results of the analyses of the products of decomposition at the end of the induction period, mentioned in the introduction are given in Table IV. Ethylamine at pressures of 600 and

TABLE IV.

	Percent	
	(1)	(2)
Hydrogen	48.25	54.87
Methane	36.83	29.16
Butane	5.26	4.17
Unsaturated	3.51	8.33
Nitrogen	6.14	3.47

650 mm was allowed to decompose at 490°C until the pressure had increased by from 15 to 25 percent.

The products were then withdrawn by means of a Töpler pump, washed with acid to remove basic material including any unchanged amine and hydrazine and the resulting gases analyzed, the butane being frozen out. The high percentage of hydrogen is striking especially if compared with the 10 percent found by Schumacher and Wiig in the final products. The amount of nitrogen is surprisingly low in view of the amount of methane. The only available explanation appears to lie in the possibility that most of the nitrogen corresponding to this methane as a product of the diethylhydrazine already decomposed at the end of the induction period, was still present as basic material and hence removed in the preliminary washing. It is well known that hydrazine itself may decompose giving either nitrogen and ammonia alone or nitrogen, hydrogen and ammonia. It may well be then that diethylhydrazine would yield ammonia or amines on partial decomposition. Schumacher finds a small amount of basic material even in the final products and in view of the probable chain mechanism of the hydrazine decomposition the presence of the nitrogen entirely as free nitrogen should not be expected.

Diethylhydrazine

The decomposition of the hydrazine itself was studied at temperatures from 510° to 540°C. The reaction proceeded without an induction period and was approximately unimolecular during a given run. The endpoint of the reaction varied between 100 and 110 percent pressure increase. The magnitude of the velocity constants calculated by the usual first-order equation for the various observations made in a given experiment show a decided falling trend. The constants quoted therefore are the extrapolated values from the limiting slope of the pressure change-time curve at zero time divided by the initial pressure. Table V gives a resumé of the results obtained.

TABLE V.

Initial Press. (mm)	Temperature (°C)	$k \times 10^4$ sec.$^{-1}$	Initial Press. (mm)	Temperature (°C)	$k \times 10^4$ sec.$^{-1}$
263	510	5.5	165	530	8.8
164	510	5.1	52	530	8.0
161	510	4.9	32	530	7.3
241	520	7.5	254	540	17.3
143	520	6.5	245	540	17.2
53	520	5.9	150	540	12.5
32	520	5.7	62	540	10.0
238	530	11.7	29	540	9.3

The general shape of these curves is similar to that found for the corresponding curves of quarter-life calculated from the later portions of the ethylamine reaction. They appear to show a divergence at higher pressures which would indicate a varying energy of activation with pressure, a condition not uncommon in chain reactions. The average energy of activation calculated by the Arrhenius equation from the velocity constants at a fixed pressure around 250 mm is 45,000 calories, whilst at 150 mm is 39,000 calories. This latter value is to be compared with the 38,000 calories found from the quarter-lives of the later portions of the ethylamine decompositions averaged around the same pressure as previously indicated. Furthermore

the absolute values of the velocities when compared for a given temperature and pressure are in agreement. Thus, the value of the quarter-life in the ethylamine decomposition at 482°C and 258 mm is 33 minutes which would correspond to a velocity constant of 1.5×10^{-4} sec.$^{-1}$. Now 258 mm of ethylamine would yield on the basis of the proposed mechanism 129 mm of diethylhydrazine. The velocity constant of 129 mm of the hydrazine at 510°C is 5.0×10^{-4} sec.$^{-1}$ which using an energy of activation of 39,000 calories gives at 482°C a value of 2.0×10^{-4} sec.$^{-1}$. Considering the approximate nature of the value based on the quarter-life this is in good agreement. It seems certain therefore that the control reaction in the ethylamine decomposition is the decomposition of diethylhydrazine.

In conclusion, it has been established that the decomposition of ethylamine proceeds by a bimolecular reaction yielding symmetrical diethylhydrazine and hydrogen followed by a subsequent decomposition of the hydrazine by a chain mechanism which overall is of first order. The former reaction is considerably more rapid than the latter and would be expected therefore to have a smaller energy of activation and smaller temperature coefficient. As the temperature is raised in the ethylamine decomposition therefore, the increase in the rate of the hydrazine decomposition will be relatively more rapid than the rate of its formation and the length of the induction period will decrease. The data given at 500°C show this to be the case, wherein the induction period is very short. One would anticipate that at 520°C the decomposition of ethylamine would show no apparent induction even at pressures as low as 50 mm. The original investigation by Taylor covered the temperature range 500 to 540°C and pressures from 50 to 400 mm, in other words was on the border line at which the induction period becomes appreciable. It is probable, however, that its complete nonobservance was due in part to the presence of traces of air in the system since the absolute rates there found are about twice as rapid as those herein quoted. The energy of activation 43,400 calories found in the earlier investigation is not considerably in error, lying in the range here found and indicates that there are no real discrepancies between the results found in both cases. The only discrepancy lies in the former interpretation of the observed results.

MARCH, 1936 JOURNAL OF CHEMICAL PHYSICS VOLUME 4

Studies on Glass

XIV. Note on the Compressibility of Glucose Glass

JOHN C. LYMAN AND GEORGE S. PARKS, *Department of Chemistry, Stanford University, California*

(Received January 4, 1936)

The coefficient of cubical compressibility of glucose glass at 24°C has been found to be 18.8 (10^{-6}) atmos.$^{-1}$ for the pressure range 7–25 atmos. The relatively large intermolecular forces in polyhydroxy substances, such as glassy glucose and liquid glycerol, are indicated by a comparison of the compressibility and expansion coefficients for these and other typical organic compounds.

A VALUE for the coefficient of isothermal compressibility of glucose glass

$$[\beta=(-1/V)(\Delta V/\Delta P)_T]$$

has been needed in connection with some of the studies on glass which are being carried on in this laboratory. It is true that Cowper and Tammann[1] previously measured this coefficient for "amorphous" glucose and obtained a mean result of 12 (10^{-6}) atmos.$^{-1}$ at 20° for the pressure interval 240–1940 atmos. However, the present requirement was for a reliable value at con-

[1] A. D. Cowper and G. Tammann, Zeits. f. physik. Chemie **68**, 281 (1909).

siderably lower pressures. Moreover, the technique of preparing clear glucose glass, free from bubbles, has been developed to a high degree in recent years here at Stanford. These considerations led us to the present determination.

After some preliminary experimentation the method developed and used extensively by Richards and his students[2] was adopted. A glass piezometer, closely following in details those described by Richards, was employed with mercury as the piezometric fluid around the sample of glucose glass. During the measurements it was placed within a strong steel bomb; various pressures, as desired, were then applied to this system from a cylinder of compressed nitrogen and were measured on a special test gauge.[3] The piezometer and bomb were kept at 24° in a carefully controlled thermostat.

The glucose glass samples were prepared by melting Pfanstiehl C. P. α-glucose crystals, heating the resulting liquid under a vacuum for ten or fifteen minutes at 170°C to eliminate air bubbles, then at atmospheric pressure pouring the material into small cylindrical molds made out of copper foil, and cooling these slowly down to room temperature in a desiccator. Full preparative details have been given in other places.[4] The small cylinders of annealed glucose glass thus obtained were carefully inspected for the inclusion of bubbles or other imperfections before use in the piezometer.

Two series of determinations on different samples of glucose glass yielded 18.2 and 19.4 (10^{-6}) atmos.$^{-1}$, respectively, for β in the pressure interval 7–25 atmos. Thus our mean result (probably accurate to within 5 percent) is 18.8 (10^{-6}) atmos.$^{-1}$ at 24°. This temperature is approximately in the middle of the "transition region"[5] in which many of the properties of carefully prepared samples of glucose glass change rather rapidly in magnitude.

TABLE I. *Some compressibility and expansion coefficients.* (At 20°C unless otherwise indicated.)

SUBSTANCE	β (10^6 atmos.$^{-1}$)	α (10^4 degree^{-1})
Ethyl alcohol (liquid)	111.3	10.8
n-Heptane (liquid)	142.4	12.2
Benzene (liquid)	94.9	12.1
Benzene (crystalline)	34.1 (0°)	—
Glycerol (liquid)	24.0	4.8
Glucose (glassy)	18.8 (24°)	1.4

It is interesting to compare this compressibility value with those for a few other typical organic compounds. We have done this in Table I, where the values for β for liquid ethyl alcohol, *n*-heptane, benzene and glycerol have been calculated from the sonic measurements of Freyer, Hubbard and Andrews.[6] They refer to 20° and 1 atmos. pressure. The value for crystalline benzene has been derived by extrapolation of the data of Richards, Bartlett and Hodges[7] and refers to 0°C and 1 atmos. pressure. As both the coefficients of compressibility (β) and of thermal expansion $\left[\alpha=(1/V)(\Delta V/\Delta T)_P\right]$ serve as rough measures of the magnitude of the intermolecular forces in a material, we have also tabulated values[8] for the latter at 20° in the last column of the table. From these data it is evident that the intermolecular forces in polyhydroxy compounds, such as liquid glycerol and glassy glucose, must be considerably greater than in ordinary liquids or even in a typical nonpolar crystal, such as crystalline benzene. Such a situation is undoubtedly a very favorable factor in the formation of a stable glass.

[2] T. W. Richards, W. N. Stull, J. H. Matthews and C. L. Speyers, J. Am. Chem. Soc. **34**, 971 (1912); T. W. Richards and E. P. R. Saerens, ibid. **46**, 934 (1924).

[3] Professor U. A. Patchett of the Department of Mechanical Engineering kindly calibrated this gauge for us.

[4] G. S. Parks, H. M. Huffman and F. R. Cattoir, J. Phys. Chem. **32**, 1366 (1928); G. S. Parks, L. E. Barton, M. E. Spaght and J. W. Richardson, Physics **5**, 193 (1934).

[5] G. S. Parks, S. B. Thomas and D. H. Light, J. Chem. Phys. **4**, 64 (1936).

[6] E. B. Freyer, J. C. Hubbard and D. H. Andrews, J. Am. Chem. Soc. **51**, 759 (1929).

[7] T. W. Richards, E. P. Bartlett and J. H. Hodges, J. Am. Chem. Soc. **43**, 1538 (1921).

[8] The sources of these α values are: *ethyl alcohol and benzene*, reference 6; *n-heptane*, G. Edgar and G. Calingaert, J. Am. Chem. Soc. **51**, 1540 (1929); *glycerol*, J. W. Lawrie, *Glycerol and the Glycols* (The Chemical Catalog Co., New York City, 1928), pp. 155–165; *glucose glass*, L. J. Snyder, Master's Thesis, Stanford University (1929).

The Kinetics of the Decomposition of Ethyl Ether at High Pressures

E. W. R. STEACIE, W. H. HATCHER AND S. ROSENBERG, *Department of Chemistry, McGill University, Montreal*

(Received December 5, 1935)

The decomposition of diethyl ether has been investigated with considerable accuracy at pressures up to 260 atmospheres at 426°C. The results confirm the previous approximate values found by Steacie and Solomon. The rate of the reaction is still increasing at the highest pressures investigated. The results may be qualitatively explained by the Rice-Herzfeld mechanism, and support the idea that the reaction is not a simple unimolecular change.

INTRODUCTION

AN investigation of the kinetics of the decomposition of ethyl ether at high pressures was described in a previous paper by Solomon and one of us.[1] In that investigation the rate of reaction was inferred from the rate of change of pressure, and on account of gas law aberrations, etc., it was only possible to claim an accuracy of about a factor of 2. In the present work the accuracy has been greatly improved by eliminating this source of error.

EXPERIMENTAL

Only minor changes were made in the apparatus previously described. The method of following the reaction, however, was completely altered, the rate being inferred from analyses rather than from the rate of change of pressure. The method used was as follows:

In making an experiment the procedure was identical with that previously described, except that pressure readings were taken merely to give the initial pressure and a rough indication of the extent of reaction. After the reaction had progressed to the desired extent, the bomb was cooled to room temperature and all the gaseous products were blown off into a large calibrated volume connected to a mercury manometer. The products were then analyzed in a Burrell gas analysis apparatus. It was thus possible to calculate the absolute amount of any gaseous product formed in the reaction. This could then be compared with the amount of the same product formed when the reaction went to completion, small differences in the initial pressure being corrected for on the assumption that the ideal gas law held. The extent to which the reaction had progressed during a given time could thus be inferred, and each experiment thus gave one point on the percent reaction-time curve. In practice the rate was inferred from the amount of saturated hydrocarbons produced, since this was the most reproducible value.

THE REACTION PRODUCTS

Analyses of the gaseous products at completion are given in Table I. It will be seen that saturated hydrocarbons are the main product of the reaction, as found in previous investigations. The amount produced is sufficiently constant to serve as a measure of the rate. With the exception of one or two low pressure experiments, the amount of carbon monoxide produced is also satisfactorily constant. The amount of unsaturated hydrocarbons is, in general, small. The large increase in the experiments at the highest pressures may be fictitious, since in these runs the gas was

TABLE I. *The products of reaction.*

Initial Pressure (cm)	Pressure Increase at Completion (%)	Gaseous Products (Percent) CO_2	C=C	CO	Saturated Hydrocarbons (+H_2)	Remarks
1860	154	12.5	7.0	9.5	70.1	
1840	153	8.6	4.3	21.5	66.0	
2380	121	13.9	5.8	13.2	67.1	
2480	135	11.5	6.6	15.6	65.9	Packed with steel turnings
1900	160	11.2	2.7	17.7	68.4	
2430	176	5.6	1.9	26.1	66.4	
7080	232	3.7	3.4	22.4	70.5	Packed with steel turnings
7280	221	6.7	3.0	18.5	71.6	Left overnight before sampling
6980	238	4.3	2.4	26.8	66.5	Coated with KCl
15300	268	5.8	13.6	16.1	64.5	
14580	270	5.7	13.7	19.4	61.2	
19020	266	6.8	10.9	19.5	62.8	
18100	281	5.2	13.9	20.2	60.7	

[1] Steacie and Solomon, J. Chem. Phys. **2**, 503 (1934).

absorbed by fuming sulphuric acid much more slowly than usual. It is therefore possible that some condensation product is formed at high pressures, which is absorbed by fuming sulphuric acid.

The comparatively large amounts of carbon dioxide are difficult to explain. It seems certain that it really is carbon dioxide, since it was not condensable at −80°C. A few experiments were made at an initial pressure of 3 atmos. These gave erratic results, and showed that the reaction is largely heterogeneous (in a stainless steel vessel) at low pressures. In these experiments the CO_2 was very high and variable. The CO_2 produced at higher pressures, however, cannot be ascribed to a heterogeneous decomposition of the ether, since at higher pressures the reaction is not appreciably heterogeneous. The carbon dioxide cannot arise from the reaction

$$2CO = CO_2 + C,$$

since large amounts of CO are left at completion, and are not diminished on standing overnight. This also seems to rule out the possible attack of the bomb by CO,

$$3Fe + 2CO = Fe_3C + CO_2.$$

A small amount of some carbonaceous material is, however, produced. In any event, the production of CO_2 does not seem to affect appreciably the amount of saturated hydrocarbons produced, and hence should be without effect on the calculated rates of reaction.

Table I also gives the percent pressure increase at completion, although with the present experimental method this is no longer of great importance. The pressure increase rises greatly at high pressures. Since the products of the reaction do not change greatly with changing pressure, it is apparent that the change in the pressure increase at completion is mainly due to increasing gas law aberrations. It is to be noted that the pressure increases at high pressures are much higher than those previously reported by Steacie and Solomon. On account of the much larger number of experiments reported here, and of the improvement of the technique as the work progressed, the present values are certainly the more accurate. In any case, however, the error introduced into Steacie and Solomon's velocity constants from this cause is well within the factor of 2 which they claimed as their experimental accuracy.

The Rate of Reaction

The reaction rate data are given in Table II.

Table II. *Reaction rate data.*

Initial Pressure (cm)	Time (min.)	% Reacted	$K \times 10^4$ (sec.$^{-1}$)	Initial Pressure (cm)	Time (min.)	% Reacted	$K \times 10^4$ (sec.$^{-1}$)
2350	11.0	18.7	3.14	7280	38.0	46.5	2.72
2460	46.5	44.9	2.13	7030	57.0	60.4	2.71
				6980	87.0	78.2	2.91
7080	13.0	34.4	5.45	7180	100.0	61.2	1.58
6800	18.0	35.3	4.00	7140	116.0	75.6	2.02
7030	32.0	50.2	3.64	6930	137.0	82.6	2.12
14480	26.0	56.1	5.53	16320	56.5	73.2	3.88
				17160	90.0	82.8	3.26
20700	17.5	42.1	5.19				
				21200	56.5	74.3	4.00
2370	76.0	57.5	1.87	19630	90.0	74.8	2.55
1910	105.5	60.1	1.45				
2340	146.0	76.1	1.63				

The values of K given in the last column are first-order constants. It is apparent that K drifts largely as the reaction progresses. The results at any pressure would agree, in fact with an order of about 1.8. To determine the effect of pressure upon the rate, the most unobjectionable method would be to extrapolate the K's to zero time and obtain the initial rates. Such an extrapolation, however, is very indefinite in view of the scattering of the values of K. It is therefore preferable to compare the values of K corresponding to some definite amount of reaction. For the sake of uniformity we have adopted 20 percent reaction for this purpose, as did Newitt and Vernon[2] and Steacie and Solomon. We thus obtain the values given in Table III. These are probably accurate to within 10 percent.

Table III. *The effect of pressure on the rate.*

Initial Pressure (cm)		
2300	7000	15000–20000
$K_{20} \times 10^4$ (sec.$^{-1}$)		
3.0	4.9	6.2

[2] Newitt and Vernon, Proc. Roy. Soc. **A135**, 307 (1932).

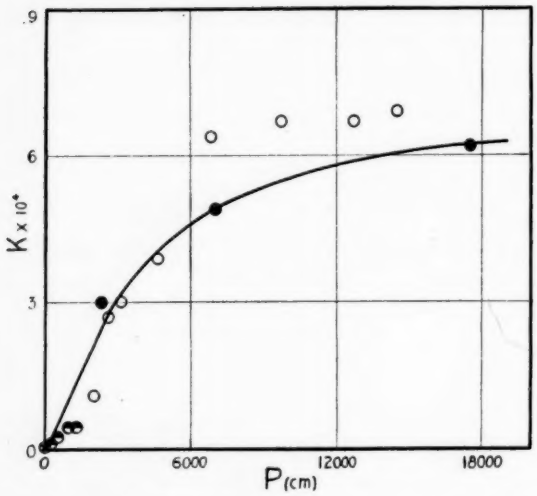

FIG. 1. The rate of reaction at 426°K. Black circles, this investigation; open circles, Steacie and Solomon; half-black circles, Newitt and Vernon; circle and cross, average low pressure value of Hinshelwood, Rice and Sickman, Kassel, and Steacie.

The data are plotted in Fig. 1, and are compared with the results of other investigations, as recalculated in the previous paper. The excellent agreement with the results of Steacie and Solomon is noteworthy, since the method of determining the rate was entirely different in the two investigations.

THE EFFECT OF SURFACE

A number of experiments were made with the reaction vessel packed with stainless steel turnings, and others with the reaction vessel coated with potassium chloride. It was found that such treatment had no measurable effect on the rate, and the reaction may therefore be considered to be homogeneous in a stainless steel vessel at high pressures.

It was obviously desirable to tie-in the results of the present investigation with those obtained at low pressures, and an attempt was made to determine the rate at 3 atmos. by the same method. It was found, however, that at these pressures the results were very erratic, and the rate was considerably increased by packing the reaction vessel. The results at this pressure have therefore been discarded.

DISCUSSION

The decomposition of ethyl ether has now been investigated over a far wider range of pressure than any other reaction, *viz.*, from 20,000 cm in this investigation to 0.01 cm in the work of Rice and Sickman.[3] It is evident that the rate of reaction increases steadily with pressure over the entire range.

Since this investigation was commenced it has become apparent that the ethyl ether decomposition is not a simple unimolecular change, but probably involves reaction chains.[4] On the basis of the Rice-Herzfeld mechanism there are two general types of free radical chain decomposition of organic compounds: (A) The chain terminates by a heavy radical combining with a light radical (CH_3 or C_2H_5). This is the mechanism proposed for the decomposition of ethyl ether, and it may be shown to lead to an approximate order of 1. (B) The chain terminates by the recombination of two light radicals, as appears to be the case in the acetaldehyde decomposition, and this leads to an order of 1.5. Which mechanism holds is governed by the activation energies of the elementary reactions, which govern the relative stationary concentrations of the various radicals.

Now it has been emphasized by Rice that free radical mechanisms of this type can only be expected to hold accurately at the start of a decomposition, before the products have accumulated to an appreciable extent. The decomposition of ethyl ether gives rise to acetaldehyde, and thus "It follows that the usual measurements of the rate of decomposition of diethyl ether are really measurements performed on mixtures with acetaldehyde and the two substances would not be expected to decompose independently since the radicals of the one enter into the decomposition of the other."[5] It follows that the decomposition of acetaldehyde will greatly increase the concentration of light radicals present, and hence the chains in the ether decomposition will in

[3] O. K. Rice and Sickman, J. Am. Chem. Soc. **56**, 1444 (1934).

[4] Leermakers, J. Am. Chem. Soc. **56**, 1899 (1934). F. O. Rice and Herzfeld, ibid. **56**, 284 (1934). F. O. Rice and K. K. Rice, *The Aliphatic Free Radicals* (Baltimore, 1935), pp. 86–90.

[5] Rice and Rice, reference 4, p. 90.

part be terminated by mechanism (B) rather than by (A). The result will be to raise the order of the reaction above 1, and thus give a rate which increases steadily with increasing pressure. In the present investigation the over-all order, as inferred from the effect of pressure on the rate, is about 1.35 and the results are therefore explicable on the basis of the free radical mechanism. Unfortunately the situation is far too complicated to permit a quantitative comparison with the theory.

In conclusion we wish to express our indebtedness to the National Research Council of Canada for a studentship awarded to one of us (S. R.) during the tenure of which this work was performed.

MARCH, 1936 JOURNAL OF CHEMICAL PHYSICS VOLUME 4

The Decomposition of Methyl Nitrite at High Pressures

E. W. R. STEACIE AND S. ROSENBERG, *Physical Chemistry Laboratory, McGill University, Montreal*

(Received December 21, 1935)

PREVIOUS work on the decomposition of diethyl ether at high pressures[1] showed that the rate increased continually with pressure up to 260 atmos., the rate at that pressure being about 40 times the previously calculated "high pressure rate." It has since been shown by Leermakers[2] that the reaction proceeds by a chain mechanism, as had been predicted by Rice and Herzfeld.[3]

The alkyl nitrites have been shown to decompose unimolecularly[4] and it appears to be very unlikely that chains occur in these reactions.[5] Nevertheless, it seemed worth while investigating the decomposition of methyl nitrite at high pressures to see if the rate would remain constant.

The apparatus, experimental procedure, preparation of materials, etc., were as previously described, except for the substitution of an oil bath for the lead bath owing to the lower temperatures required. The rates were inferred from the change in pressure accompanying the reaction. The results are given in Table I.

TABLE I. *Temperature 217.5°C.*

RUN NO.	P_0 (cm)	k(sec.$^{-1}$)	% ΔP AT COMPLETION
Steacie & Shaw	up to 65	1.0×10^{-3}	82.5
1	103	1.3	142
5	109	1.9	94
4	682	1.7	56
2	1320	1.7	118
3	2980	2.3	76
6 (Packed)	79	2.3	92

It is apparent that the pressure increase at completion is very erratic. The rate in run 6, where the surface is about double that in the empty vessel, is considerably higher than that in the corresponding unpacked runs, and the reaction is thus partly heterogeneous. Considerable error is also to be expected from gas law aberrations. In consequence the results are probably accurate only to within a factor of about 2. Furthermore most of the errors will tend to make the rate high. Hence it may be concluded that, within the rather large experimental error, there is no appreciable increase in the rate of decomposition of methyl nitrite on going from 65 cm to 35 atmos. This furnishes further support to the conclusion that the reaction is really unimolecular.

We wish to acknowledge our indebtedness to the National Research Council of Canada for a studentship awarded to one of us (S. R.) during the tenure of which this work was performed.

---

[1] Steacie and Solomon, J. Chem. Phys. **2**, 503 (1934); Steacie, Hatcher, and Rosenberg, ibid., this issue.
[2] Leermakers, J. Am. Chem. Soc. **56**, 1899 (1934).
[3] F. O. Rice and K. F. Herzfeld, J. Am. Chem. Soc. **56**, 284 (1934).
[4] Steacie and Shaw, Proc. Roy. Soc. **A146**, 388 (1934); **A151**, 685 (1935); J. Chem. Phys. **2**, 345 (1934); **3**, 344 (1935).
[5] F. O. Rice and Radowskas, J. Am. Chem. Soc. **57**, 350 (1935).

The Distribution of Molecules in a Model Liquid

W. E. MORRELL AND J. H. HILDEBRAND, *Department of Chemistry, University of California*

(Received January 3, 1936)

A three-dimensional model molecular assemblage has been constructed permitting a determination of the relative frequency of occurrence of the varying intermolecular distances. The model simulates the expansive effect of temperature. A good approximation is obtained to the distribution of molecules in liquid mercury determined by Menke by the aid of x-ray diffraction.

THE number of molecules of a pure fluid in a spherical shell of radius r and thickness dr is $(N/\mathrm{v})\ 4\pi r^2 dr$ (where N is Avogadro's number and v is the molal volume), provided r is large. When r becomes small, however, a function of r, which has been designated by W, must be introduced, because the positions of the molecules in the shell are influenced by the positions of their neighbors. The number of molecules in the shell is then $(N/\mathrm{v})\ 4\pi W r^2 dr$. We may define W as the average number of molecules per unit volume (v/N) at distance r from a central molecule.

The determination of this distribution function, W, would permit important conclusions to be drawn regarding intermolecular forces and such related problems as solubilities.[1] Its purely mathematical analysis, in the case of rather condensed systems, where the molecular field surrounding each molecule must be approximately constant, offers attractive possibilities complicated by difficulties which have thus far not been surmounted. Probably the most successful mathematical treatment to date is that of Kirkwood,[2] who, by statistical-mechanical methods, obtained a complicated "approximate molecular pair distribution function, typical of dense fluids." Experimental determination of the distribution function by the aid of x-ray diffraction has been carried out in the cases of mercury and liquid gallium by Menke,[3] and at two different temperatures for water by Katzoff.[4] Menke's distribution function for mercury is reproduced in Fig. 2A. Kirkwood's curve only roughly approximates this experimental curve.

Another type of investigation which throws light upon the variation of W with r is the use of models and direct measurement. Thus Menke,[3] by merely pouring steel spheres onto a flat surface and measuring each time the distance between two black ones, then tabulating these distances, obtained a curve for two dimensions which had the characteristics of his W curve for mercury. Very similarly, Prins[5] poured seeds onto a glass plate and photographed them. He then drew concentric circles on the negatives around "central" seeds, counted the numbers between circles, and obtained the two-dimensional "W" for this case, or the number per unit area at various distances from the central seed. Here also, curves were obtained which at least roughly resemble the distribution function for mercury.

The present work is an extension of this use of models, under conditions, however, which should more nearly duplicate those in an actual liquid. We have used three dimensions instead of two, practically neutralized the force of gravity on the individual particles, put the "molecules" in motion, and have taken more measurements and at smaller intervals.

The model "molecules" were gelatin spheres. These spheres were made by allowing drops of a hot gelatin solution (15 grams per 100 cc of water) to fall into a column of "crystal" oil surrounded by an ice bath, the gelatin becoming hard before the spheres reached the bottom of the column. A few black spheres were made by mixing lamp black into part of the hot gelatin. The oil was washed from the balls with ether, then the ether washed away with water.

An environment for the spheres was made by heating part of the clear gelatin solution over a

[1] J. H. Hildebrand and S. E. Wood, J. Chem. Phys. **1**, 817 (1933).
[2] J. G. Kirkwood, J. Chem. Phys. **3**, 300 (1935).
[3] H. Menke, Physik. Zeits. **33**, 593 (1932).
[4] S. Katzoff, J. Chem. Phys. **2**, 841 (1934).
[5] J. A. Prins, Naturwiss. **19**, 435 (1931).

water-bath for some 12–16 hours—until it no longer solidified when cooled. This solution retains practically the same density and refractive index as the spheres, or can be adjusted to these conditions by the addition of a little water. The solid balls, then, when placed in this solution would neither sink nor rise to the surface and were practically invisible. On the other hand, the few black spheres put into the mixture were clearly and sharply defined.

The solution and spheres were placed in a small plate-glass cell. Shadow pictures of the mixture were made by means of a mercury spark. A small metal frame clamped the film firmly against two sides of the box, and by use of a mirror each exposure was made simultaneously from two directions at right angles. Before each exposure, while a new film was being placed in the frame, the cell was tipped in various directions and shaken somewhat, then as quickly as the cell was in position and before the motion of the spheres had completely ceased, the picture was snapped.

One of the resulting photographs is shown in Fig. 1.

The black spheres on the negatives were numbered consecutively from top to bottom for the sake of convenience in recording their positions. Their distances from the axes at the right and bottom of each half of the film, scratched on the walls of the glass cell, were measured by the aid of a vernier caliper. Given the X, Y, and Z positions of each black sphere, the values for ΔX, ΔY, and ΔZ for each possible pair were obtained merely by subtractions. The distance, r, between each pair was given by $r=(\Delta X^2+\Delta Y^2+\Delta Z^2)^{\frac{1}{2}}$. We found that the thousands of repetitions of this problem were most conveniently handled on a slide rule with an appropriate square and square root scale.

The distances between all possible pairs of black spheres having been thus calculated from a series of photographs, the number of times that each distance occurred was tabulated. If this number be x, the total number of measurements obtained from the series can be designated $\sum_0^\infty x$. Then $x/\sum_0^\infty x$ is the relative frequency with which this particular distance occurred in the series, or it is the relative chance that a particular black sphere would at a certain time be found at a given distance r from a particular ball arbitrarily chosen as the central one. Since there are N spheres in the box, the chance that any of them, no matter which, would at that time be at distance r from the central one is $(N-1)x/\sum_0^\infty x$, or this is the probable number of balls which at any time would be found at distance r from the central one. The number which would probably be found within a spherical shell of inner radius r_1 and outer radius r_2 is $(N-1)\sum_{r_1}^{r_2} x/\sum_0^\infty x$. The number per cc within this shell would be

$$(N-1)\sum_{r_1}^{r_2} x/\sum_0^\infty x \int_{r_1}^{r_2} 4\pi r^2 dr.$$

Hence the number of spheres per unit volume at distance r from the central sphere would be

$$V(N-1)\sum_{r_1}^{r_2} x/N\sum_0^\infty x \int_{r_1}^{r_2} 4\pi r^2 dr,$$

and this by definition is W. Integrating, the expression becomes:

$$W=3V(N-1)\sum_{r_1}^{r_2} x/4\pi N\sum_0^\infty x(r_2^3-r_1^3). \quad (1)$$

By means of this equation and the data obtained from the photographs, the value of W at each value of r was calculated. The results of four series of measurements are plotted in Fig. 2B, C, and D.

In these figures the points represented by the solid dots were obtained by taking $r_2-r_1=0.05$ cm, and the circles by using $r_2-r_1=0.09$ cm. The points on D were determined only with $r_2-r_1=0.05$ cm. The values of the various constant quantities occurring in Eq. (1), to-

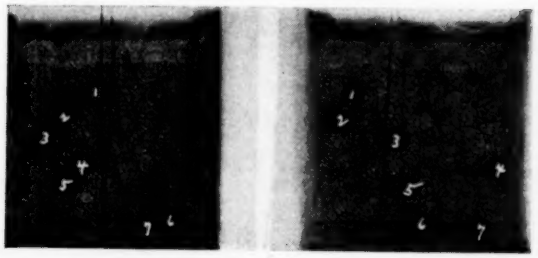

FIG. 1.

TABLE I.

SERIES	TOTAL NO. MEASUREMENTS $\int_0^\infty (\Sigma x)$	TOTAL NO. SPHERES (N)	NO. BLACK SPHERES	DIAMETER OF SPHERES	VOLUME OF "SYSTEM" (V)	"EXPANSION"
B	1121	614	7	0.422 cm	60 cc	1.84
B′	820	300	6	0.48 cm	45 cc	1.92
C	1120	371	7	0.432 cm	60 cc	2.84
D	1035	500	10	0.39 cm	30.5 cc	1.45

gether with other information concerning each series, are summarized in Table I.

The "expansion" is the ratio of the total volume of the mixture to that which would be occupied by the balls, together with the space between them, if they were allowed to settle into a completely regular, closest-packed arrangement. In other words, it is the ratio of V to 0.707 D^3N, where D is the diameter of the spheres.

The "expansions" of two of the series, B and B′, were practically equal, hence they were plotted together in B.

It will be noted that the less "expanded" the mixture, the higher and sharper is the first maximum. This is exactly what should be expected, and agrees also with the results of Prins.[5] The extreme case would be a regular, close-packed arrangement, either hexagonal close packing or cubic close packing. In these cases the distribution functions become discontinuous. These are given for comparison in Fig. 2E.

These varying "expansions" were introduced to simulate the effect of temperature. As a sample of the degree of expansion of an ordinary liquid we may cite carbon disulfide, whose volume at 25°C is 1.25 times its volume extrapolated to absolute zero.

A curve showing these close-packing effects more markedly was obtained in our preliminary measurements. In this case glass spheres were used instead of gelatin, a few being colored with water paints. They were immersed in a solution of bromoform and carbon tetrachloride, the mixture being so adjusted as to have the same refractive index as the glass. However, the spheres were denser than the liquid, hence sank to approximately close-packed, though jumbled, arrangements. The positions of the colored ones were read directly, instead of being measured from photographs. (This method of measurement was also used in D.)

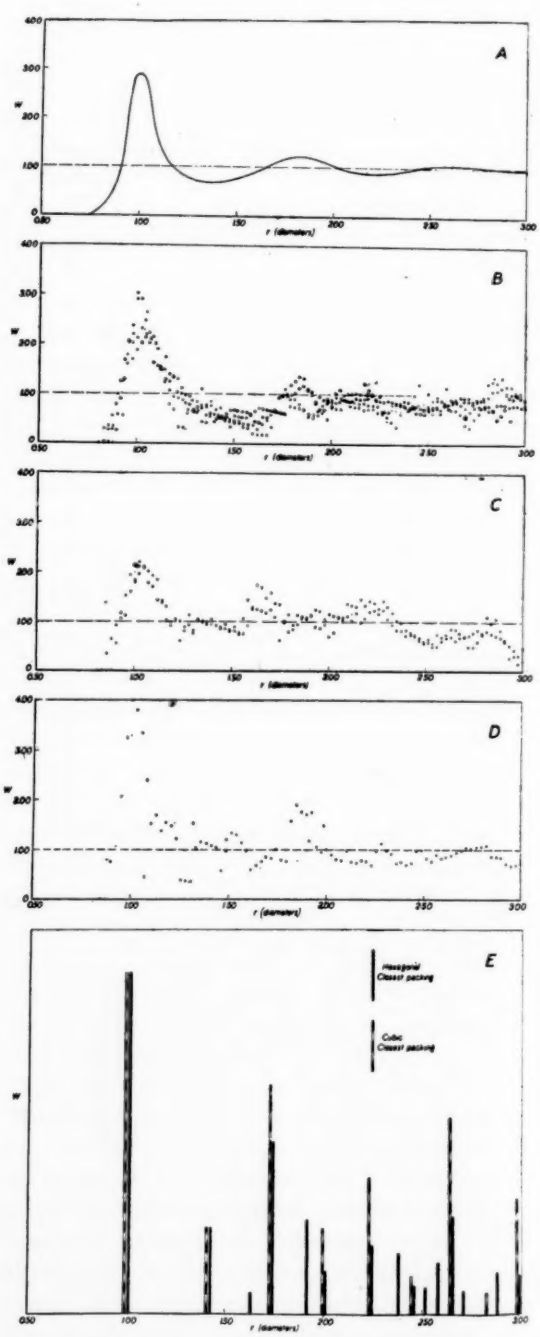

FIG. 2. A, Menke's[3] distribution function for mercury; B, two distribution functions, superimposed, obtained with gelatin spheres, "expansions" 1.84 and 1.92; C, "expansion" 2.84; D, "expansion" 1.45; E, discontinuous distribution functions for regular close-packed arrangements.

In opposition to close-packed arrangements, very high "expansions," or a gas-like structure, should give distribution functions with a very low first maximum or no peak at all, and practically no fluctuations from unity at distances greater than one diameter.

Because of the smallness to the cell used in these experiments, the values of W tend to sag below the unity line at the larger distances, since these larger distances could not occur relatively as frequently as they would in a box of infinite size. This effect, within the region considered, could have been practically eliminated by the use of a larger container. This, however, would have greatly increased the number of observations necessary to supply the same number of measurements at the shorter distances, and it is at these smaller distances that the determination of the distribution function is of most value. Beyond a couple of diameters the function fluctuates little from unity, as Menke's curve shows. Within a couple of diameters this sagging effect plays very little part, so the added labor incident to the use of a larger cell was not considered worth while.

Thus by the use of a model molecular assemblage we have been able to duplicate the principal characteristics of the molecular distribution function obtained for mercury. Presumably the atoms in liquid mercury are distributed much as are the spheres in these model liquids. This distribution, while practically random with respect to a central molecule at distances greater than a couple of diameters, is far from random at smaller distances. Within these shorter distances the distribution shows remnants of a regular, close-packed, or crystalline structure.

It might be noted in this respect that Kratky,[6] from a study of Menke's curve for mercury and comparison with curves which he calculated from assumptions of various possible types of packing, concludes that the residual ordered arrangement in liquid mercury is of the hexagonal close-packed type. Probably a better conclusion would be that it is a mixture of both hexagonal and cubic packings, which are represented by Fig. 2E. Thus glass spheres poured into a pile will pack cubically as often as hexagonally. If a layer of such spheres be arranged in hexagonal or honeycomb fashion, then a second layer on top of the first, then the first sphere of a third layer be added, it will be found that it can take either of two positions relative to the lower layers. Either it can be put directly above a sphere of the first layer or it can be placed on the continuation of a straight line joining the centers of a sphere of the first layer and an adjacent sphere in the second layer.[7] The first case gives hexagonal packing, the second, cubic, and there is no *a priori* reason why the one should occur in preference to the other. It seems likely that both types should occur in liquid mercury, especially since the thermal motions prevent a completely regular, close-packed arrangement. Indeed, an examination of Kratky's curves shows that an average of the two types would match Menke's curve for mercury better than does the hexagonally-packed curve alone.

It would be interesting and enlightening to extend the study of the distribution functions by means of model liquids to cases involving spheres of different sizes, and these at various "mole fractions." The method might also be extended to "molecules" of other forms, such as sausage-shaped, where orientation as well as distance would have to be considered.

A knowledge of these distribution functions for various types of liquids and solutions, and their variations with concentration and temperature, would permit a forward step in the study of the liquid state.

We wish to acknowledge certain suggestions for the construction of our model system made by Professor J. E. Gibson.

[6] O. Kratky, Physik. Zeits. **34**, 482 (1933).

[7] See W. H. Bragg and W. L. Bragg, *The Crystalline State* (G. Bell and Sons, London, 1924), p. 144.

LETTERS TO THE EDITOR

This section will accept reports of new work, provided these are terse and contain few figures, and especially few halftone cuts. The Editorial Board will not hold itself responsible for opinions expressed by the correspondents. Contributions to this section must reach the office of the Managing Editor not later than the 15th of the month preceding that of the issue in which the letter is to appear. No proof will be sent to the authors. The usual publication charge ($3.00 per page) will not be made and no reprints will be furnished free.

The Rearrangement of Molecules in Monomolecular Films: Polycyclic Compounds of the Five Ring Series

Monomolecular films of certain compounds whose molecules contain five benzene rings have been found to exhibit a remarkable phenomenon; that is, a rapid rearrangement of the molecules occurs in the film in such a way that the pressure almost entirely disappears. Thus with betuline the initial or immediate pressure at a molecular area of 24.5 sq. A is 17 dynes per cm while after this there is at this area an almost exponential fall of pressure with time to a practically constant value, in 30 seconds, of 1.0 dyne. Nevertheless a rapid compression to 33.5 sq. A, or by about 1/34 of the area, increases the pressure by 21 times to 21 dynes, or to 4 dynes more than the previous initial compression. At an area of 28 sq. A the initial pressure of 40 dynes falls to 5.5 dynes in 30 seconds, but on rapid compression to 26.2 sq. A rises to 50 dynes per cm.

At a pressure adjusted every 5 minutes to 16 dynes the area decreased in an hour by 18 percent, but by only about a fourth of this at 1.0 dyne. If the pressure is adjusted to constancy more frequently the area decreases more rapidly. Fig. 1 gives the values of the film pressures and surface potentials of betuline (polar groups Ring I at positions 2 and 3) and oleanolic acid (I, 3 and V, IV, 17), and Fig. 2 of the isomers sumaresinolic and siaresinolic acid (positions I, 2, 3 and V, IV, 17). The substances β-amyrine or vitamin E (position I, 2) and betuline diacelate (I, 2, 3) do not exhibit this rearrangement except at the highest pressures (Fig. 3).

In the figures the unbroken lines give the initial values and the dotted lines the values obtained after the rearrangement. The experimental points for these values lie very closely on the dotted lines. In order to show just how closely the initial values for different experiments lie on a single curve, the experimental values for these curves are represented by points. To obtain these points one worker compressed the film by a definite decrease of area which depended upon the slope of the curve, while the other, by turning the torsion head of the balance, kept the float and thus the beam of light in a constant position until just the moment when the compression was completed.

The molecular areas obtained for all of the substances are about what would be expected from their structure except in the case of betuline, which gives abnormally low areas, below 37 sq. A, not only for the final state but even for the initial state of the film at pressures above ten dynes. Mr. Robert T. Florence is beginning a study of this problem by various optical means, including the use of the ultramicroscope and the effects of the film on polarized light.

Of the relations exhibited by the surface potential (ΔV) the most remarkable is the difference shown by the two isomers. Thus sumaresinolic acid exhibits a maximum value of 400 mv while siaresinolic acid gives the very high value of 615 mv.

The values of $m = \Delta V/n$, where n is the number of molecules in the film per sq. cm are related to the dipole moments (u) of the molecules in the film in an unknown way; but in general m increases with u. The values of u for the

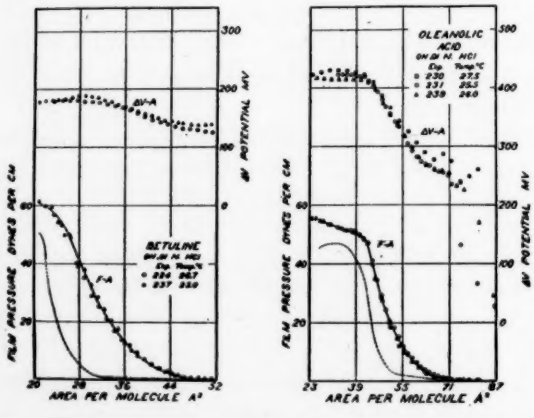

FIG. 1. Film pressures and potentials. The unbroken line gives the initial pressure, and the dotted line the pressure thirty seconds later.

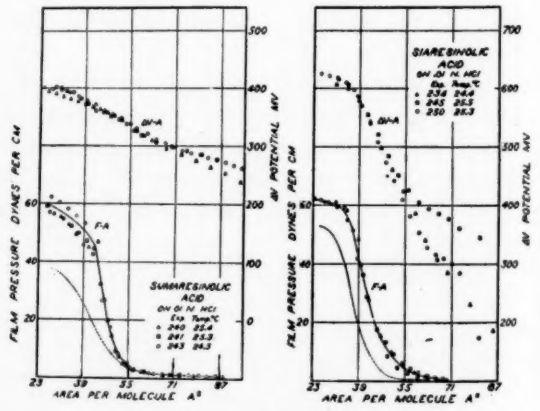

FIG. 2. Film pressures and potential for two isomers.

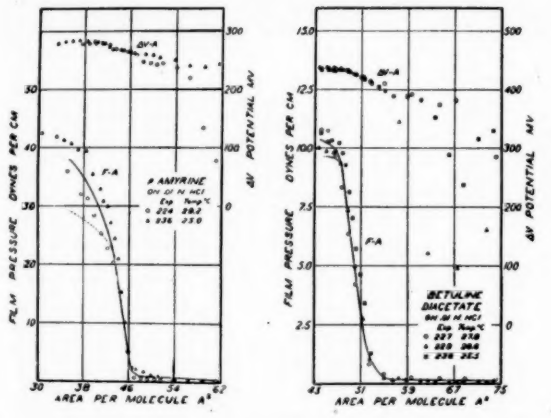

FIG. 3. Film pressures and potentials for vitamin E and betuline diacetate.

film as given by investigators in England are not dipole moments at all, but only values of $m/4\pi$. In units of 10^{-18} e.s.u. per molecule the maximum values of m are approximately 2.2 for betuline, 2.1 for amyrine, 6.0 for oleanic acid, 6.8 for sumaresinolic acid, 7.5 for betuline diaceto and 7.8 for siaresinolic acid. These values are much higher than those given by films of fatty acids, alcohols, etc., which lie in general between 2 and 3 when the number of carbon atoms is between 12 and 18.

WILLIAM D. HARKINS
HERMAN E. RIES, JR.
EVERETT F. CARMAN

George Herbert Jones Laboratory,
University of Chicago,
February 11, 1936.

The Infrared Absorption Spectrum of HDS and D_2S

The infrared absorption spectrum of the molecules HDS and D_2S has been investigated between 1.5μ and 12.0μ, by using a prism spectrometer of the Wadsworth type, with the result that several vibration-rotation bands characteristic of each were found. The two samples of gas studied were prepared with D_2O of two different purities. The HDS was made by dropping 55 percent D_2O on chemically pure aluminum sulfide, and the D_2S was made by dropping 99.2 percent D_2O on aluminum sulfide, in each case being very careful to trap out any "heavy water" vapor. The purity of the samples was thus assured. The cell of HDS contained, of course, some H_2S, and some D_2S also, and all the previously known bands of H_2S [1] were found in its spectrum in addition to the new ones. The purity of the D_2S could not be doubted and the bands found were attributed to it alone.

The positions of the bands found in D_2S are as follows: 3.65μ, 4.55μ, and 10.8μ. Two of these regions have been studied with a prism-grating spectrometer with the result that their rotational structure has been very completely resolved. The band at 3.65μ appears to be of the *P*, *Q*, *R* type with a very broad and partially resolved *Q* branch. The band at 10.8μ has also been resolved, but it does not have a *Q* branch and is probably more nearly the doublet type.

In HDS none of the bands have as yet been studied with the grating and resolved. The positions of the bands given by the prism data are: 2.1μ, 3.15μ, 4.1μ, 9.0μ. By combining these new bands with the ones already known in H_2S in a table it can be seen how the bands corresponding in HDS, and D_2S are shifted toward longer wave-lengths in the anticipated manner.

TABLE I.

H_2S	HDS	D_2S
1.9μ	2.1μ	—
2.65	3.15	3.65μ
3.70	4.1	4.55
7.9	9.0	10.8

The grating measurements on the remaining bands have been begun and will be reported in this journal in the near future. We wish to express our appreciation to Professor H. L. Johnston of the Chemistry Department of Ohio State University, for his kind cooperation in furnishing us with the quantities of "heavy water" used in making the samples of gas.

ALVIN H. NIELSEN*
HARALD H. NIELSEN

Mendenhall Laboratory of Physics,
Ohio State University,
January 22, 1936.

[1] Rollefsen, Phys. Rev. **34**, 604 (1929); Nielsen, ibid. **37**, 727 (1931).
* Now at University of Tennessee, Knoxville.

On Some Gas-Kinetic Properties of Light and Heavy Hydrogen

The knowledge of certain gas-kinetic quantities as the coefficients of viscosity, of thermal conductivity and diffusion which are mutually interrelated has become of considerable importance, particularly since their measurement has been used for the determination of the concentration of the *ortho* and *para* modifications in the case of the two hydrogens. We have therefore closely investigated the influence of the statistical weights of the various molecules on these coefficients. It thereby turned out for example, that in the neighborhood of 70°K, the coefficient of viscosity of pure parahydrogen should be approximately six percent smaller than that of ordinary hydrogen. This difference decreases at lower and higher temperatures, but is expected to increase again when the temperature becomes extremely low. A corresponding effect for deuterium should be vanishingly small. The calculations have been made on the basis of the rigid sphere model and the numbers given might therefore still depend on the actual force of interaction between the molecules. We shall later on report in more detail on the application of the theory to other gas-kinetic quantities and to other gases.

O. HALPERN
E. GWATHMEY

Physics Department,
New York University, University Heights,
February 3, 1936.